Dissertation
submitted to the Department of Earth Sciences
of the Freie Universität Berlin

Christopher Lüthgens

The age of Weichselian main ice marginal positions in north-eastern Germany inferred from Optically Stimulated Luminescence (OSL) dating

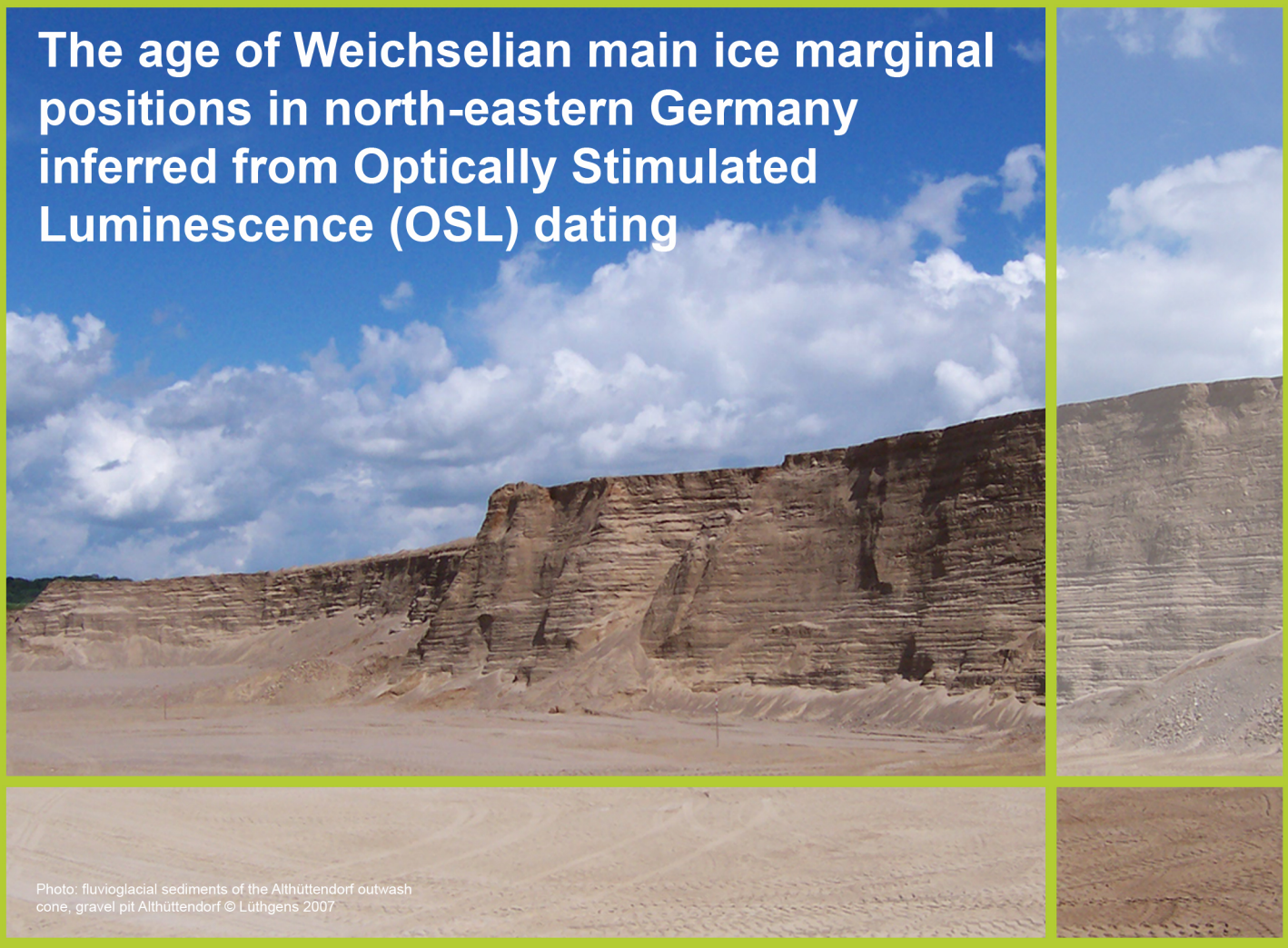

Photo: fluvioglacial sediments of the Althüttendorf outwash cone, gravel pit Althüttendorf © Lüthgens 2007

Freie Universität Berlin

The age of Weichselian main ice marginal positions in north-eastern Germany inferred from Optically Stimulated Luminescence (OSL) dating

Datierung weichselzeitlicher Haupteisrandlagen
in Nordost-Deutschland mit Hilfe von
Optisch Stimulierter Lumineszenz (OSL)

Inauguraldissertation
zur Erlangung des akademischen Grades Dr. rer. nat.
im Fach Geographie

am Fachbereich Geowissenschaften
der Freien Universität Berlin

vorgelegt von
Christopher Lüthgens

Berlin 2011

Erstgutachterin: Prof. Dr. Margot Böse

Zweitgutachter: Prof. Dr. Manfred Frechen

Tag der Disputation: 09.02.2011

Table of contents

* Sections 4, 5, 6, 8, 9 have been published previously. The internal structure of these sections was not altered from the original publications and is not stated here in detail.

List of figures

Figures from sections 4, 5, 6, 8, 9 have been published previously. The numbering of these figures was not altered from the original publications and is not stated here.

List of tables

Tables from sections 4, 5, 6, 8, 9 have been published previously. The numbering of these tables was not altered from the original publications and is not stated here.

Acknowledgements

First of all, I would like to thank my supervisor Prof. Dr. Margot Böse for giving me the chance to work on this fascinating topic in the first place and for her constant helpfulness and support throughout the course of my work. This study is rooted in a research project funded by the German Research Foundation (Deutsche Forschungsgemeinschaft, DFG) and conducted in cooperation between the working group of Prof. Dr. Margot Böse at the Institute of Geographical Sciences, Physical Geography, Freie Universität Berlin and the luminescence dating laboratory run by Dr. Matthias Krbetschek, Quaternary Geochronology Section of the Saxon Academy of Sciences at the Institute of Applied Physics of the TU Freiberg. Therefore I would like to thank Dr. Matthias Krbetschek and Mrs Ingrid Stein for their support in the Freiberg lab, especially for the sample preparation and radionuclide analyses. Special thanks go to Dr. Frank Preusser and the team at the luminescence dating laboratory of the University of Bern for giving me the chance (and sufficient measurement time) to carry out the single grain OSL measurements.

Furthermore, I would like to thank all colleagues who contributed to the research papers (in order of appearance): Margret Fuchs (Technical University of Dresden), who assisted in the compilation of the first Excel sheets for automated D_e calculations, Margot Böse (Freie Universität Berlin) for the fine gravel analysis of the Luckenwalde section, Tobias Lauer (Leibniz Institute for Applied Geosciences) for the post-IR YOSL measurements in the Freiberg lab, Jaqueline Strahl (Landesamt für Bergbau, Geologie und Rohstoffe Brandenburg) for providing results from pollen analysis of the Eemian of Vevais, Dirk Wenske (Freie Universität Berlin) for processing the SRTM data for the digital elevation model of the Oderbruch basin, Thomas Rosenberg (University of Bern) for providing the correction factors for the beta source of the single grain OSL reader of the Bern luminescence lab and the anonymous reviewers of the papers for their fruitful comments. I would also like to thank all those who assisted in the field work - I couldn't have moved all these cubic metres of sediment on my own! Thanks to Karolin Ortelbach and Nina Dörschner for their assistance in the sediment lab and the evaluation of the grain size data. Special thanks to Anne Beck for proofreading part of this manuscript. Thanks also to the owners of the various gravel pits for granting access to their property and permitting the necessary excavations. I would also like to thank all the colleagues at the Institute of Geographical Sciences, especially the 'residents of the Böse & Schütt corridor' for the excellent working atmosphere. A very special thanks to Dirk Wenske for always having an open door, for many fruitful discussions and for a whole lot of Taiwanese Oolong Tea!

Last but not least I would also like to thank those 'outside' science, who accompanied me all the way through this challenge and never stopped believing – my mom, for her support, her patience and for always being there, regardless of what times she had to go through herself – my dad, my number one inspiration, I miss you … – good friends, with whom I had the pleasure to share some of the best days in my life – Nina, my love and life, for making me complete!

Christopher Lüthgens

Abstract

During the past 130 years, classification of the Weichselian Pleniglacial in north-eastern Germany was mainly based on morphostratigraphical interpretations. In general, three main ice marginal positions are distinguished. The ice advance to the southernmost, relatively weakly developed ice marginal position of the Brandenburg phase has traditionally been ascribed to the Last Glacial Maximum (LGM) of the Scandinavian Ice Sheet (SIS). The Frankfurt phase is usually interpreted as a halt during the downmelting of the glacier. The most prominent ice marginal position in north-eastern Germany is that of the Pomeranian phase.

Owing to the absence of recent geochronological data of the Weichselian ice advances, the commonly used ages of ice marginal positions are only estimates or are based on extrapolations from ^{14}C ages of underlying organic sediments. However, during the past few years a number of studies have been conducted to set up a chronology based on geochronometrical data. In this study fluvioglacial sediments from outwash plains associated with the Brandenburg phase and the Pomeranian phase were dated by means of Optically Stimulated Luminescence (OSL) of single aliquots and single grains of quartz. Recently, additional ages from Surface Exposure Dating (SED) of erratic boulders using cosmogenic ^{10}Be have been published. To compare the results from these different approaches, the type and position of the sampled material within the glacial landscape system have to be considered. Consequently, different geomorphological processes are datable using either OSL or SED techniques. Therefore a process-based interpretation for numerical ages from OSL and SED in glacigenic landscapes is introduced.

From the results of the OSL analyses from the Brandenburg and Pomeranian phases as well as a thorough reassessment of the available ^{10}Be exposure ages, a synthesis was achieved in terms of ice dynamics and ice retreat patterns during Marine Isotope Stage (MIS) 2. One of the main findings is the evidence for a twofold LGM, with the older phase (LGM-1) corresponding to the Brandenburg phase, which was dated to <34 ka (maximum age), and the younger phase (LGM-2) represented by the Pomeranian phase, which was dated to 20.1 ±1.6 ka (initial formation of outwash plains) and 19.4 ±2.4 ka (final sedimentation of sandur sediments).

The first Weichselian deglaciation pattern for north-eastern Germany was established, based on results from numerical dating methods, and the last glacial-interglacial cycle was dated for the first time from a terrestrial Saalian-Eemian-Weichselian sedimentary sequence in the research area.

Zusammenfassung

Die im Laufe der letzten 130 Jahre entwickelte Klassifikation für das weichselzeitliche Pleniglazial in Nordost-Deutschland basierte im Wesentlichen auf morphostratigraphischen Interpretationen. Im Allgemeinen werden drei Haupteisrandlagen unterschieden. Der Eisvorstoß zur südlichsten, relativ schwach entwickelten Eisrandlage der Brandenburger Phase wurde traditionell dem Last Glacial Maximum (LGM) des Skandinavischen Eisschildes (Scandinavian Ice Sheet, SIS) zugeschrieben. Die Frankfurter Phase wird in der Regel als Eishalt im Zuge des Zurückschmelzens der Gletscher gedeutet. Die am deutlichsten ausgeprägte Eisrandlage in Nordost-Deutschland ist die der Pommerschen Phase.

Aufgrund des Fehlens aktueller geochronologischer Daten für die weichselzeitlichen Eisvorstöße, sind die für den Raum gebräuchlichen Altersangaben nur Schätzungen oder basieren auf Extrapolation von ^{14}C Altern liegender organischer Sedimente. Im Laufe der letzten Jahre wurden jedoch mehrere Studien mit dem Ziel durchgeführt, eine Chronologie basierend auf geochronometrischen Daten zu entwickeln. Im Rahmen dieser Studie wurden glazifluviatile Sedimente von Sanderflächen der Brandenburger und der Pommerschen Eisrandlage mit Hilfe von Optisch Stimulierter Lumineszenz (OSL) an Aliquoten und Einzelkörnern aus Quarz datiert. Kürzlich wurden zusätzliche, auf Oberflächen-Expositionsdatierungen (Surface Exposure Dating, SED) mit Hilfe von kosmogenem ^{10}Be basierende Alter veröffentlicht. Um die Vergleichbarkeit der mit Hilfe dieser unterschiedlichen Verfahren gewonnenen Erkenntnisse zu gewährleisten, ist es notwendig, die Art und Lage des beprobten Materials im Kontext des glazialen Landschaftssystems zu berücksichtigen. Folglich können mit Hilfe von OSL- und SED-Verfahren unterschiedliche geomorphologische Prozesse datiert werden. Dementsprechend wurde ein prozessbasiertes Interpretationsverfahren für OSL- und SED-basierte, numerischer Alter in glazialen Landschaftssystemen entwickelt.

Basierend auf den Ergebnissen der OSL-Datierungen der Brandenburger und der Pommerschen Phase, sowie einer grundlegenden Neuinterpretation verfügbarer ^{10}Be-Alter, konnte eine Synthese in Bezug auf das Rückschmelzverhalten und die Eisdynamik im Marinen Isotopenstadium (MIS) 2 erzielt werden. Eine der wesentlichen Erkenntnisse ist der Nachweis eines zweifachen LGM. Die ältere Phase (LGM-1) entspricht der Brandenburger Phase, die auf <34 ka (Maximalalter) datiert wurde. Die jüngere Phase (LGM-2) entspricht der Pommerschen Phase, die auf 20.1 ±1.6 ka (initiale Bildung von Sanderflächen) bis 19.4 ±2.4 ka (letztmalige Sedimentation auf den Sanderflächen) datiert wurde.

Zusätzlich zur Einführung einer ersten Chronologie des weichselzeitlichen Eisrückzuges auf der Grundlage von numerischen Datierungsmethoden wurde im Untersuchungsgebiet erstmals der letzte Glazial-Interglazial-Zyklus an einer terrestrischen Sedimentabfolge, die saalezeitliche, eemzeitliche und weichselzeitliche Sedimente umfasst, datiert.

1. Introduction

Studies of past climate may help to improve knowledge of the forcing factors of climate change and the sensitivity of the earth's climate to these factors. Multiple evidence including geomorphological, sedimentological and palaeontological findings has proved that the climate of the earth was subject to permanent change. Today's measurements and observations substantiate the continuation of those fluctuations (IPCC, 2007). With regard to the current discussion about global warming and possible consequences such as sea-level rise and desertification, a thorough reconstruction of past climatic changes is essential. The analysis of amplitudes of fluctuations occurring in natural systems is a requirement in order to enhance understanding of the effects of man-induced changes. However, the available data especially from terrestrial archives are still scarce, and past climate system dynamics offer a challenge to scientific understanding.

Records of climatic change on regional scales are relevant because they represent individual components for reconstructing the complex patchwork of past global climate. This study intends to provide such a component and aims to contribute to the reconstruction of the timing and dynamics of the deglaciation of the last Scandinavian Ice Sheet (SIS) by Optically Stimulated Luminescence (OSL) dating of fluvioglacial (sandur) sediments related to main ice marginal positions (IMPs) in north-eastern Germany.

1.1. Aims of this study

The major aim of this study is to establish a reliable numerical chronology of the distinct Weichselian ice marginal positions in NE Germany. During the past 130 years the classification of the Weichselian Pleniglacial in north-eastern Germany has mainly been based on morphostratigraphical interpretations (cf. section 2). Owing to the absence of recent geochronological data of the Weichselian ice advances, the ages of ice marginal positions that are commonly used for that region are only estimates or based on extrapolations from ^{14}C ages from underlying organic sediments (cf. section 2.3.1). A reliable chronology of the Weichselian ice decay based on numerical ages is unfortunately still lacking (Terberger et al., 2004). International research has shown that the dynamics of the margin of the SIS during the Weichselian glaciation were highly variable in different regions (e.g., Marks, 2002). The uncertainties implied herein impede a simple correlation of ice marginal features from adjacent countries such as Denmark, Poland, and the Baltic States with those in NE Germany and the adaptation of their respective ages.

To achieve the geochronological aim of the study, Optically Stimulated Luminescence (OSL) dating techniques, primarily based on the single aliquot regenerative dose protocol (SAR) (Murray & Wintle, 2000, 2003; Wintle & Murray, 2006) for the dating of quartz, have been applied (cf. section 3.3). In contrast to ^{14}C dating, OSL enables the determination of depositional ages directly from glacial sediments. This geochronological aim consequently determines the methodological aims of this study, namely to enhance the application of OSL dating techniques to fluvioglacial (cf. section 1.2) sediments. This has previously been a challenging task, the major problem being the incomplete resetting of the OSL signal prior to deposition (cf. section

3.4). Another aim evolved during the progress of this study, as first results from surface exposure dating (SED) of erratic boulders from the research area became available. OSL and SED are the two most frequently used techniques for the dating of ice marginal positions. With comparable OSL and SED based ages available, this study aims to clarify the chances and limitations implied by either method with respect to the dating of ice marginal positions (cf. section 4).

1.2. Choice of the research area and representative sampling sites

To achieve geochronological significance, the appropriate choice of the research area in general and the sampling sites in particular is crucial. Within a glacial landscape that was formed and reshaped by multiple ice advances during the last three glaciation cycles (cf. section 2), the unambiguous assignment of glacial landforms to a specific ice advance remains challenging. However, in contrast to the Jutland peninsula (comprising Denmark and Schleswig-Holstein in Germany) and parts of Mecklenburg-Vorpommern, for example, the ice marginal positions of the Weichselian glaciation in Brandenburg are located well apart from each other (cf. section 2.2). In addition, this area has a long tradition of Quaternary research and was the type area where the glacial theory was established in Germany by the end of the 19th century. Brandenburg was therefore chosen as the general research area. Of the three main IMPs usually differentiated here, only two represent ice advances of the SIS (cf. section 2.2): the Brandenburg IMP and the Pomeranian IMP. The Frankfurt IMP is only weakly developed and is assumed to represent a halt in the downmelting of the SIS from the maximum extent of the Brandenburg phase and was therefore excluded from the investigations in this study. With the research area thus specified, the prerequisites implied by the dating method to be applied come into play. OSL dating of sediments enables the determination of the point in time when the sediments were last exposed to daylight (cf. section 3). In contrast to subglacially or englacially deposited sediments such as tills, subaerially deposited fluvioglacial sediments of outwash plains (sandar) are likely to have been exposed to daylight before burial. In addition, outwash plains are often found to be geared with terminal moraines and can therefore be assigned to specific ice marginal positions. Owing to the possibly longer transport distances, fluvioglacial sediments deposited within meltwater channels and ice marginal valleys (IMVs) may even have had a greater chance of having been properly exposed to daylight before burial than sandur sediments. However, the fact that the complex system of channels and IMVs drained meltwater originating from different IMPs impedes an unambiguous assignment of the sediments to a specific IMP. Hence, sandur sediments were identified as being most suitable to achieve the geochronological aims of this study. Sub-research areas and individual sampling sites were accordingly defined for the Brandenburg and Pomeranian IMPs (overview maps provided as appendices 13.2.1, 13.2.2 and 13.2.4). They are described in detail in section 2.4 and in the individual research papers (sections 5, 6, 8, 9).

To be able to crosscheck the OSL ages obtained with an independent age control, an additional sampling site had to be identified. Unfortunately, a suitable section within the age

range of radiocarbon dating was not available. Accordingly, a sampling site offering age control from results of plalynological analyses was chosen (cf. section 2.4). Additionally, the sediments exposed there gave the opportunity to enhance understanding of the development and deglaciation history of the adjacent Oderbruch basin.

1.3. The structure of this cumulative paper

The results from this study have already been published as research papers in international, peer-reviewed scientific journals. Following a general introduction of the research area and the individual sampling sites, as well as an introduction to OSL dating in general and the SAR protocol for the dating of quartz in particular, these individual research papers will therefore be presented in this cumulative paper as they have been published. The respective chapters will be indicated and a link to the latest online version of the published articles will be provided. Any reproduction of these chapters requires the agreement of the respective copyright owners. However, the structure of this cumulative paper and the order of presentation of the individual articles guarantees a self-contained and comprehensive presentation of the research conducted in this study. In addition to the already published work, new analyses and results are also presented, discussed and incorporated into the overall conclusions.

2. Research area

This section provides a general overview of the geomorphology, stratigraphy and chronology of the research area situated in Brandenburg, north-eastern Germany (Figure 01, appendix 13.2.1), and briefly introduces the different sampling locations. A differentiated description of the sites is provided within the different research papers (cf. sections 5, 6, 8, 9).

2.1. Pre-Weichselian Quaternary history of north-eastern Germany

The base of the Quaternary sediments in north-eastern Germany is characterised by a system of NE-SW oriented channels deeply incised (~200 m on average, max. 500 m below sea level) into the pre-Quaternary subsurface. The formation of these channels by subglacial meltwaters is assumed to have set in during the downmelting of the first ice advance of the Elsterian glaciation (Lippstreu, 1995) and continued during the second Elsterian ice advance. By the end of the Elsterian glaciation the channels were completely filled with glacial sediments. A possible influence on recent morphology can therefore be excluded. The Elsterian glaciation is tentatively correlated with Marine Isotope Stage (MIS) 10 (Litt et al., 2007). During the subsequent Holsteinian interglacial, fluvial and limnic processes prevailed in the young morainic landscape formed by the Elsterian glaciation. On the basis of results from ^{230}Th/U dating of peat, Geyh & Müller (2005) correlate the Holsteinian interglacial with MIS 9. However, the results from this study have been controversially discussed (Scourse, 2006; Geyh & Müller, 2006). A succession of alternating cold and warm phases marks the beginning of the subsequent Saalian complex (Litt et al., 2007). Krbetschek et al. (2008)

Figure 01: North-eastern Germany and neighbouring areas of Denmark and Poland (light grey); administrative areas of Brandenburg (grey) and Berlin (dark grey).

Main Weichselian ice marginal positions according to Liedtke (1981): W_2 – Pomeranian phase (green line), W_{1F} – Frankfurt recessional phase (dashed blue line), W_{1B} – Brandenburg phase (red line).

Sampling sites: 1 Luckenwalde (LUC-I,II), 2 Frankenfelde (LUC-III), 3 Beelitz (BEE), 4 Vevais (VEV), 5 Eberswalde (EBE), 6 Macherslust (MAC), 7 Althüttendorf (ALT-I,II)

successfully dated fluvial sediments from this so-called Lower Saalian (Ehlers et al., 2004) using infrared radio-fluorescence (IR-RF; Trautmann et al., 1999; Krbetschek et al., 2000) and conclude that the period spanned the time from ~300 ka to ~150 ka. Two major ice advances occurred during the Saalian complex: the older ice advance of the Drenthe stadial and that of the Warthe stadial. Both are correlated with MIS 6 (Litt et al., 2007). Geomorphological and stratigraphical evidence suggests that, as a consequence of the interaction of a highly dynamic advancing ice sheet with the young

morainic topography shaped during the preceding Drenthe stadial, glacitectonic processes and formation of push morainic areas primarily took place during the Warthe stadial (Lippstreu, 1995). However, the maximum extent of the SIS during the Saalian did not reach as far south as during the Elsterian (Figure 02). Taking into account the age of ~150 ka as the upper boundary of the Lower Saalian reported by Krbetschek et al. (2008), as well as the onset of the subsequent Eemian interglacial at ~130 ka, the Upper Saalian (Ehlers et al., 2004) might only have spanned roughly 20 ka. Eemian deposits, mostly limnic sediments recovered from drilling cores, have frequently been identified within the research area. Hermsdof & Strahl (2008) have recently compiled all recorded occurrences and the results from related palynological analyses of Eemian sediments in Brandenburg. The correlation of the Eemian interglacial with MIS 5e has been widely accepted in scientific discourse throughout the past few years (summarised in Brauer et al., 2007).

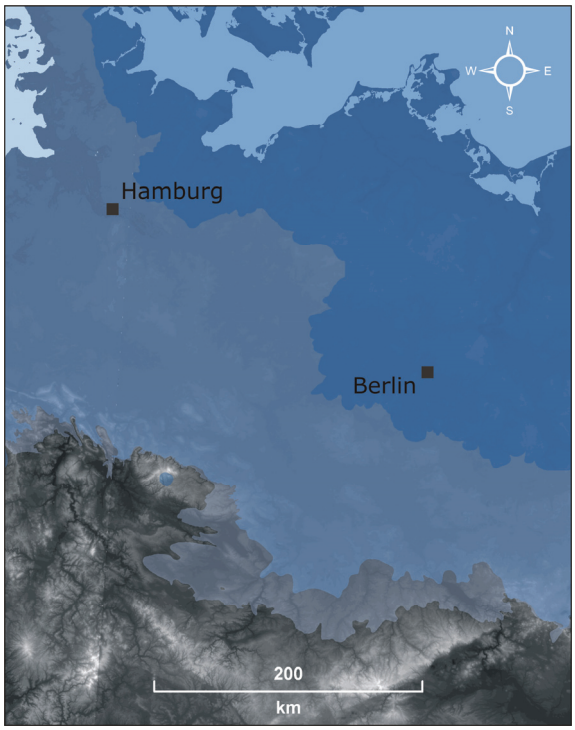

Figure 02: Maximum extents (from south to north) of the Elsterian (light blue), Saalian (blue) and Weichselian (dark blue) glaciations in north-eastern Germany and neighbouring areas (data provided by Ehlers & Gibbard, 2004). Figure based on a digital elevation model (DEM) derived from hole-filled seamless SRTM data (processed by Jarvis et al., 2006).

2.2. The Weichselian cold stage in north-eastern Germany

Like the Saalian, the onset of the Weichselian cold stage was also characterised by alternating cold and warm phases. Glacitectonic and lithological evidence reported from Denmark (e.g., Houmark-Nielsen, 2007) indicates that a first advance of the Scandinavian Ice Sheet (SIS) through the Baltic Sea basin might already have occurred in MIS 4. Corresponding fluvioglacial inter-till deposits have recently been dated to ~50 ka (MIS 3; Houmark-Nielsen, 2007) by means of quartz OSL. Although it has been proposed that several localities along the Baltic Sea coast of Mecklenburg-Vorpommern represent such an early ice advance, up to now no clear evidence supports such an assumption. In general, three main Weichselian ice marginal positions are usually distinguished in north-eastern Germany (Figure 01), but only two are assumed to represent ice advances (compare 2.2.1 & 2.2.2). The Brandenburg ice marginal position (IMP) represents the southernmost extent of the Weichselian glaciation in the research area (W_{1B}), situated well north of the maximum extent of the previous glaciations (Figure 02). It is followed to the north by the Frankfurt IMP (W_{1F}) and the Pomeranian IMP (W_2). Based on the conceptual model of the “Glaziale Serie” (glacial series - typical sequence of geomorphological units formed at a stationary ice margin) of Penck (1879), this pattern of ice

marginal positions was named and thereby established by Woldstedt in 1925 already, shortly after Keilhack (1910) finally established the concept of polyglaciation in northern Germany primarily introduced by Penck in 1879. Woldstedt's pattern was solely based on morphostratigraphical findings and implied a deglaciation chronology with the southernmost IMP representing the oldest ice advance and a succession of constantly younger IMPs northward towards the Baltic Sea basin. This includes not only the three main IMPs depicted in figure 01, but also a complex pattern of intermediary systems of recessional terminal moraines, which have been controversially discussed within scientific discourse (e.g., Böse, 1994, 2005). This introduction will therefore focus on the three main ice marginal positions as stated above.

2.2.1. Brandenburg (W_{1B}) and Frankfurt (W_{1F}) phase

Ice marginal positions related to the Brandenburg and Frankfurt phase are relatively weakly developed and have mainly been reconstructed along ridges of outwash plains (sandar). Terminal moraines (mainly consisting of meltout till) or even pushmoraines only rarely occur in the Brandenburg IMP and are almost absent in the Frankfurt IMP. This implies a presumably rapid and short-lived ice advance that adapted to the morphology inherited from the penultimate glaciation. Within the research area, push morainic complexes originating from Saalian times are known to have been preserved in some places (Böse, 2005). The ice advance to the southernmost Brandenburg IMP has traditionally been ascribed to the LGM as reconstructed from marine and ice core data. The area between the Brandenburg IMP and the Pomeranian IMP (encompassing the Frankfurt IMP) is dominated by fluvioglacial deposits and landforms as well as dead ice topography. Kames and minor outwash plains frequently occur, but can hardly be assigned to specific IMPs (Böse, 2005). The Frankfurt IMP is considered to represent a halt in the course of the downmelting of stagnant or even dead ice related to the ice advance to the Brandenburg IMP (Lippstreu 1995; Böse, 2005; Litt et al., 2007). The area south of the Pomeranian IMP is furthermore characterised by intensive fluvioglacial erosion related to the development of a complex system of ice marginal valleys (IMV, "Urstromtäler") and interconnecting meltwater channels. Specific IMVs have frequently been assigned to specific IMPs: Glogau-Baruth IMV & Brandenburg IMP, Warsaw-Berlin IMV & Frankfurt IMP, Thorun-Eberswalde IMV & Pomeranian IMP. However, the drainage of meltwater has been shown to be highly complex (e.g., Juschus, 2001) and IMVs and meltwater channels were still in use even when the SIS had already retreated north of the Pomeranian IMP.

2.2.2. Pomeranian (W_2) phase

The ice marginal position formed during the Pomeranian phase shows the most prominent terminal moraines in north-eastern Germany and represents a strong readvance of the SIS (Böse, 2005). It is still a matter of discussion how far north the SIS retreated prior to the Pomeranian phase. Most authors (e.g., Lippstreu, 1995; Böse, 2005) favour a retreat back into the Baltic Sea basin, whereas others (e.g., Kliewe & Jahnke, 1972; Liedtke, 2001) argue that there was no evidence for an interstadial between the $W_{1B/F}$ and the W_2 phases, and the SIS ice margin therefore must

have remained south of the Baltic Sea basin. Towards the end of the Weichselian glaciation the SIS retreated further north, with various oscillations and readvances (the most prominent of which occurred during the Mecklenburg phase, forming the terminal moraines of the Rosenthal and Velgast IMPs) documented by ice marginal features north of the Pomeranian IMP (Böse, 2005).

2.3. The late Weichselian

The late Weichselian is again characterised by alternating cold and warm phases. It marks the retreat of the SIS to the north of the Baltic Sea depression. Preusser (1999) dated kame sediments from the decaying ice of the Mecklenburg phase in the Lübeck bay to ~15 ka, using green light stimulated luminescence (GLSL) and thermoluminescence (TL) techniques. By the time of the Younger Dryas cooling, active glaciers of the SIS had retreated to the north of the Baltic Sea depression and formed the Salpausselkä IMP. The latter was dated to ~11.5 ka by means of SED of erratic boulders by Tschudi et al. (2000). During the late Weichselian, periglacial and aeolian processes prevailed in north-eastern Germany. The melting of buried dead ice had significant influence on the topography as soon as kettle holes and subglacial channels evolved at the surface. In general, limnic and/or organic sedimentation within these depressions did not set in before the Bölling interstadial (Böse, 2005).

2.3.1. Geochronology of the main Weichselian IMPs

The available geochronometrical data for the main ice marginal positions were recently reviewed by the German Stratigraphic Commission (Litt, 2007). Table 01 shows a summary of the relevant data. However, that chronology is solely based on extrapolations of ^{14}C ages and on estimates. It represents the status quo of the time when this study was initiated. In the course of this study additional ages became available, derived from surface exposure dating (SED) of erratic boulders from north-eastern Germany (Heine et al., 2009; Rinterknecht et al., in press). They are discussed in detail in the research paper dealing with the age of the Pomeranian IMP (section 9). A reinterpretation of these SED ages is also included in the summarising discussion (cf. section 11).

Table 01: ^{14}C based chronology of the main IMPs in NE Germany*

IMP	Age**	Method
Brandenburg (W_{1B})	~20 ka BP	Estimate[1]
	<24 cal. ka BP	^{14}C[2]
Frankfurt (W_{1F})	~18.8 ka BP	Estimate[3]
	<23.8 cal. ka BP	^{14}C[4]
	<32 cal. ka BP	^{14}C[5]
Pomeranian (W_2)	~16.2 ka BP	Estimate[6]
	<17.6 cal. ka BP	^{14}C[7]

[1] Cepek (1965), Liedtke (1981), Kozarski (1995)
[2] Age of organic sediments underlying glacial sediments of the Brandenburg phase (Marks, 2002).
[3] Age extrapolated from underlying ^{14}C ages, assuming an estimated rate of ice build-up and decay Kozarski (1995).
[4] Age of organic sediments underlying glacial sediments of the Poznan (Frankfurt) phase near Konin, Poland (Marks, 2002).
[5] Age of an organic silt layer ("Mudde vom Segrahner Berg") underlying glacial sediments of the Frankfurt phase (Lüttig, 2005).
[6] Age extrapolated from underlying ^{14}C ages, assuming an estimated rate of ice build-up and decay Kozarski (1995).
[7] Age of organic sediments (Liedtke, 1996; Marks, 2002), origin and stratigraphical position unclear from primary sources.

* Summarised from Litt et al. (2007), no age uncertainties specified.
** Calibration of ^{14}C ages according to Stuiver et al. (1998) by Litt et al. (2007).

2.4. Sampling sites

As outlined in section 1.2, the dating efforts within this study were concentrated on the two main ice marginal positions in north-eastern Germany representing advances of the SIS, namely the Brandenburg and the Pomeranian IMPs, with an additional sampling location offering a crosscheck of the obtained OSL ages with independent age control. Possible sampling locations had to enable access to fluvioglacial (sandur) sediments suitable for OSL dating with an unambiguous assignment to a specific IMP. A section from the Beelitz outwash cone to the terminal moraine and outwash plain near Luckenwalde was chosen to represent the Brandenburg IMP within this study (Figure 03). Three suitable sampling sites were identified within this area: an abandoned gravel pit near Beelitz and the active gravel pits near Frankenfelde and Luckenwalde. A section from the Althüttendorf outwash cone to the western boundary of the Oder valley was chosen to represent the Pomeranian IMP (Figure 04), and the Althüttendorf gravel pit, an abandoned clay pit near Macherslust and the Klosterbrücke outwash fan were identified as suitable sampling sites. A sediment succession encompassing glaciofluvial to fluvial sediments as well as limnic sediments exposed near the village of Vevais provided the only chance to crosscheck the obtained OSL ages with an independent age control. Palynological analyses allow a secure classification of the limnic sediments as being of Eemian origin. Table 02 provides the exact position of each of the mentioned sites. Additionally, the names of the locations are linked to the sample codes used within this study. The maps provided as appendices 13.2.1, 13.2.2 and 13.2.4 show the position of the sampling locations within their regional context and provide a simplified overview of the main geomorphological features of the respective region. Detailed descriptions of the different sites are available within the related articles (links see table 02). In addition, excerpts from the geological survey map (GÜK 200) are provided as supplementary material (appendices 13.2.3 & 13.2.5). Furthermore, detailed excerpts from topographical maps (TK25) and geological maps (GK25) are provided for each sampling site (appendices 13.2.7-13.2.20).

Table 02: Sampling locations

Name	Sample code	Related IMP	UTM* coordinates	Altitude a.s.l. (m)	Related article
Althüttendorf	ALT_I	W_2	33N 424235 5868772	70	Section 9
	ALT_II	W_2	33N 424060 5868389	70	Section 9
Beelitz	BEE	W_{1B}	33N 359294 5795101	70	Section 5
Eberswalde	EBE	W_2	33N 426814 5856926	42	Section 9
Frankenfelde	LUC_III	W_{1B}	33N 372165 5774668	68	Section 6
Luckenwalde	LUC_I	W_{1B}	33N 372881 5772414	72	Section 6
	LUC_II	W_{1B}	33N 372916 5772535	72	Section 6
Macherslust	MAC	W_2	33N 421750 5855962	60	Section 9
Vevais	VEV	n/a	33N 441648 5838632	30	Section 8

* Universal Transverse Mercator (UTM) projection, zone 33N.

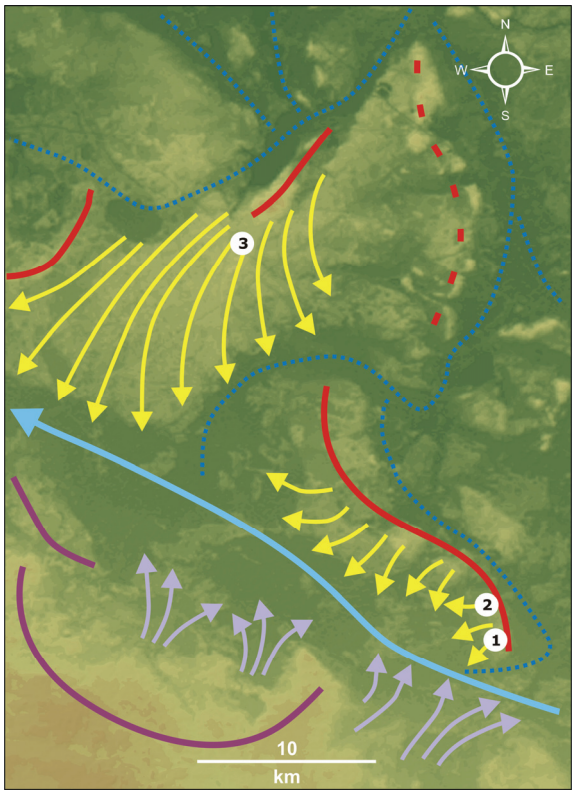

Figure 03: Simplified geomorphological overview of the W_{1B} research area: Outwash plains (yellow arrows), Brandenburg IMP (red line), Glogau-Baruth IMV (light blue arrow), fluvioglacial channel system (broken dark blue lines), periglacial valley incision and formation of outwash fans (grey arrows), Saalian push moraines (purple lines). Sampling locations: Beelitz (1), Frankenfelde (2), Luckenwalde (3).

Figure based on a digital elevation model (DEM) derived from hole-filled seamless SRTM data (processed by Jarvis et al., 2006).

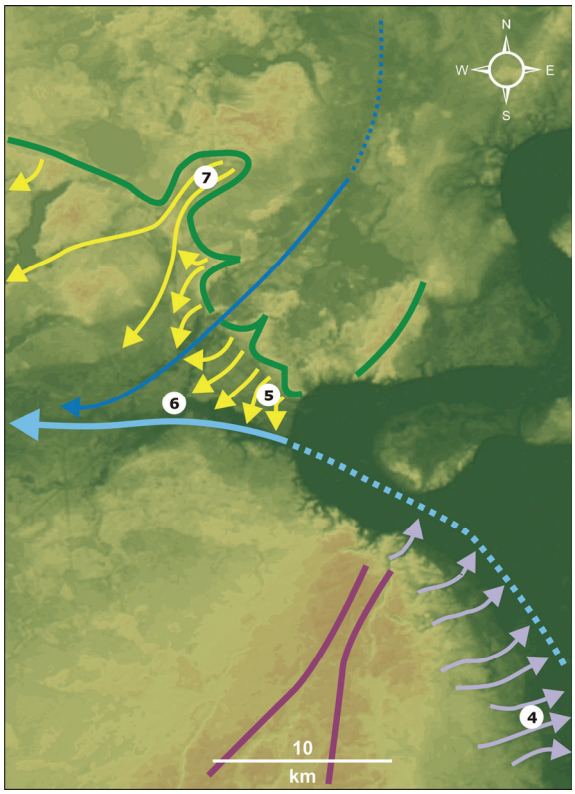

Figure 04: Simplified geomorphological overview of the W_2 research area: Outwash plains (yellow arrows), Pomeranian IMP (green line), Thorun-Eberswalde IMV (light blue arrow), meltwater of recessional phases intersecting the Pomeranian IMP at Chorin (dark blue arrow), periglacial valley incision and formation of outwash fans (grey arrows), interlobate Saalian push moraines (purple lines). Sampling locations: Vevais (4), Eberswalde (5), Macherslust (6), Althüttendorf (7).

Figure based on a digital elevation model (DEM) derived from hole-filled seamless SRTM data (processed by Jarvis et al., 2006).

In the following please also see figure 03 and appendices 13.2.2 & 13.2.3. The Beelitz sampling site is situated on the Beelitz outwash cone, which dips over a distance of ~14km from its inner fringe towards the Baruth ice marginal valley. It has been described as a type region of the Brandenburg ice marginal position (Böse, 2005). A complex system of meltwater channels connected to the Baruth ice marginal valley divides the Brandenburg IMP east of the Beelitz outwash cone into separate “islands” consisting mainly of fluvioglacial sediments. The gravel pits near Frankenfelde and Luckenwalde are both situated on the southernmost of these elevations. Here the small outwash plain of Luckenwalde dips southwest over a distance of ~2 km from its peak elevation towards the Baruth IMV. South of the Baruth IMV, push morainic complexes of the Saalian glaciation form the southern margin of the Fläming upland, part of the old morainic landscape.

In the following please also see figure 04 and appendices 13.2.4 & 13.2.5. The sampling site near the village of Vevais is part of the “Wriezener Terrasse”, an elevated level of discharge on the western border of the

Oderbruch basin formed during the existence of a Thorun-Eberswalde ice marginal valley. Near Oderberg, the Pomeranian IMP was intersected by fluvial erosion of the Oder river. From Oderberg the Pomeranian IMP continues to the north-west, with its course revealing the lobate character of the ice sheet. The Althüttendorf outwash cone was deposited in an interlobate position. Nowadays one of the largest gravel pits in Brandenburg is situated on the outwash cone, granting excellent access to the sandur sediments. The small “Klosterbrücke” outwash cone marks the latest sandur formation attributed to the Pomeranian IMP. By contrast, the sediments exposed within the abandoned clay pit near Macherlust are related to meltwater discharge from IMPs north of the Pomeranian terminal moraines.

2.5. Sampling for OSL dating

The OSL samples for this study were collected using the equipment shown in figure 05. Opaque plastic tubes of about 20 cm length and 6 cm diameter were driven into the freshly cleaned sediment face (Figure 06). Under darkroom conditions the light-exposed parts of the samples (inner front and back part of the sampling cylinders) were removed and used to determine in situ and saturation water content. Additional samples for radionuclide analyses were taken from the direct surroundings of the OSL samples. Pure quartz grains were extracted for the OSL measurements using a procedure of sieving, H_2O_2 and HCl treatment (removal of organics and carbonates), feldspar flotation (separation of feldspar contaminants), density separation (2.62–2.67 g/cm^3), HF/HCl etching (removing the outer ~10 µm of the grains affected by alpha radiation (Mejdahl and Christiansen, 1994), and final sieving. A summary of the basic luminescence sampling and preparation procedures is provided by Preusser et al. (2008).

Figure 05: OSL sampling equipment consisting of an opaque plastic tube equipped with cutter (top), opaque plastic caps to seal the tube after sampling (middle) and soft hammer for driving the tube into the sediment (bottom).

Figure 06: The author taking an exemplary sample (not dated) in the Althüttendorf gravel pit, June 2007; photo taken by Dirk Wenske.

3. Optically stimulated luminescence (OSL) dating of quartz

Luminescence dating techniques make it possible to determine when sediments were last exposed to daylight throughout a transportation event before subsequent burial and therefore the time of sealing from daylight within a sedimentary archive. Whereas the specific sample preparation techniques, measurement procedures and evaluation techniques are described in detail in the research papers, this section provides a short introduction to the basic principles of luminescence dating in general and the Single Aliquot Regenerative (SAR) dose protocol for the dating of quartz developed by Murray and Wintle (2000, 2003; reviewed in Wintle & Murray, 2006), which was used for the major part of the dating work in this study in particular. Additionally, the basic problem of incomplete resetting of the OSL signal (also termed incomplete bleaching) and the different approaches developed in order to overcome this problem in OSL dating are introduced.

3.1. Basic principles of luminescence dating

Luminescence dating techniques are based on the nature of non-conductive minerals such as quartz or feldspar that store measurable radiation damage within their crystal lattices (Bøtter-Jensen et al., 2003b). Ionising radiation caused by the decay of naturally occurring radionuclides (^{40}K, ^{87}Rb) and radioactive series (^{235}U, ^{238}U and ^{232}Th) as well as cosmogenic radiation has the effect that excited charge carriers are trapped in deficiencies within the crystal lattice and are stored in these luminescence traps for geologically relevant periods of time (Figure 07, a/b). As the number of trapped charge carriers correlates with the stored energy per mass unit [J/kg = Gy], the mineral grains function as natural dosimeters. Once stimulated by light or heat (input of energy), trapped electrons recombine with defects within the crystal lattice functioning as luminescence centres (Figure 07, c/d). That recombination process causes a light glow (luminescence). The intensity of that signal is a measure for the amount of energy stored within the crystal (Bøtter-Jensen et al., 2003b;

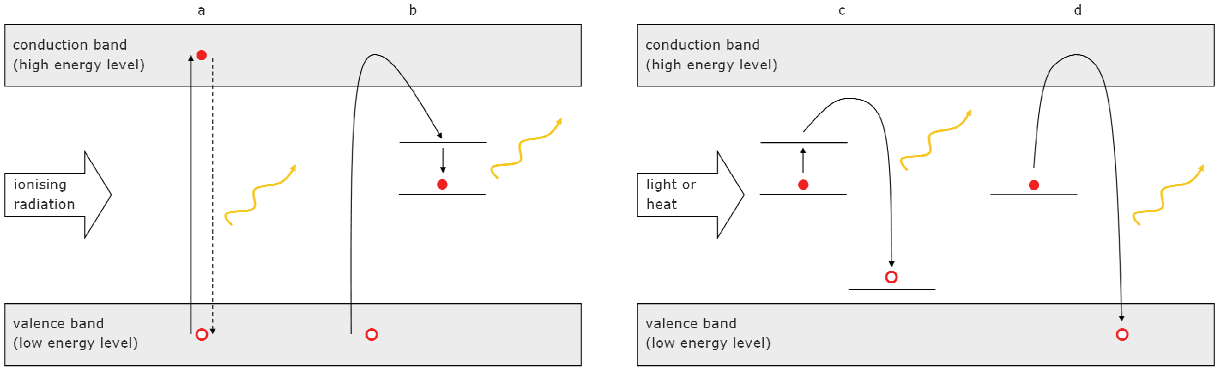

Figure 07: A valence electron is excited by ionising radiation and is transferred to a higher energy level (conduction band), leaving a hole in the valence band (a/b). Most excited electrons instantly recombine with a hole in the valence band and dissipate their energy in the course of that process which is sometimes accompanied by photon emission (a). Only few excited electrons transition to localised energy states below the conduction band (b). This electron trapping creates a latent luminescence signal. Stimulation of the trapped electrons by light or heat empties the traps. Electrons might either recombine with holes above (c) or within (d) the valence band, either transitioning an unstable level below the valence band (c) or directly via the valence band (d). In the course of that recombination process energy loss might be released in the form of light (luminescence). Figure based on and modified from Bøtter-Jensen et al. (2003b), Preusser et al. (2008).

Preusser et al., 2008). Once the rate of stored energy per time is known [Gy/ka], it is possible to calculate the time elapsed since the crystal was last exposed to daylight. This can be described as a general age equation:

$$age\left[ka\right] = \frac{equivalent\ dose\left[Gy\right]}{dose\ rate\left[Gy/ka\right]}.$$

The increase of the latent luminescence signal stored within the crystal lattice over time is limited by the number of available traps and will therefore reach a saturation dose. In contrast to the simplified model (Fig. 07), different types of traps and recombination centres exist within natural minerals. Depending on the depth of the trap (with shallow traps not suitable for dating purposes at all because electrons do not necessarily remain captured within such traps), different amounts of energy are required to stimulate the recombination process. The emission of a luminescence signal can be stimulated in different ways, e.g., by heat (Thermally Stimulated Luminescence – TL), visible light (Optically Stimulated Luminescence – OSL), or infrared light (Infrared Stimulated Luminescence – IRSL). Comprehensive summaries of the development of the different luminescence techniques and recent new approaches are provided, e.g., by Lian & Roberts (2006) and Wintle (2008b). Whereas luminescence dating of sediments was initially conducted using TL techniques (e.g., Wintle & Huntley, 1979), the 1980s saw the introduction of optical dating techniques (OSL (Huntley et al., 1985) and IRSL (e.g. Hütt et al., 1988)), which brought about a ground-breaking approach for the dating of sediments. Only optically sensitive traps are used to determine the equivalent dose, which has the advantage that these are more quickly and more thoroughly bleachable than thermally sensitive traps (Godfrey-Smith et al., 1988). This is essential for dating sediments prone to insufficient bleaching because possible overestimations of equivalent dose and subsequently of age are minimised.

3.2. Determination of dose rate

To achieve a precise age, apart from the equivalent dose, the dose rate within the sediments must also be precisely determined. Three types of naturally occurring ionising radiation have to be taken into account for the calculation of the dose rate for luminescence dating: cosmic radiation (from space), external radiation (from neighbouring grains) and internal radiation (from within the grains). The cosmic radiation can be calculated with regard to geographical position (intensity increasing polewards), altitude (intensity increasing with altitude) and overburden (by sediment and/or water; shielding effect increasing with overburden thickness). External radiation from ^{40}K and the decay chains of ^{235}U, ^{238}U and ^{232}Th consists of α-radiation (range about 20 µm), β-radiation (range about 2 mm) and γ-radiation (range about 30 cm) occurring within the sediment body (Preusser et al., 2008). For the calculation of the external dose rate, the moisture content (average water content since deposition) of the sediment is of great importance because the attenuation of ionising radiation is much greater when the sediment pores are filled with water rather than air. Internal radiation is caused by the presence of radioactive elements within the crystal lattice of minerals. In alkali feldspars it mainly consists of β-radiation from ^{40}K; in quartz the contribution

of internal radiation to the overall dose rate is usually considered to be negligible.

Within this study, the external radiation was determined by high resolution gamma spectrometry (Aitken 1985, DeCorte et al. 2004, Krbetschek et al. 1994, Lang et al. 1996, Preusser & Kasper 2001, Wagner, 1998) of bulk samples from the direct surroundings of the OSL samples. In order to take the gradient of deposition of energy into account, coarse grain (90-160 µm and 200-250 µm) samples for luminescence dating were prepared as carbonate and organic free mineral separates. The outer layer affected by alpha radiation was removed by etching of the grains (Mejdahl & Christiansen, 1994). The α-radiation component could therefore be neglected in age calculations. The overall dose rate was calculated using the software ADELE (Kulig, 2005), which was also used for the final age calculations.

3.3. Determination of equivalent dose using the SAR protocol

To determine the equivalent dose, the natural luminescence signal is compared with that of laboratory irradiated subsamples (aliquots). Apart from the classic multiple aliquot techniques, single aliquot techniques have been established since the 1990s. Here all measurement steps necessary to determine the equivalent dose are conducted using the same aliquot. In contrast to multiple aliquot techniques, the equivalent dose of a large number of single aliquots can be determined, which significantly reduces the measurement error. Different approaches using single aliquots have been put forward, but nowadays the Single Aliquot Regenerative (SAR) protocol of Murray and Wintle (2000, 2003; Wintle & Murray, 2006) has been established in luminescence dating laboratories worldwide and is constantly being refined and enhanced. For the dating of sediments prone to incomplete bleaching, the use of quartz grains is preferred as opposed to feldspar because the OSL signal of quartz bleaches faster than that of feldspar. In addition the OSL signal from feldspar is known to show anomalous fading, a loss of OSL signal over time (Wintle, 1973). Although different methodological approaches have been developed to solve it (Huntley and Lamothe, 2001; Auclair et al., 2003; Tsukamoto et al., 2006; Thomsen et al., 2008), that problem has not yet been overcome. Therefore, quartz SAR OSL measurements were used as the standard technique within this study. Only in one case were feldspar measurements successfully conducted in order to overcome dose rate related problems (Section 8).

Table 03: Generalised SAR protocol*

Step	Treatment	Observe
1	Give dose[a], D_i	-
2	Preheat (160-300°C for 10 s)	-
3	Stimulation with blue LEDs for 40 s at 125°C	L_i [b]
4	Give test dose, D_T	-
5	Cutheat (160-300°C)	-
6	Stimulation with blue LEDs for 40 s at 125°C	T_i [b]
7	Start from top	-

[a] For the first cycle (natural sample) i=0, D_0 is the natural dose.
[b] The observed luminescence signals for L_i and T_i are derived from the stimulation curve.

* Based on Murray & Wintle (2000, 2003), modified from Wintle & Murray (2006)

Table 03 shows a basic SAR sequence after Murray and Wintle (2000, 2003) used to derive a dose response curve as shown in figure 08. The assumptions underlying the SAR

procedure have been summarised in detail by Wintle and Murray (2006). The basic principle can be described as follows: each OSL measurement is preceded by a preheating step in order to empty shallow, unstable luminescence traps (step 2). In the first SAR cycle the natural luminescence signal corresponding to the natural dose (D_0) is measured. In subsequent SAR cycles the aliquot is given known doses (step 1) and the corresponding luminescence signal is measured (step 3). After each luminescence measurement a test dose which remains constant throughout all SAR cycles is given to the aliquot (step 4). After another preheating step (termed cutheat, step 5) the luminescence signal corresponding to the given test dose is measured (step 6). This allows for the correction of possibly occurring sensitivity changes due to the repeated stimulation and irradiation of the aliquot. The measurement cycle is repeated for multiple known doses. Finally, a dose response curve can be fitted to the individual L_i / T_i values for the known dose points and allows for the determination of the equivalent dose (D_e) of the natural OSL signal (figure 08).

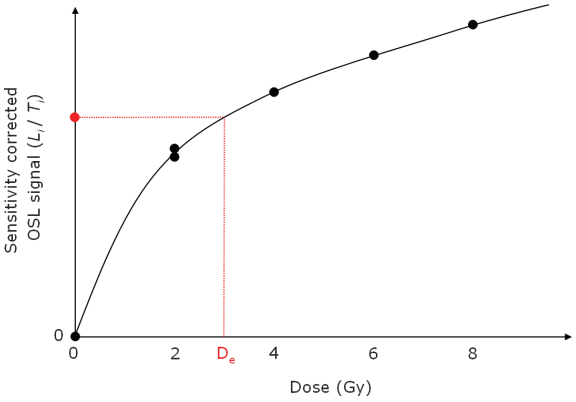

Figure 08: Idealised dose response curve for a SAR protocol with 7 cycles including recycling point (2 Gy) and zero point. In this example, the natural OSL signal corresponds to a D_e of ~3 Gy.

Two quality checks are incorporated into the SAR sequence: tests for recuperation and recycling. Recuperation is expressed as a fraction of the OSL response to a given zero dose. In an ideal case, recuperation should be zero. To be able to calculate the recycling ratio, the OSL response to an identical dose is measured twice. The quotient of the repeated measurements should equal one in an ideal case. As a guideline, deviations of recuperation values up to 0.05 and deviations of 5% from unity for recycling ratios are regarded as acceptable (Murray & Wintle, 2000). Aliquots exceeding these threshold values should be discarded from further calculations.

To test the suitability of a SAR protocol for specific samples, dose recovery tests have to be conducted. Here, a number of aliquots is artificially bleached (luminescence signal is set to zero) in the laboratory and subsequently given a known dose. The dose is then measured by applying a SAR protocol as described above. The equivalent dose calculated from the SAR measurements should ideally equal the dose given to the aliquots prior to the SAR measurements (corresponding to a measured/given dose ratio of 1; Wintle & Murray, 2006).

Additional quality tests and rejection criteria (e.g., tests for feldspar contamination, IR depletion ratio cf. Duller, 2003) were applied in the course of the OSL measurements conducted for this study. These criteria are described in detail within the different research papers. The Software Analyst (Duller, 2007) was used for the evaluation of all SAR data. Finally, the “true” equivalent dose of a sample can be derived from the dose distributions of the individual D_es obtained from the individual aliquots. Once the dose rate is also known, a

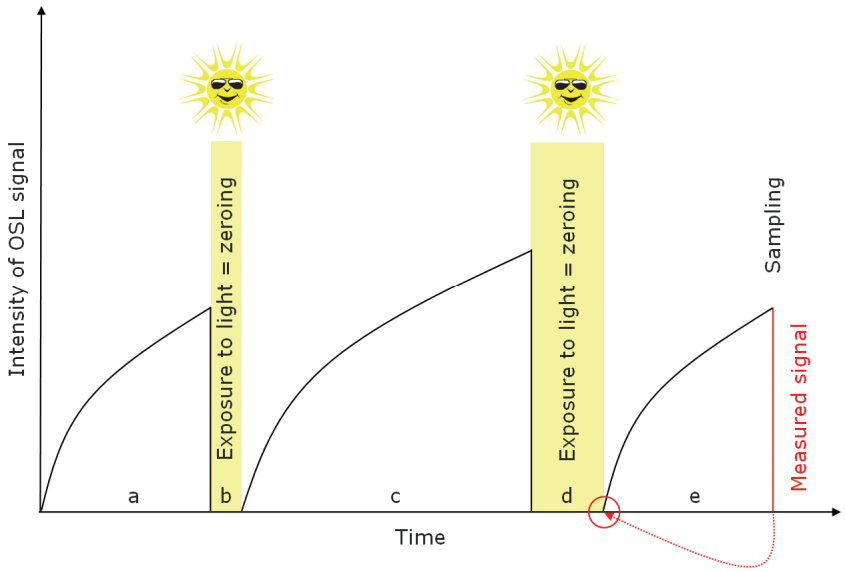

Figure 09: Once buried, the OSL signal within sediments starts to grow (a, c, e) until mobilisation and exposure to daylight during transport events (b, d). Sufficient sunlight exposure completely resets the accumulated OSL signal during transport (b, d). The OSL signal measured for a completely bleached sample therefore corresponds to the age of the last depositional event (d/e).

depositional age can be calculated by applying the general age equation as stated above. Dose distributions of well bleached sediments ideally show a tight normal distribution and the "true" D_e is determined by calculating a central mean value. The Central Age Model (CAM) developed by Galbraith et al. (1999) is most commonly used for these calculations.

3.4. Incomplete resetting of the OSL signal

Incomplete resetting (bleaching) of the OSL signal occurs whenever sediments are not exposed to sufficient daylight during transport events. The chance of insufficient resetting of the OSL signal to occur during transport is highly dependent on the depositional environment. Whereas aeolian sediments are generally regarded as thoroughly bleached (Figure 09), waterlain sediments in general (e.g., Juyal et al., 2006; Wallinga, 2002; Olley et al., 1998) and especially fluvioglacial (sandur) sediments (e.g., Thrasher et al., 2009 and references cited therein) have frequently been shown to be prone to incomplete bleaching (Figure 10) due to cloudy meltwaters, high sedimentation rates and short transport distances. Various approaches have been proposed to detect and correct for incomplete bleaching, either conducting comparative measurements, investigating properties of the luminescence signal itself, or analysing D_e distributions obtained from SAR measurements. Table 04 provides a condensed summary of the major approaches and gives reference to key publications. The detailed application of these methods within this study is described in the respective research papers (cf. sections 4, 5, 6, 8, 9). Comprehensive overviews are provided in Fuchs & Owen (2008) and Thrasher et al. (2009).

The OSL signal derived from single aliquots is always an averaged signal consisting of the individual luminescence signals from individual grains. By using a fine to medium sand sized fraction of quartz grains, the number of grains per aliquot can be controlled, enabling the measurement of small aliquots or even single grains. Because only a small proportion of

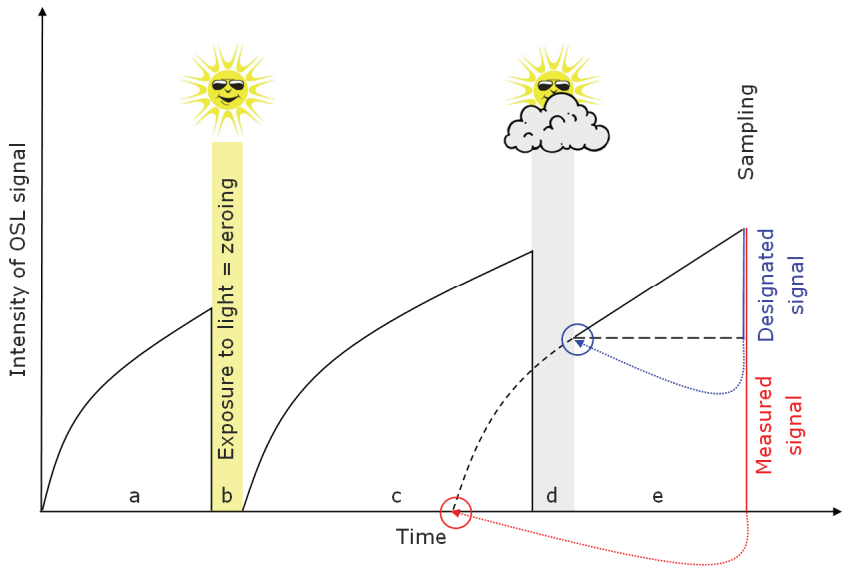

Figure 10: Sufficient exposure to daylight during transport completely zeroes the OSL signal accumulated during phases of burial (a/b/c). However, sediment grains may not be exposed to sufficient daylight during transport (d) and the OSL signal may not be completely zeroed. In that case an unknown residual is added to the OSL signal accumulated since the last depositional event (designated signal corresponds to depositional event d/e). The measured OSL signal is significantly higher, which causes significant age overestimation.

grains (usually 5-10%) emits a luminescence signal at all, Duller (2008) suggests reducing the aliquot size for the dating of sediments probably affected by incomplete bleaching. The resulting reduction of the number of grains per aliquot (eventually down to the single grain level, figure 11) has the effect that the measured OSL signal is composed of fewer individual signals emitted from individual grains and therefore enables the differentiation of fractions of well bleached and incompletely bleached grains within heterogeneously bleached samples. To account for this effect, medium (4mm diameter) and small aliquots (2mm diameter) as well as

Table 04: Approaches developed to detect incomplete bleaching

Comparative approaches	Key publications
OSL using coarse grain and fine grain fractions	Olley et al. (1998), Wallinga (2002)
Measurements of quartz OSL and feldspar IRSL[1]	Godfrey-Smith et al. (1988), Fuchs et al. (2005)
Analysis of the OSL signal	**Key publications**
D_e versus illumination time plot	Huntley (1985), Bailey (2003)
Correlation of OSL intensity and corresponding D_e	Li (1994, 2001), Wallinga (2002)
Signal component separation using LM OSL[2]	Bailey et al. (1997), Singarayer et al. (2005)
Analysis of equivalent dose distributions	**Key publications**
Asymmetry of D_e distributions	Wallinga (2002), Bailey & Arnold (2006)
Thresholds for scatter in D_e from dose recovery tests	Fuchs & Lang (2001), Fuchs & Wagner (2003)
Thresholds for scatter in D_e from well bleached analogues	Galbraith et al. (2005), Fuchs et al. (2007)
Observed overdispersion	Duller (2008), Thrasher et al. (2009)

[1] Infrared stimulated luminescence (IRSL)
[2] Linearly Modulated OSL (LM OSL)

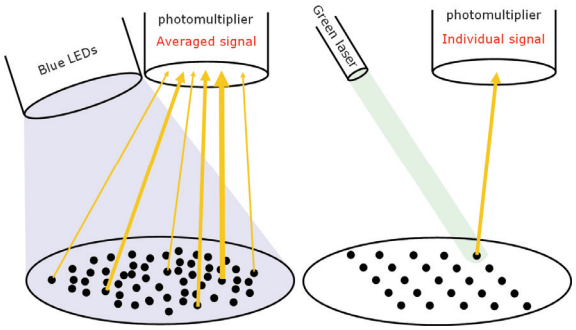

Figure 11: OSL signal recorded by the photomultiplier installed in an OSL reader system: averaged signal from single aliquots (left) and individual signal from single grains (right).

single grains of quartz were used for the OSL measurements in this study. A comprehensive review of single grain quartz OSL is provided by Duller (2008).

3.5. Statistical age models

Whenever incomplete bleaching is detected for a sample, different statistical age models are available to calculate the "true" equivalent dose and subsequently a depositional age for such samples. In general, these models are based on the assumption that incompletely bleached sediments consist of a mixture of well bleached and incompletely bleached grains (Duller, 1994). Within the dose distribution of the individual aliquots obtained from single aliquot or single grain measurements for a specific sample, the low end of the dose distribution is assumed to reflect the well bleached proportion of grains and therefore the true burial dose. Table 05 summarises the most important statistical age models and gives reference to key publications, including the Central Age Model (CAM, Galbraith et al., 1999) described above and the Finite Mixture Model (FMM, Roberts et al., 2000). The latter allows the identification of different populations of D_e within heterogeneous D_e distributions caused by post depositional sediment mixing. The decision which model should be applied to which dataset primarily depends on the statistical characteristics of the dataset to be analysed, as each model has individual shortcomings. This decision process and comparative calculations for suitable age models are described in the individual research papers.

Table 05: Statistical age models

Age model	Suitable in case of	Key publications
Central Age Model (CAM)[1]	Complete bleaching	Galbraith et al. (1999)
Mean of the lower 5%[2]	Incomplete bleaching	Olley et al. (1998)
3 and 4 parameter Minimum Age Model (MAM-3, MAM-4)[3]	Incomplete bleaching	Galbraith et al. (1999)
Sample specific threshold based D_e determination[4]	Incomplete bleaching	Fuchs & Lang (2001)
Leading edge technique[5]	Incomplete bleaching	Lepper & McKeever (2002)
Finite Mixture Model (FMM)[6]	Sediment mixing	Roberts et al. (2000)

[1] Within the calculation of the mean, the observed overdispersion (σ_b) is taken into account, which describes the spread in the D_e distribution additional to the spread expected from the errors on the individual D_e values.
[2] The true D_e is calculated as the mean of the lower 5% of a positively skewed D_e distribution.
[3] The equivalent dose estimate is derived from the truncation point of a truncated log-normal distribution. In contrast to the MAM-3, the MAM-4 allows for the allowance of an expected overdispersion.
[4] A running mean value is calculated for the sorted (low to high) D_e distribution and compared with a threshold based on the experimental error obtained from dose recovery tests.
[5] The true D_e is derived from the inflexion point of a Gaussian curve which is fitted to the rising limb of a positively skewed dose distribution.
[6] Allows for the identification of different populations of D_e within distributions, each of which is assigned with an individual D_e error. The best component fit is indicated by the lowest value for the Bayesian Information Criterion (BIC) (Rodnight, 2006).

4. From morphostratigraphy to geochronology - on the dating of ice marginal positions

Proceeding from the general introduction of the research area and the basics of OSL dating, this section focuses on the following issues:

- The position of this study in the context of the history of Quaternary research in northern Germany.
- The change in approach to the stratigraphy of glacial deposits that has taken place within the last decade (within German Pleistocene stratigraphy and beyond).
- Chances and problems concerning the integration of different dating methods, especially OSL and SED of erratic boulders, to ascertain ages for depositional features within the glacial landscape.
- The use of age-derived isochroneity in ice marginal positions, rather than morphostratigraphical definitions.

This section has already been published. Please see below for corresponding information.	
Title:	From morphostratigraphy to geochronology - on the dating of ice marginal positions
Journal:	Quaternary Science Reviews
Volume / Issue:	n/a
First author:	Christopher Lüthgens
Co-author(s):	Margot Böse
Date of acceptance:	12 October 2010
Date of online publication:	19 November 2010
Link (WWW):	From morphostratigraphy to geochronology
DOI:	http://dx.doi.org/10.1016/j.quascirev.2010.10.009
PDF:	PDF (1765 K)
Status at press time:	Article in Press, Corrected Proof

5. The age of the Brandenburg ice marginal position – Part 1: The Beelitz outwash cone

The following sections present the OSL dating results obtained within this study. The order of presentation of the results follows the succession of ice marginal positions from south to north (cf. section 2). This section accordingly deals with the first numerical ages for the Brandenburg IMP in north-eastern Germany. Methodologically this section focuses on the comparison of different indicator values for the detection of incomplete resetting of the OSL signal as well as the comparability of results from different statistical age models developed in order to correct for the effect of incomplete bleaching in the evaluation of SAR based D_e distributions.

In addition to the published material, topographical and geological maps of the sampling site are provided as supplementary material in appendices 13.2.9 & 13.2.10.

This section has already been published. Please see below for corresponding information.	
Title:	Optically stimulated luminescence dating of fluvioglacial (sandur) sediments from north-eastern Germany
Journal:	Quaternary Geochronology
Volume / Issue:	Volume 5, Issues 2-3, April-June 2010, Pages 237-243
First author:	Christopher Lüthgens
Co-author(s):	Matthias Krbetschek, Margot Böse, Margret C. Fuchs
Date of acceptance:	24 June 2009
Date of online publication:	08 July 2009
Link (WWW):	OSL dating of fluvioglacial (sandur) sediments
DOI:	http://dx.doi.org/10.1016/j.quageo.2009.06.007
PDF:	PDF (721 K) Supplement PDF (69 K)
Status at press time:	Printed (Supplementary material only available online)
Copyright notice:	Reproduction of this section only by permission of the rightholder.

6. The age of the Brandenburg ice marginal position – Part 2: The Luckenwalde end moraine and outwash plain

Within the following section numerical ages for the Luckenwalde end moraine and outwash plain (Brandenburg IMP) are presented. To provide support of the results obtained from OSL dating, stratigraphical analyses including detailed mapping of four sediment sections as well as petrographic gravel analyses of selected samples were conducted.

Additional topographical and geological maps are provided as supplementary material to this publication in appendices 13.2.13 & 13.2.14. Unfortunately an error most probably caused by transformation of one of the data tables throughout the publication process could not be corrected before the final printed publication of the article. Therefore a corrected version of the table is provided in the following. Again, it is important to note that the error only occurred in the course of the publication process and all calculations and conclusions of the manuscript were originally based on the correct values presented here and therefore don't need to be altered.

This section has already been published. Please see below for corresponding information.	
Title:	On the age of the young morainic morphology in the area ascribed to the maximum extent of the Weichselian glaciation in north-eastern Germany
Journal:	Quaternary International
Volume / Issue:	Volume 222, Issues 1-2, 1 August 2010, Pages 72-79
First author:	Christopher Lüthgens
Co-author(s):	Margot Böse, Matthias Krbetschek
Date of acceptance:	17 June 2009
Date of online publication:	09 July 2009
Link (WWW):	On the age of the young morainic morphology
DOI:	http://dx.doi.org/10.1016/j.quaint.2009.06.028
PDF:	PDF (759 K)
Status at press time:	Printed
Copyright notice:	Reproduction of this section only by permission of the rightholder.

Erratum: Corrected version of "Table 4 – OSL data summary"

This table substitutes the original table on top of page 77 in the published article (Changes only affect the dose rate column).

Table 4
OSL data summary

location	sample	depth (cm)	n	c_v of natural D_e (%)	c_v of D_e from drt[1] (%)	significance[2] of Δ c_v (nat.) & c_v (drt)	range of D_e values (Gy)	skewness of D_e distri-bution (γ_1)	w.c. (%)[3]	dose rate (Gy/ka)	dose (Gy)[4]	$\sigma^{(b)}$ (%)[5]	age (ka)
"Weinberge"	LUC_I-3	1310	21	19.76	3.99	yes	99.0	0.3	4.7	0.71	110.17 ± 8.05	13.5	155.44 ± 21.5
"Weinberge"	LUC_I-4	1280	33	24.36	4.66	yes	119.7	1.2	3.5	0.70	96.65 ± 5.25	16.3	137.24 ± 17.7
"Weinberge"	LUC_II-1	780	36	27.67	5.61	yes	218.0	1.2	4.4	0.88	115.16 ± 7.13	20.6	130.76 ± 9.5
"Weinberge"	LUC_II-2	680	22	22.72	8.83	yes	136.5	0.6	3.2	0.84	126.19 ± 10.60	12.7	150.31 ± 13.9
"Weinberge"	LUC_II-3	450	25	32.70	9.92	yes	256.4	1.6	6.7	0.89	122.73 ± 9.38	17.2	137.81 ± 11.9
"Weinberge"	LUC_II-4	270	9	21.51	12.5	no	93.3	0.2	3.8	0.79	102.11 ± 12.80	12.3	129.84 ± 17.4
"Weinberge"	LUC_II-5	100	32	22.72	8.83	no	144.1	1.6	4.0	0.80	110.15 ± 6.17	12.6	137.59 ± 10.0
"Frankenfelde"	LUC_III-1	420	10	37.55	9.63	yes	143.2	0.9	6.8	0.94	50.20 ± 8.56	35.5	53.10 ± 9.3
"Frankenfelde"	LUC_III-2	275	11	35.71	9.87	yes	133.9	-0.6	4.0	1.02	34.79 ± 6.86	45.7	34.39 ± 6.9
"Frankenfelde"	LUC_III-3	160	11	41.89	9.45	yes	147.1	0.9	4.1	0.96	52.41 ± 7.29	40.1	54.89 ± 7.9

[1]dose recovery tests of 6 (LUC_I, LUC_II) or 8 (LUC_III) discs per sample, recovery dose similar to expected D_e
[2]p=0,95, α=0,05
[3]estimated average water content
[4]values calculated using the Minumum Age Model (MAM-3, Galbraith 1999)
[5]overdispersion values calculated using the Central Age Model (CAM, Galbraith 1999)

7. The age of the Brandenburg ice marginal position – Part 3: The Beelitz outwash cone revisited

Both the age of 34.1 ±3 ka from the Beelitz outwash cone (cf. section 5) and the age of 34.4 ±7 ka from the Luckenwalde outwash plain (cf. section 6) have to be regarded as maximum ages for the formation of the Brandenburg IMP. However, the ages from both sites are in good agreement. Incomplete bleaching was detected for all samples from the Brandenburg IMP. As suggested by Duller (2008), comparative measurements for two samples from the Beelitz site were conducted using reduced aliquot sizes. However, the expected drop in D_e and consequently in age could not be observed (cf. section 5). To investigate this problem further and to be able to state the age of the Brandenburg IMP more precisely, additional measurements using single grains of quartz were conducted for the samples BEE-2 and BEE-3. The results from these measurements will be presented and discussed in the following. Please see section 5 for details concerning the geomorphology of the study area and the stratigraphy of the Beelitz sampling site.

7.1. Methods and procedures

Pure quartz separates were extracted from the bulk samples using the procedures as described in the respective subchapters of sections 5. The fraction of 200-250 µm was separated for single grain measurements, and grains were placed onto aluminium sample holders, each containing 100 grains. The measurements were carried out in the luminescence dating laboratory of the University of Bern, using a RISØ TL-OSL DA 20 automated luminescence reader system (Bøtter-Jensen et al. 2000, 2003a) equipped with a green (532 nm) and an infrared (830 nm) laser for single grain measurements.

Based on the results from dose recovery tests (recovery ratios close to 1.00 for both samples), the SAR protocol shown in table 06 was used for D_e determination. One thousand grains were measured for sample BEE-2 and 1200 grains for sample BEE-3. To correct for inhomogeneity of the Sr-90 beta irradiator (5.6 Gy min^{-1}), the dose received at the individual single grain positions on the sample holders was calibrated as suggested by Ballarini et al. (2006). The luminescence signal was integrated over the first 0.5s of stimulation with background integration over the last 0.25 s of stimulation.

A more detailed description of the single grain procedures applied here is provided in section 9. Details concerning the dose rate determination have been described in the respective chapter of section 5.

Table 06: Single Aliquot Regenerative (SAR) dose protocol for single grains[1]

Run	Treatment
1	Dose (except before first run)
2	Preheat (260° C for 10 s)
3	Optical stimulation with IR laser (only for last run)
4	Optical stimulation with green laser for 0.5 s at 125° C
5	Test dose
6	Cutheat (220° C for 10 s)
7	Optical stimulation with green laser for 0.5 s at 125° C
8	Start from top

[1] Seven regeneration cycles including zero dose, recycling point and test for IR depletion according to Duller (2003)

7.2. Results

7.2.1. Luminescence signal characteristics

A high variation in the OSL properties of single grains of quartz was observed. In general, the values summarised in table 07 are in good agreement with results from previous studies (summarised in Duller, 2008), as well as the results from single grain measurements for samples from the Pomeranian IMP conducted within this study (cf. section 9). Furthermore, both samples show rather similar values. However, there is a strikingly high percentage of grains characterised by an L_N/T_N ratio above the maximum L_X/T_X value to be calculated from the generated dose response curve. The BEE samples both show values of about 8 times the maximum value obtained for samples from the Pomeranian IMP (0.4% for sample ALT_II-1, cf. section 9). For the samples from the Pomeranian IMP, the grains falling into this category show a natural OSL signal well above a dose response curve in or close to saturation as observed from previous studies (e.g., Jacobs et al. 2006 and references therein; Stone & Thomas 2008). Such grains (Figure 12a) are also present in the BEE samples, but their overall percentage only amounts to 0.7% for

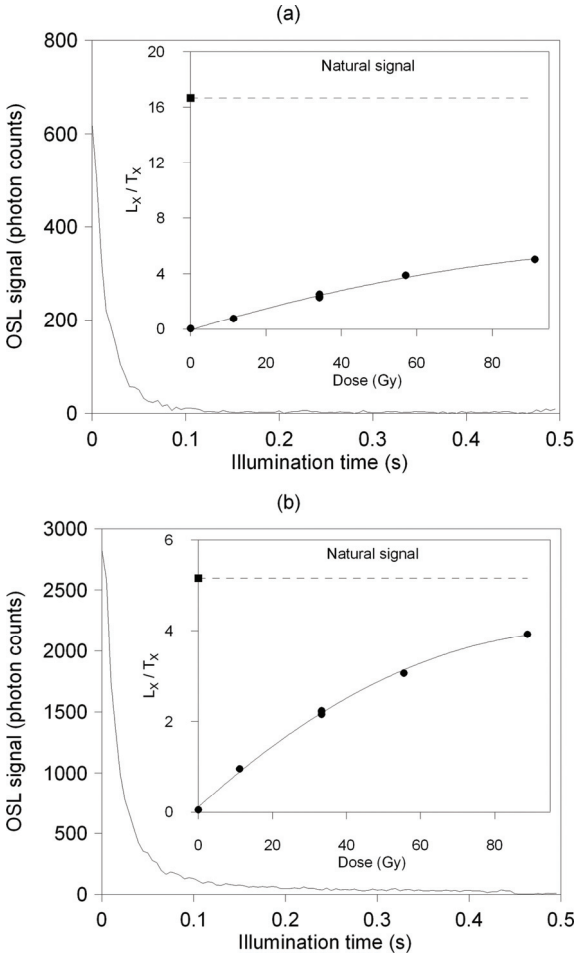

Figure 12: Shinedown and dose response curves of two single grains measured for sample BEE-3. (a) Grain showing a natural OSL signal well above the dose response curve. (b) Grain showing a natural OSL signal barely above the dose response curve.

Table 07: Single grain characteristics of samples BEE-2 and BEE-3

Sample	n[1] (100%)	No signal (%)[2]	Dim grains (%)[3]	Feldspar grains (%)[4]	L_N/T_N > max. L_X/T_X (%)[5]	Accepted grains (%)[6]
BEE-2	1000	86.8	7.3	1.0	3.4	1.5
BEE-3	1200	86.4	7.0	1.5	3.0	2.1

[1] Total number of grains measured per sample
[2] Percentage of grains not emitting any detectable luminescence signal
[3] Percentage of grains emitting only a dim OSL signal (rejected for insufficient test dose signal)
[4] Percentage of grains failing the IR depletion test and therefore identified as feldspar grains
[5] Percentage of grains characterised by an L_N/T_N ratio above the maximum L_X/T_X value to be calculated from the generated dose response curve
[6] Percentage of grains fulfilling all quality requirements as proposed by Lüthgens et al. (submitted for publication; cf. section 9)

BEE-2 and 0.8% for BEE-3. The remaining grains also show a natural OSL signal above the maximum L_X/T_X value to be calculated from the generated dose response curve. However, the shape of the dose response curves (Figure 12b) indicates that by applying higher regenerative doses an intersection of the natural L_N/T_N value with the dose response curve might have been achieved. The proportion of such grains amounts to 2.7% for BEE-2 and 2.2% for BEE-3. This exceeds the proportion of accepted grains of 1.5% for BEE-2 and 2.1% for BEE-3 for both samples. Similar behaviour was only observed in very rare cases from the single aliquot measurements. Therefore it is likely that the effect was obscured by signal averaging (cf. section 3.4).

7.2.2. Analysis of D_e distributions and resulting OSL ages

Because of the circumstances described in the previous section, the D_e distributions of the two samples have to be regarded as incomplete. All values that might have been obtained from grains carrying a charge corresponding to more than ~90 Gy (highest dose point) are missing. The analysis of D_e distributions for the detection of incomplete bleaching (cf. section 3.4) is therefore inapplicable. However, the results from single aliquot measurements had already revealed the samples to be incompletely bleached (cf. section 5). Therefore it is still possible to derive a burial dose from the D_e distributions of the two samples by applying the Finite Mixture Model (FMM, Roberts et al., 2000; for a more detailed description of the statistical age model see section 8). The calculations on which this model is based are not affected by the described truncation of the D_e distributions. Within an incompletely bleached sample, the well bleached proportion of grains is supposed to be represented by a statistically independent population of D_e values at the lower end of the dose distribution. By applying the FMM this population can be separated and a corresponding average value can be calculated. Table 08 shows the results from the D_e calculations using the FMM, as well as the resulting ages calculated using the software ADELE (Kulig, 2005).

Table 08: FMM results and age calculations for samples BEE-2 & BEE-3

	FMM[1]				
Sample	Component[2]	De (Gy)	n	dose rate (Gy/ka)[3]	age (ka)[4]
BEE-2	1	24.29 ±2.97	7	0.8	30.6 ±4.0
	2	59.19 ±7.54	8	n/a	n/a
BEE-3	1	20.46 ±1.43	14	0.8	24.8 ±2.0
	2	72.34 ±6.26	11	n/a	n/a

[1] According to Roberts et al. (2000), threshold of $\sigma_{(b)}$ = 19% for FMM calculations derived from analogue well bleached samples from the Pomeranian IMP (cf. section 9) as suggested e.g. by Galbraith et al. (2005); observed overdispersion values: BEE-2 $\sigma_{(b)}$ =45.5 %; BEE-3 $\sigma_{(b)}$ =63.0 % calculated using the Central Age Model (CAM, Galbraith et al., 1999).
[2] The best fit was achieved for two components for both samples as indicated by the BIC.
[3] Procedures of dose rate determination described in the respective chapter of section 5, different grain size for single grain measurements accounted for in calculations here.
[4] No ages were calculated for the second component, as these values represent the proportion of incompletely bleached grains within the samples.

7.3. Single aliquot vs. single grain results

Two samples previously dated using single aliquot techniques were reinvestigated by applying single grain dating techniques for the dating of quartz. The single grain based equivalent doses and the resulting ages are significantly lower than the values previously obtained from single aliquot measurements (summarised in table 09). This is not surprising considering that both samples had already been identified as incompletely bleached on the basis of the results from single aliquot measurements. Accordingly the observed drop in D_e is larger for sample BEE-2, which had already revealed poorer bleaching characteristics than sample BEE-3 in single aliquot measurements. The fact that D_e values as well as the resulting ages for the single grain based results overlap within error may indicate that the different bleaching characteristics that influenced the results on the single aliquot level (with both samples clearly showing significantly different results, cf. table 09) have been overcome on the single grain level. Because both samples were taken from the same stratigraphical unit, it seems plausible to calculate an average age of 27.7 ±4 ka (stating the largest observed uncertainty from the individual ages as error). This age is not significantly different from the single aliquot based results previously stated for the Beelitz outwash cone of 34.1 ±3 ka (cf. section 5) and 34.4 ±7 ka for the Luckenwalde outwash plain (cf. section 6) and might confirm the assumption that the ice advance to the Brandenburg IMP occurred earlier in MIS 2 than previously estimated (cf. section 2.3.1).

However, a final assessment of the reliability of the single grain based results remains challenging because comparable results obtained from well bleached samples are not available for the Brandenburg IMP. As is shown in section 9, single grain OSL measurements for samples from the Pomeranian IMP have been proven to provide reliable equivalent doses, based on comparative measurements of single grains and single aliquots for well bleached and incompletely bleached samples. However, owing to the different OSL characteristics outlined above, it remains questionable whether the overdispersion threshold used for the FMM calculations ($\sigma_{(b)}$ = 19%, as derived from well bleached fluvioglacial samples from the Pomeranian IMP, cf. section 9) is also adequate for samples from the Brandenburg IMP. This issue will be discussed in further detail in the summarising discussion provided in section 11.

Table 09: Single grain and single aliquot equivalent doses and ages for samples BEE-2 and BEE-3.

	Single aliquots[1]		Single grains	
Sample	D_e (Gy)	Age (ka)	D_e (Gy)	Age (ka)
BEE-2	44.6 ±4.2	54.8 ±5.6	24.29 ±2.97	30.6 ±4.0
BEE-3	28.8 ±2.2	34.1 ±3.0	20.46 ±1.43	24.8 ±2.0

[1] Results from small aliquots (cf. section 5).

8. An excursus: The Eemian of Vevais – A comparison with independent age control and the reconstruction of the development of the Oderbruch basin

Near the village of Vevais, east of Berlin (maps provided as supplementary material in appendices 13.2.17 & 13.2.18), a sediment succession encompassing deposits from the last glacial-interglacial cycle is accessible. This profile was chosen as a sampling site for two reasons. First, it offered the chance to crosscheck OSL ages obtained from fluvioglacial sediments with an independent age control from palynological findings. Furthermore, the section is situated in a key position, in both stratigraphical and geographical senses, for the reconstruction of the development of the Oderbruch basin. Five samples for OSL dating were taken: two from below Eemian sediments (pre-interglacial), one from Eemian sediment (interglacial) and two from above Eemian sediments (post-interglacial). Owing to dose rate related problems the ages obtained from the initially conducted quartz OSL measurements turned out to be severely underestimated for some of the samples. Additional Infrared Stimulated Luminescence (IRSL) and post-Infrared Yellow OSL (post-IR YOSL) measurements of feldspar as well as a subtraction dating method were applied in order to solve these problems. The results of these analyses are presented within the following section.

This section has already been published. Please see below for corresponding information.	
Title:	Timing of the last interglacial in Northern Europe derived from Optically Stimulated Luminescence (OSL) dating of a terrestrial Saalian-Eemian-Weichselian sedimentary sequence in NE-Germany
Journal:	Quaternary International
Volume / Issue:	n/a
First author:	Christopher Lüthgens
Co-author(s):	Margot Böse, Tobias Lauer, Matthias Krbetschek, Jaqueline Strahl, Dirk Wenske
Date of acceptance:	23 June 2010
Date of online publication:	27 July 2010
Link (WWW):	Timing of the last interglacial in Northern Europe
DOI:	http://dx.doi.org/10.1016/j.quaint.2010.06.026
PDF:	PDF (1941 K)
Status at press time:	Article in Press, Corrected Proof
Copyright notice:	Reproduction of this section only by permission of the rightholder.

9. Age of the Pomeranian ice-marginal position inferred from OSL dating of single grains of quartz

Three sampling sites were investigated in order to determine the age of the Pomeranian IMP: the Klosterbrücke outwash fan near Eberswalde (supplementary maps provided as appendices 13.2.11 & 13.2.12), the Althüttendorf outwash cone (supplementary maps provided as appendices 13.2.7 & 13.2.8) and an abandoned clay pit near Macherslust (supplementary maps provided as appendices 13.2.15 & 13.2.16). Within the following section the results obtained from OSL dating of single grains of quartz will be presented. Based on these results, previous surface exposure ages obtained from erratic boulders associated with the Pomeranian ice marginal position will be critically discussed.

This section was submitted for publication to BOREAS and is currently under review. In order to enhance readability the manuscript draft was adjusted to the overall layout of this cumulative paper. However, the overall structure of the manuscript as well as the format of citations, references, figure captions etc. were not altered from the journal's specifications.

This section has already been published. Please see below for corresponding information.	
Title:	Age of the Pomeranian ice-marginal position in northeastern Germany determined by Optically Stimulated Luminescence (OSL) dating of glaciofluvial sediments
Journal:	BOREAS
Volume / Issue:	n/a
First author:	Christopher Lüthgens
Co-author(s):	Margot Böse, Frank Preusser
Date of acceptance:	09 March 2011
Date of online publication:	11 May 2011
Link (WWW):	Age of the Pomeranian ice-marginal position in northeastern Germany
DOI:	http://dx.doi.org/10.1111/j.1502-3885.2011.00211.x
PDF:	PDF (3506 K)
Status at press time:	Article in Press, Corrected Proof
Copyright notice:	Reproduction of this section only by permission of the rightholder.

10. A comparison of single aliquot and single grain quartz OSL for samples from the Pomeranian IMP

In addition to the single grain measurements presented in the previous section, comparative measurements of medium and small aliquots of quartz were conducted for the samples from the Pomeranian IMP to investigate the signal contribution of individual grains to multigrain aliquots of different sizes. As shown for samples from the Brandenburg IMP in section 7, the reduction of aliquot size does not necessarily result in a reduction of D_e for incompletely bleached samples. This may be due to a significant effect of signal averaging even on the small aliquot level.

10.1. Study area, methods and procedures

The study area as well as the sampled profiles have been described in detail in the previous section. Please also see section 9 for details concerning preparation procedures and dose rate determination. Sample preparation (cf. section 9) and single aliquot OSL measurements were carried out at the Freiberg luminescence laboratory. The fraction of 90-160 µm was separated for the single aliquot measurements. Aliquots were prepared with 4 mm (medium) and 2 mm (small) diameter single grain layers in aluminium cups. The average number of grains on each aliquot was determined by microscopic counting of the grains on randomly chosen aliquots. About 800 grains fit onto a 4 mm aliquot, and about 200 grains onto a 2 mm aliquot. These numbers are in good agreement with those estimated from Duller (2008). The prepared aliquots were tested for remaining feldspar contamination by IR (880nm) stimulation at low power. Aliquots showing a significant luminescence signal were excluded from further analyses. Single aliquot measurements were carried out on a RISØ TL-OSL DA 15 automated luminescence reader system (Bøtter-Jensen et al., 2000) equipped with a Sr-90 beta irradiator (5.6 Gy/min). Stimulation was carried out using blue LEDs (470nm) at 90% power. The OSL emission was detected in the UV through a 7.5mm U 340 (Hoya) optical filter. Based on results of dose recovery tests (recovery ratios close to 1.00 for all samples, figure 14 a SAR protocol (Murray & Wintle, 2000, 2003) with six regeneration cycles including zero dose and recycling point was used to determine the equivalent dose (Table 10).

Table 10: SAR protocol for single aliquots

Run	Treatment
1	Dose (except before first run)
2	Preheat (260° C for 10 s)
3	Optical stimulation with blue LEDs for 50 s at 125° C
4	Test dose
5	Cutheat (220° C for 10 s)
6	Optical stimulation with blue LEDs for 50 s at 125° C
7	Dose (only for last run)
8	Optical stimulation with IR LEDs (only for last run)
9	Start from top

10.2. Luminescence signal characteristics

All samples show OSL signals clearly dominated by a fast component. Typical shine down and dose response curves for medium and small aliquots are shown in figure 13. Despite variations in peak luminescence intensities, the Althüttendorf samples show a generally brighter luminescence signal than the

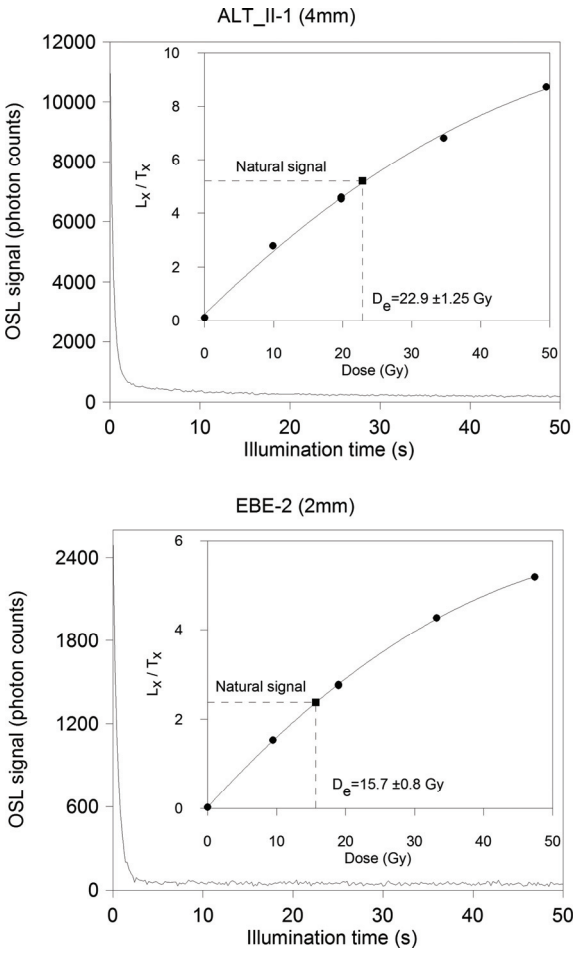

Figure 13: Representative OSL shinedown curves and typical dose response curves (inset) for medium (top, sample ALT_II-1) and small (bottom, sample EBE-2) aliquots.

Eberswalde and Macherslust samples (Table 11). For medium (4 mm) aliquots the Althüttendorf samples show an average of ~40000 photon counts recorded within the first second of stimulation with a background of 800-900 counts recorded within the last 10 seconds of stimulation. The Eberswalde and Macherslust samples show average values of only around 50% of the Althüttendorf sample values for medium aliquots. For small (2 mm) aliquots this general trend is no longer present. Luminescence intensities scatter within a broader range with the brighter samples averaging at around 18000 counts and the dimmer ones ranging from ~4600-8500 counts within the first second of stimulation. Recycling

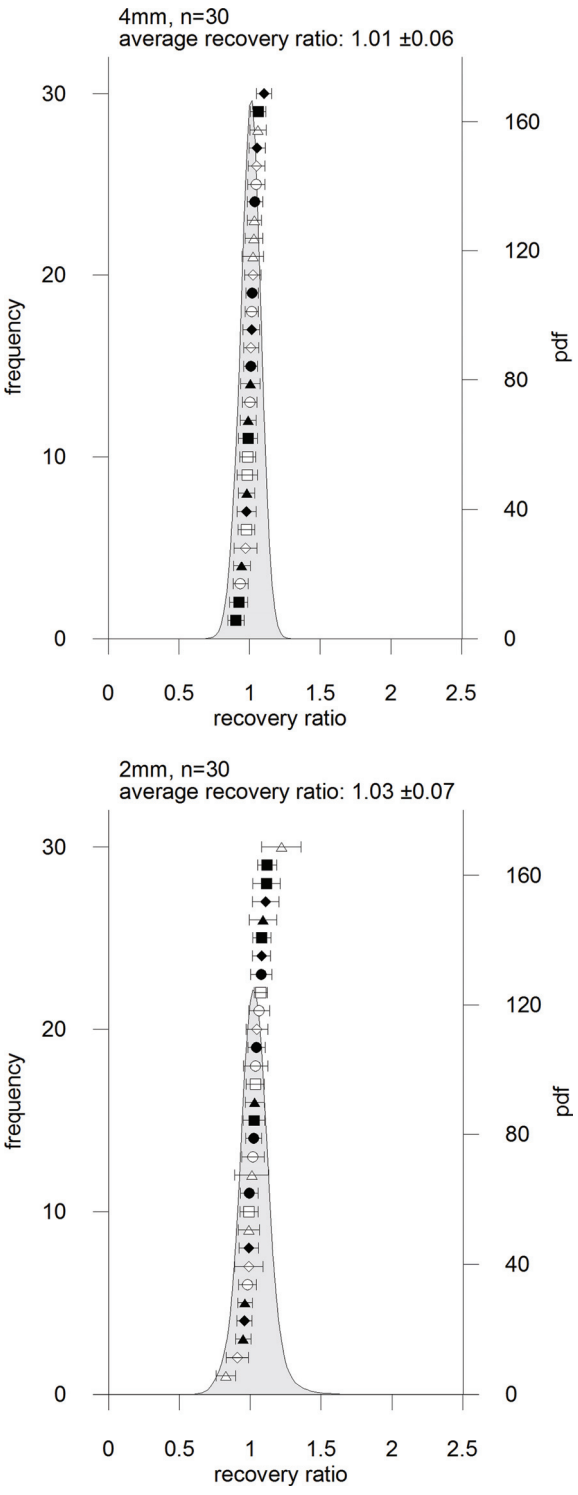

Figure 14: Results from dose recovery tests for all samples (top - medium aliquots; bottom – small aliquots; given dose of ~19 Gy similar to expected natural dose): ALT_I-1 open circles, ALT_I-2 filled circles, ALT_II-1 open squares, ALT_II-2 filled squares, EBE-1 open triangles, EBE-2 filled triangles, EBE-3 open diamonds, MAC-1 filled diamonds.

Table 11: Luminescence properties of single aliquot and single grain measurements

sample	size	n[1]	Natural OSL signal intensity (photon counts)[2]					
			peak			background		
			min	max	mean	min	max	mean
ALT_I-1	4mm	29	7295	282532	42608	434	1877	838
	2mm	32	1158	21420	6910	158	509	261
	SG[3]	46	163	21975	2834	18	833	100
ALT_I-2	4mm	33	9169	203578	38009	414	1490	804
	2mm	37	1623	80326	18711	140	754	365
	SG[3]	40	190	18642	1964	26	623	104
ALT_II-1	4mm	33	11270	512708	43699	511	1773	987
	2mm	35	2260	261650	17895	186	1118	336
	SG[3]	32	138	10672	1463	19	322	82
ALT_II-2	4mm	37	11429	117352	40424	386	2104	932
	2mm	33	2467	25444	7585	171	454	261
	SG[3]	50	127	26841	3062	25	797	131
EBE-1	4mm	39	3295	60374	20236	239	827	430
	2mm	33	898	18287	4647	68	214	121
	SG[3]	29	78	31183	2768	7	1017	130
EBE-2	4mm	40	4701	314198	25909	248	638	394
	2mm	36	1340	26502	8425	170	699	244
	SG[3]	32	134	14352	2041	28	422	120
EBE-3	4mm	39	3598	84124	19534	233	665	401
	2mm	35	2048	57327	8489	124	447	219
	SG[3]	28	311	56617	4748	38	992	184
MAC-1	4mm	41	5905	184193	25520	191	846	332
	2mm	43	1877	69642	18640	156	844	276
	SG[3]	49	189	68370	3793	17	2071	131

[1] number of accepted aliquots/ grains
[2] peak integrated over the first second of stimulation, background integrated over the last 10s of stimulation for single aliquots; peak integrated over the first 0.1s of stimulation, background integrated over the last 0.25s of stimulation for single grains
[3] Single grain values taken from section 9.

ratios are close to unity within error for all single aliquot measurements. Aliquots showing a recycling ratio of >5% were discarded from further calculations. Recuperation is low on average. Aliquots showing recuperation values of >0.05 were discarded from further calculations as well (Murray and Wintle, 2000, 2003). A closer look at the recorded peak signal intensities (Table 11) reveals the following characteristics, which occur independently from the different sample characteristics described above:

- For the minimum OSL peak intensities, the observed brightness drops with aliquot size for all samples (medium aliquots showing the brightest signal, followed by small aliquots and single grains).
- For the maximum OSL peak intensities, medium aliquots always show the brightest signals, but for some samples the brightness recorded for single grains is similar to or even exceeds the brightness recorded for small aliquots (Table 11).

- For the observed mean OSL peaks the order of brightness again corresponds to aliquot size (from medium to small aliquots to single grains).

This might indicate that some of the small aliquots are dominated by a luminescence signal originating from only few individual grains. This seems plausible when the low percentages of grains that emit a significant OSL signal are taken into account. Sample EBE-3 may serve as an example: only 3.1% of the grains emit a significant OSL signal (excluding dim grains, cf. section 9), corresponding to ~6 grains on a small aliquot, but to ~25 grains on a medium aliquot.

10.3. Modelling of synthetic multigrain aliquots from single grains

To be able to assess the signal contribution from individual grains to the multigrain aliquots in more detail, a straightforward modelling approach was developed. Synthetic aliquots were generated from the single grain datasets (1000 grain per sample, cf. section 9) of each sample. Grains identified as feldspar grains were removed before modelling the synthetic aliquots. For each aliquot size, 200 synthetic aliquots were generated by repeated random selection of 10, 25, 50, 100, 200, 400 and 800 grains respectively from the single grain dataset. The luminescence signal of the individual grains was determined by integrating the first 0.1s of the luminescence signal recorded as response to the first test dose of the SAR cycle. The luminescence signals of the single grains were summed up, and the individual proportion of each grain to the resulting cumulative luminescence signal of the synthetic aliquot was determined. From the resulting datasets of 200 synthetic aliquots for each aliquot size, the mean signal proportions of the grains were calculated and plotted versus the cumulated OSL signal (adapted and modified from Duller, 2006). Additionally, the aliquot showing the highest signal proportion within the first 10 % of grains and the aliquot showing the lowest signal proportion within the first 10 % of grains were extracted from the datasets for each aliquot size. These provide boundary values for the range of signal proportion distributions around the mean values. Cumulative signal plots were compiled for a selection of the modelled synthetic aliquot sizes. In these plots, the graph for an ideal aliquot showing identical signal contribution to the cumulative OSL signal from each grain would be depicted as a diagonal straight line from the origin. A shift of the maximum curvature towards the top left corner of the plot (which defines the point of 100% of the cumulative OSL signal being concentrated in one single grain) indicates a higher concentration of the luminescence signal within fewer grains. These analyses were conducted for all samples from the Pomeranian IMP, two of which will be presented here. Sample ALT_II-1 was chosen because it is characterised by the lowest average natural OSL signal. Additionally, as indicated by the rather low value of the maximum recorded luminescence intensity, the dataset is not assumed to contain very bright grains (Table 11). By contrast, sample MAC-1 shows significantly higher luminescence intensity on average and the highest maximum value recorded for the natural luminescence signal of a single grain of all samples (Table 11). Selected cumulative signal percentage plots of sample ALT_II-1 are presented in figure 15, those of sample MAC-1 are provided in figure 16 for comparison. Both samples show a higher percentage of the cumulative OSL signal

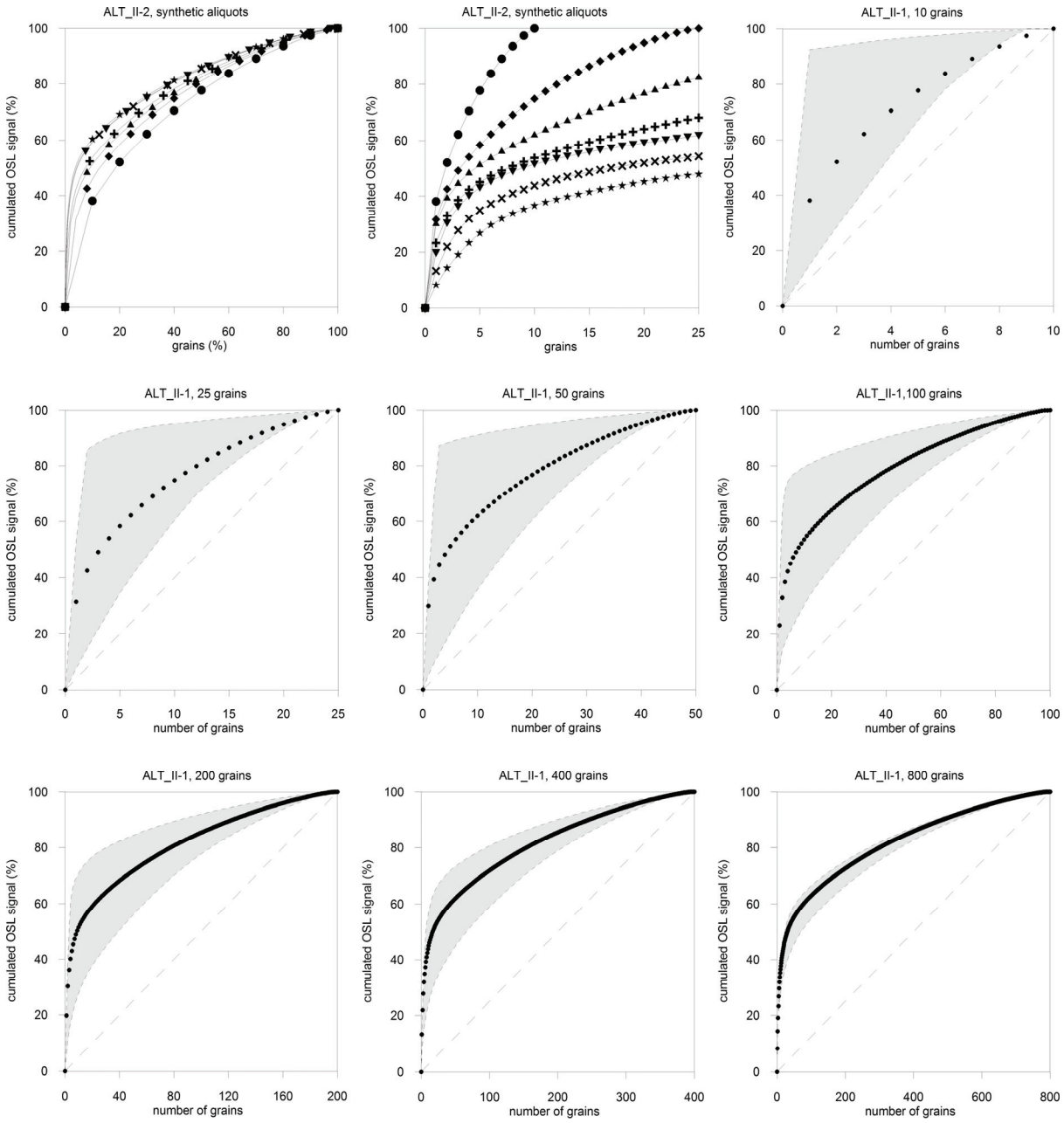

Figure 15: Synthetic aliquots modelled for sample ALT_II-1; top left: cumulated OSL signal percentage plotted versus the percentage of grains for all modelled aliquot sizes (symbology: circles 10 grains, diamonds 25 grains, tip up triangles 50 grains, cross symbols 100 grains, tip down triangles 200 grains, X symbols 400 grains, star symbols 800 grains); top middle: cumulated OSL signal percentage plotted versus the absolute number of grains (only first 25 grains displayed for aliquot sizes >25 grains; symbology as described before); top right and subsequent plots: cumulated OSL signal plotted versus the overall number of grains displayed for 10 (top right), 25 (middle left), 50 (middle middle), 100 (middle right), 200 (bottom left), 400 (bottom middle) and 800 (bottom right) grains: dots represent the average signal contribution for each grain on the aliquot calculated from the 200 synthetic aliquots modelled for each aliquot size, the shaded area describes the minimum and maximum signal concentrations observed from the 200 synthetic aliquots modelled for each aliquot size with the diagonal (dashed line) indicating an ideal aliquot with each grain contributing the same signal percentage to the overall OSL signal (all grains showing equal brightness).

concentrated in the same proportion of grains with larger aliquot sizes (top left plot in figures 15 and 16). This reflects the effect of a larger number of grains making up the same percentage for the different aliquot sizes (10% of grains amount to a single grain for a 10 grain aliquot as opposed to 80 grains for an 800 grain aliquot). When the contribution to the cumulated

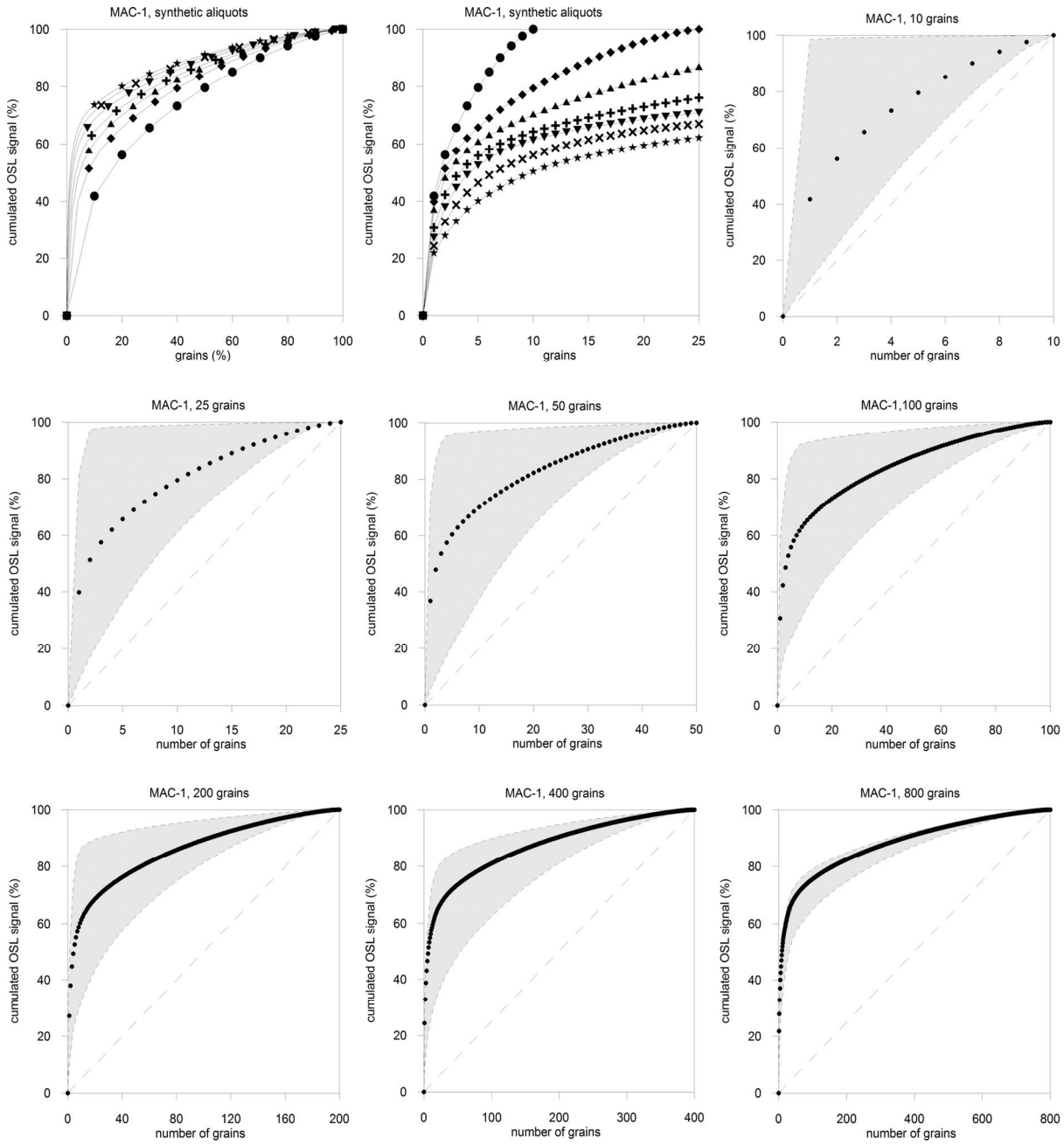

Figure 16: Synthetic aliquots modelled for sample MAC-1; top left: cumulated OSL signal percentage plotted versus the percentage of grains for all modelled aliquot sizes (symbology: circles 10 grains, diamonds 25 grains, tip up triangles 50 grains, cross symbols 100 grains, tip down triangles 200 grains, X symbols 400 grains, star symbols 800 grains); top middle: cumulated OSL signal percentage plotted versus the absolute number of grains (only first 25 grains displayed for aliquot sizes >25 grains; symbology as described before); top right and subsequent plots: cumulated OSL signal plotted versus the overall number of grains displayed for 10 (top right), 25 (middle left), 50 (middle middle), 100 (middle right), 200 (bottom left), 400 (bottom middle) and 800 (bottom right) grains: dots represent the average signal contribution for each grain on the aliquot calculated from the 200 synthetic aliquots modelled for each aliquot size, the shaded area describes the minimum and maximum signal concentrations observed from the 200 synthetic aliquots modelled for each aliquot size with the diagonal (dashed line) indicating an ideal aliquot with each grain contributing the same signal percentage to the overall OSL signal (all grains showing equal brightness).

OSL signal is analysed with regard to the absolute numbers of grains (top middle plot in figures 15 and 16), it is shown that the smaller the aliquot size, the higher the relative contribution of individual grains to the overall signal. What is striking is that for all aliquot sizes 25 grains or less contribute more than 50% of the overall OSL signal. The rise of the

cumulative plots is rather exponential for the 10 brightest grains and subsequently shifts towards a linear shape for the remaining grains. This suggests that these remaining grains (15 grains for a 25 grain aliquot up to 790 grains for an 800 grain aliquot) contribute similarly low proportions to the overall OSL signal. To be able to detect incomplete resetting of the OSL signal from multigrain aliquot measurements, it is crucial that the recorded OSL signal is dominated by only few individual grains. The plots for different modelled aliquot sizes (top right to bottom right plots in figures 15 and 16) show the rising effect of signal averaging with increasing aliquot sizes. For small aliquots (10-200 grains) a large variation in signal composition can be detected around the mean, whereas the variation is only very limited for medium aliquots (400-800 grains). The existence of aliquots showing a possibly high concentration of the cumulative OSL signals within only few grains enables the detection of incomplete bleaching from a SAR dataset. According to the results from the synthetic aliquot modelling, this seems to be possible for aliquots with up to a maximum of 200 grains for the samples analysed within this study. For larger aliquots the signal averaging is assumed to obscure the scatter caused by incomplete resetting of the OSL signal. Additionally, it has to be pointed out that this maximum number of grains is strongly dependent on the signal characteristics of the individual samples. As described above, sample MAC-1 was identified as a bright sample in single aliquot measurements. Based on single grain analyses this brightness is caused by the existence of very few extremely bright individual grains within the sample (brightest grain showing ~25000 counts within the first 0.1s of stimulation). Sample ALT_II-1 also contains only few bright grains, but these grains are significantly dimmer than those found in sample MAC-1 (brightest grains showing up to ~5000 counts within the first 0.1s of stimulation). As a result the effect of signal averaging is higher even for smaller aliquot sizes for this sample as indicated by less variation around the mean detected from the synthetic aliquot modelling (Figures 15 and 16).

10.4. Observations from modelling vs. observations from measurements

Based on these observations from the modelling approach, significant averaging effects were surely present in the medium aliquot (~800 grains) measurements and might already have had a significant effect on the small aliquot (~200 grains) measurements within this study. This should be comprehensible by comparing the equivalent doses and resulting ages derived from the single grain measurements (cf. section 9) with those from the single aliquot measurements. For the well bleached samples all aliquot sizes should lead to indiscernible values, whereas the incompletely bleached Eberswalde samples should show a drop in D_e and accordingly in age. Equivalent dose determination for the single aliquots was carried out according to the same principles as for the single grains (cf. section 9). The results of the bleaching assessment for the single aliquots are provided in table 12; the results of D_e determination and age calculations are summarised in table 13, which additionally includes the single grain based values (cf. section 9) for comparison. The results from the bleaching assessment for the single aliquot measurements yielded the same results for both medium and small

Table 12: Bleaching characteristics of samples from the Pomeranian IMP

Sample	Size[1]	n	Skewness	$2\sigma_{skew}$[2]	Signifi-cance[3]	Kurtosis	$2\sigma_{kurt}$[4]	Signifi-cance[5]	$\sigma_{(b)}$[6]	RSD_{IDR}[7]	RSD_{DRT}[8]
ALT_I-1	4	29	0.77	0.91	no	0.27	1.82	no	7.26	10.44	4.08
	2	32	0.00	0.87	no	-0.67	1.73	no	9.34	15.47	2.89
ALT_I-2	4	33	0.82	0.85	no	0.65	1.71	no	14.64	16.71	1.21
	2	37	0.44	0.81	no	-0.29	1.61	no	12.35	16.13	2.96
ALT_II-1	4	33	1.60	0.85	yes[9]	3.52	1.71	yes[9]	10.08	15.71	0.34
	2	35	0.56	0.83	no	-0.37	1.66	no	18.73	23.24	3.23
ALT_II-2	4	37	0.29	0.81	no	-0.43	1.61	no	14.43	15.87	6.29
	2	33	0.34	0.85	no	-0.33	1.71	no	12.59	14.89	3.43
EBE-1	4	39	1.90	0.78	yes	4.03	1.57	yes	8.75	26.94	1.31
	2	33	1.23	0.85	yes	2.75	1.71	yes	19.79	27.29	13.69
EBE-2	4	40	1.83	0.77	yes	4.13	1.55	yes	10.73	24.35	2.27
	2	36	2.38	0.82	yes	6.15	1.63	yes	13.85	32.20	5.60
EBE-3	4	39	2.61	0.78	yes	7.70	1.57	yes	3.55	24.62	2.76
	2	35	1.95	0.83	yes	3.69	1.66	yes	2.85	24.38	5.80
MAC-1	4	41	0.54	0.77	no	0.39	1.53	no	7.98	10.42	4.44
	2	43	0.27	0.75	no	-0.71	1.49	no	6.63	10.89	5.94

[1] Number of accepted aliquots
[2] Two times the standard deviation of skewness, calculated according to Tabachnick & Fidell (1996)
[3] Significant skewness detected when skewness value exceeds $2\sigma_{skew}$ (Bailey & Arnold, 2006)
[4] Two times the standard deviation of kurtosis, calculated according to Tabachnick & Fidell (1996)
[5] Significant kurtosis detected when kurtosis value exceeds $2\sigma_{kurt}$ (Bailey & Arnold, 2006)
[6] Overdispersion value calculated using the Central Age Model (Galbraith et al., 1999)
[7] Coefficient of variation (relative standard deviation) of the natural dose distribution, RSD_{IDR} in sensu Preusser et al. (2007)
[8] Coefficient of variation (relative standard deviation) of dose recovery test dose distributions, RSD_{DRT} in sensu Preusser et al. (2007)
[9] The fact that sample ALT_II-1 shows significant skewness for medium aliquots is surprising, as this is not present in the datasets of small aliquots and single grains for that sample (skewness caused by incomplete bleaching should rather be obscured by averaging of the OSL signal for medium aliquots). A Grubbs outlier test (normality assumption, 95% significance level) was applied to the 4mm dataset and revealed that the skewness is caused by only few high outliers. Their occurrence can-not be explained by the luminescence characteristics of the respective aliquots and therefore remains unclear. On the basis of these considerations, the 4mm dataset of sample ALT_II-1 should also be treated as a well bleached sample.

aliquots. Furthermore, the Eberswalde samples, which had been identified as incompletely bleached samples on the single grain level, were also identified as incompletely bleached samples on the single aliquot level.

As expected, the well bleached samples show indiscernible D_e values and ages for all aliquot sizes. A closer look at the D_e values calculated for the incompletely bleached Eberswalde samples shows that the results are indiscernible within error for medium and small aliquots of each sample. This corroborates the results from the synthetic aliquot modelling, which revealed signal averaging to be significant for both aliquot sizes (200 and 800 grains). On the single grain level all three samples show a drop in D_e. However, owing to the relatively large errors of the single grain based D_es, the CAM and minimum age model results still slightly overlap in some cases. This suggests that incomplete resetting of the OSL signal might have affected the samples only slightly.

10.5. Chances and limitations of the modelling approach

The basic population for the synthetic aliquot modelling was derived from the single grain OSL measurements of 1000 grains for each

sample. As shown previously, the percentage of grains emitting a detectable OSL signal is rather similar for all samples (~90%), whereas the percentage of grains passing the rejection criteria varies from 2.8% to 5% on the single grain level for the different samples. The latter is mainly dependent on the brightness of the individual grains because dim grains often have to be rejected owing to insufficient response to the test dose. For the single aliquot modelling all grains apart from those identified as feldspar grains were included in the basic population. Therefore not the percentage of bright grains but rather the question whether these bright grains show similar or varying brightness in the OSL signal becomes more important. Within the MAC-1 sample, very few extremely bright grains were identified in the single grain measurements, whereas such grains are missing in the ALT_II-1 sample. By contrast, the single aliquot measurements of the ALT_II-1 sample have shown the highest peaks in luminescence intensity of all samples (Table 11). It is therefore very likely that such extremely bright grains as identified from the MAC-1 single grain dataset are also present in

Table 13: OSL data summary – single aliquots vs. single grains from the Pomeranian IMP

Sample	Depth (cm)	Water content (%)[1]	Aliquot size[2]	n	D_e (Gy)[3]	Dose rate (Gy/ka)[4]	Age (ka)
ALT_I-1	14.6	8 ±4	4	29	30.8 ±0.6	1.3	22.4 ±0.6
			2	32	32.3 ±0.8		24.0 ±1.5
			sg	46	28.3 ±1.1		21.7 ±1.4
ALT_I-2	7.0	8 ±4	4	33	31.0 ±0.9	1.5	19.7 ±1.5
			2	37	28.1 ±0.7		17.8 ±1.4
			sg	40	29.7 ±1.3		19.4 ±1.6
ALT_II-1	13.5	8 ±4	4	33	24.6 ±0.5	1.3	18.8 ±1.4
			2	35	25.5 ±0.9		19.5 ±1.6
			sg	32	27.1 ±1.5		21.3 ±1.9
ALT_II-2	7.0	8 ±4	4	37	28.3 ±0.7	1.4	19.0 ±1.5
			2	33	27.3 ±0.7		18.3 ±1.4
			sg	50	26.2 ±1.0		18.1 ±1.5
EBE-1	2.3	8 ±4	4	39	17.2 ±0.6	0.8	20.2 ±1.4
			2	33	14.5 ±1.1		17.0 ±1.6
			sg	29	16.6 ±1.8		20.0 ±2.5
EBE-2	1.5	8 ±4	4	40	18.2 ±1.1	0.9	20.7 ±1.7
			2	36	18.1 ±0.8		20.7 ±1.5
			sg	32	17.0 ±1.8		19.8 ±2.4
EBE-3	0.7	8 ±4	4	39	21.4 ±0.6	1.0	21.3 ±1.4
			2	35	20.0 ±0.6		20.0 ±1.3
			sg	28	18.0 ±2.2		18.4 ±2.5
MAC-1	4.5	20 ±5	4	41	31.9 ±0.5	2.0	15.9 ±1.0
			2	43	32.0 ±0.5		15.9 ±1.0
			sg	49	28.8 ±1.0		14.7 ±1.0

[1] Estimated average water content, cf. section 9
[2] Aliquot sizes: sg – single grains, 2mm - ~200 grains, 4mm - ~800 grains
[3] Calculated using the Central Age Model (CAM) according to Galbraith et al. (1999) for the ALT and MAC samples, calculated using the MAM-4 according to Galbraith et al. (1999) for the EBE samples, cf. section 9
[4] Overall dose rate, cf. section 9

the ALT_II-1 sample. For future modelling approaches it is therefore suggested to measure more than 1000 grains per sample to obtain a basic population for the synthetic aliquot modelling, which more closely resembles the natural variation of individual grain properties occurring in a certain sample. Furthermore, a threshold value for a maximum averaging effect still needs to be defined. However, the analysis of the modelled synthetic aliquots has clearly demonstrated the importance of single grain analyses to determine a suitable aliquot size for single aliquot measurements in order to be able to detect incomplete bleaching. For the analysed samples the effect of signal averaging is most likely to become a limiting factor in terms of bleaching assessment for aliquots containing 200 or more grains. This might also explain why a significant drop in D_e could not be proved for a reduction of aliquot size from medium (4mm diameter, ~800 grains) to small (2mm diameter, ~200 grains) aliquots for incompletely bleached samples (cf. sections 5, 7).

On the basis of the findings from the straightforward modelling approach proposed here, we strongly suggest using single grain measurements as a tool to characterise the signal contribution to the overall cumulated OSL signal from individual grains in order to be able to set up a maximum aliquot size that still allows the detection of incomplete bleaching. Samples showing a rather uniform signal contribution would require the measurement of smaller aliquot sizes as opposed to samples showing large variation in relative signal intensity and the existence of few very bright grains. For the latter, larger aliquots might still allow the detection of incomplete resetting from a SAR dataset. Additionally the aliquot size should be defined by the number of grains and not by aliquot diameter (as usually done). Differences in grain size distribution within the grain size fraction used for the measurements and different aliquot preparation procedures might result in significantly different numbers of grains on aliquots with the same diameter.

10.6. A welcome side-effect

Various authors (e.g. Vandenberghe et al., 2003; Mayya et al., 2006; Lomax et al., 2007) have pointed out that microdosimetriy may have a significant effect on equivalent dose distributions on the single grain level. The inhomogeneous distribution of beta radiation within sediments is assumed to result in different dose rates for individual grains. These small-scale variations in radiation dose are regarded as an additional extrinsic source of scatter apart from incomplete bleaching. Like the latter, they are assumed to cause asymmetry in single grain D_e distributions (Duller, 2008; Mayya et al., 2006). As stated above, the Althüttendorf and Macherslust samples did not show significantly skewed dose distributions for all measured aliquot sizes. Furthermore, there is no clear trend of rising skewness values with decreasing aliquot size for the individual samples. By contrast, the Eberswalde samples have shown positively skewed dose distributions for all aliquot sizes (not only on the single grain level as would be expected for skewness caused by microdosimetric effects) and also lack a trend of increasing skewness for small aliquots and single grains. It is therefore concluded that microdosimetric effects, if present, do not have a significant influence on the single grain D_e distributions obtained from sandur sediments of the Pomeranian IMP.

10.7. Concluding remarks

In a straightforward modelling approach based on the luminescence intensities of 1000 single grains for each sample, the cumulative signal composition of multigrain aliquots was investigated. This modelling approach might serve as a powerful tool in assessing the maximum aliquot size for multigrain aliquots in order to prevent signal averaging from inhibiting the detection of incomplete resetting of the OSL signal.

The comparison of equivalent doses and corresponding ages from different aliquot sizes and single grains of quartz has proved the single grain based ages obtained for the Pomeranian IMP to be reliable. No significant influence of microdosimetric effects could be observed.

11. Summarising discussion

The results of the individual subchapters of this study have already been discussed in detail in the corresponding sections. Here, the main findings and issues will be briefly summarised and discussed in a broader perspective in order to achieve a coherent, synthetic evaluation of the overall results of this study. In addition, perspectives for future research based on the results of this study will be introduced.

11.1. Quartz OSL dating of fluvioglacial (sandur) sediments

As expected from previous research (cf. section 1.2), incomplete resetting of the OSL signal prior to deposition turned out to be the main challenge in OSL dating of fluvioglacial (sandur) sediments within this study. Analysis of a set of different indicator values (e.g., skewness and kurtosis of dose distributions, cf. sections 5 and 9) showed that all fluvioglacial samples from the Brandenburg IMP and some of the samples from the Pomeranian IMP were incompletely bleached. As suggested by Galbraith et al. (2005) and Preusser et al. (2007), for example, the comparison of threshold values for different measures of scatter (RSD, overdispersion) derived from well bleached analogue samples turned out to be a practicable, reliable approach for the identification of incompletely bleached samples and the subsequent calculation of the burial dose using different minimum age models (cf. section 5 & 9). For the samples from the Beelitz outwash cone (cf. section 5 & 7), well bleached samples from periglacial cover sediments were used to establish threshold values for incomplete bleaching and subsequent D_e calculation. Well bleached fluvioglacial samples from neighbouring sampling sites (Althüttendorf, cf. section 9) provided the threshold values for the equivalent dose calculations for the incompletely bleached Eberswalde samples (cf. sections 9 & 10). As to the choice of an appropriate statistical age model, comparative calculations conducted within this study have shown that the results from different minimum age model approaches agree within error with samples from Beelitz and Eberswalde (cf. section 5 & 9). These findings are in good agreement with those of Fuchs et al. (2007), for example. The decision which model should be applied for a specific sample should therefore be based on the characteristics of the respective dose distribution.

As suggested by Duller (2008) for the measurement of incompletely bleached samples, single grain and small aliquot measurements were conducted for samples from the Brandenburg and Pomeranian IMP (cf. sections 5, 6, 7, 9, 10). For the samples from the Pomeranian IMP comparative measurements of ~800 grain (medium) and ~200 grain (small) aliquots for well bleached samples have proved the single grain measurements to be reliable (cf. section 9 & 10). However, the single grain measurements also revealed different luminescence characteristics for samples from the Pomeranian IMP and the Brandenburg IMP (for example, expressed by significantly higher overdispersion values for samples from the Brandenburg IMP, cf. section 7). For the latter no single grain data from well bleached analogue samples are available. Given that, the reliability of the ages based on these measurements remains questionable to a certain degree. Additional single grain OSL measurements are needed in order to provide a larger population of D_e values for statistical

analyses. With respect to the very low proportion of D_e values passing the applied set of rejection criteria (cf. section 7), it seems advisable to use the results from single grain measurements to determine an adequate aliquot size for small aliquot measurements (cf. section 10). The modelling approach introduced in section 10 might serve as a powerful tool for that purpose. However, a threshold value for a critical averaging effect to be derived from the synthetic aliquot modelling still needs to be established and verified. Once that is achieved, aliquot sizes can be determined on a robust statistical basis and deduced individually for each sample. The latter is of great importance because the single grain measurements conducted within this study revealed different luminescence characteristics (especially concerning the brightness of individual grains) even for samples from identical stratigraphical units.

For some of the samples from the Vevais section, dose rate related problems (a common difficulty in limnic and related environments, Preusser et al., 2008) impeded reliable age determination by means of quartz OSL dating techniques (cf. section 8). Unfortunately, it was therefore not possible to 'calibrate' the latter with the independent age control from the pollen record as originally intended (cf. section 1.2 & 2.4). To solve the dose rate related problems, IRSL and post-IR YOSL dating techniques for the dating of feldspar as well as a subtraction dating approach were applied. Although already developed in 1981 by McKerrel and Mejdahl, the subtraction dating approach has only rarely been used in recent studies (e.g., Davids et al., 2010). Based on the given palynological age control from a sequence of lake marls encompassed within the sediment succession, the ‘subtraction ages’ were proved to be reliable.

11.2. Interpretation of geochronometrical data derived from glacial landscapes

Within section 4 a process-based interpretation for numerical ages from OSL and SED in glacigenic landscapes was introduced. OSL of sandur sediments and SED of glacigenic boulders on endmoraine crests were identified as the most suitable techniques for the dating of ice marginal positions. However, whereas OSL of sandur sediments makes it possible to date the presence of an active ice margin at a certain IMP, SED of glacigenic boulders dates the final stabilisation of the landscape surface. This implies a significant time lag between the ages obtained by the two methods because secondary deglaciation (in sensu Everest & Bradwell, 2003) and the persistence of periglacial processes delay the stabilisation of the landscape surface after the initial retreat of active ice from an IMP (cf. section 4). The comparison of OSL ages of sandur sediments from the Pomeranian IMP with exposure ages of erratic boulders (cf. section 9) have reliably validated this process-based interpretation pattern. However, the combination of both SED and OSL dating methods allows a detailed reconstruction of regional deglaciation patterns, as will be shown in section 11.3. Based on these findings, a reassessment of previously published exposure ages for erratic boulders and their significance for the dating of IMPs is recommended (cf. section 9). By applying the Finite Mixture Model to a set of exposure ages attributed to the Pomeranian IMP it was possible to discern significantly different populations of boulder ages from the dataset (cf. section 9), with the oldest population showing

ages in agreement with those derived from OSL dating of sandur sediments. This application of the FMM as a 'maximum age model' may serve as a tool for the proposed reassessment of previously published exposure ages. Nevertheless, the calculation of average ages needs to be handled with care because they might obscure geochronological details and regional differences in landscape development (cf. sections 4 & 9).

11.3. Geochronological implications

11.3.1. Timing of the last glacial-interglacial cycle and the onset of the Weichselian glaciation

Despite methodological challenges, reliable ages for the last glacial-interglacial cycle were derived from the Saalian-Eemian-Weichselian sedimentary sequence exposed near the village of Vevais (cf. section 8). The onset of the Eemian was dated to 126 ±16 ka. The beginning climatic transition from the Eemian to the Weichselian cold stage was dated to 109 ±9 ka. This is in excellent agreement with the marine isotope record (MIS 5e equivalent to the Eemian interglacial) as well as the results from the continuous varve record of Lago Grande di Monticchio (Brauer et al., 2007). There is still no evidence for an ice advance to the north-eastern German lowland as early as MIS 4 (reliable evidence of such an advance exists for Denmark, Houmark-Nielsen, 2007).

11.3.2. A new deglaciation chronology for north-eastern Germany

The Brandenburg IMP

The ice advance to the Brandenburg IMP was formerly estimated to have occurred at about 20-24 ka (cf. section 2.3.1). In the course of this study, three ages from SED using ^{10}Be of erratic boulders from between the Brandenburg and Frankfurt IMPs were published (Heine et al., 2009). The ages range between 19.0 ± 0.8 ka and 21.2. ± 0.7 ka (corrected for snow and vegetation cover and erosion, corresponding to 18.3 ±0.9 ka and 20.5 ±0.7 ka without corrections) and provide a minimum age for the Brandenburg IMP in the area. For Poland, Marks (in press) states an age of 24 ka for the Lezno phase which corresponds to the Brandenburg phase in Germany. This age is based on the reinterpretation of ^{10}Be (Rinterknecht et al., 2006a) and ^{36}Cl (Dzierzek and Zreda, 2007) ages of erratic boulders from the area attributed to the Lezno phase. Dzierzek and Zreda (2007) themselves state an age of 27-28 ka for the LGM ice advance in north-eastern Poland. However, Rinterknecht et al. themselves (2006b) report an age of 19 ±1.6 ka for the age of the "LGM" moraine, by calculating an error-weighted mean from 15 ^{10}Be ages of erratic boulders from IMPs attributed to the LGM in Lithuania and Belarus. In 2008 they reported an age of 18.3 ±0.8 ka for the initial retreat of the SIS from the LGM position (Grūda moraine) in Lithuania (Rinterknecht et al., 2008), based on the same dataset already published in Rinterknecht et al. (2006a). The same applies to the LGM in Belarus. Rinterknecht et al. (2007) give an age of 17.7 ±2.0 ka for the initial retreat of the ice from its LGM position (Orsha moraine) in Belarus. However, they also argue that the ice advance to the LGM moraines in Belarus did not occur before 19.2 ±0.2 cal. kyr BP in the north-eastern part of the country and 22.3 ±1.5 cal. kyr BP in the western part of the country (based on results from radiocarbon dating).

In this study, the following ages were obtained from fluvioglacial sandur sediments from the Brandenburg IMP :

- 34.1 ±3 ka (based on single aliquot measurements, maximum age from the Beelitz outwash cone, cf. section 5)
- 34.4 ±7 ka (based on single aliquot measurements, maximum age from the Luckenwalde outwash plain, cf. section 6)
- 27.7 ±4 ka (based on single grain measurements from the Beelitz outwash cone, cf. section 7).

When the time lag between initial sandur formation and final boulder deposition is taken into account (cf. section 4, also observed for the Pomeranian IMP, cf. section 9), the single grain based age is in good agreement with the oldest boulder age of Heine et al. (2009) from the hinterland of the Brandenburg IMP and Marks' (2010) interpretation of the exposure ages from Poland. The age of 27-28 ka stated by Dzierzek and Zreda (2007) for the LGM ice advance in Belarus even matches the single grain based age very well. The fact that most of the ages calculated by Rinterknecht et al. (2006a/b, 2007, 2008) are significantly younger may be explained by the way the ages are calculated. By stating an error-weighted mean, different phases of exposure documented within the dataset may get lost. In fact, three individual boulders from Lithuania and Belarus show ages > 22 ka (within error, the dataset contains 15 boulder ages, two of which are > 50 ka due to inheritance effects and four of which show Younger Dryas to Holocene ages due to post-depositional exhumation). The single grain based OSL age of sandur sediments from the Brandenburg IMP therefore indicates an ice advance that occurred at around 24-32 ka, which is in good agreement with results from SED. However, given the various uncertainties affecting single grain OSL ages (cf. section 7) it seems to be more appropriate to state the single aliquot based maximum ages of ~34 ka for the Brandenburg IMP. More dating work is obviously needed to be able to state the age of the Brandenburg IMP more precisely.

The Pomeranian IMP

The OSL ages obtained for samples from outwash plains of the Pomeranian IMP have been discussed in detail in sections 9 & 10. The initial sandur formation was dated to 20.1 ± 1.6 ka (Althüttendorf outwash cone). The final sandur formation was dated to 19.4 ± 2.4 ka (Klosterbrücke outwash fan, Eberswalde). Final stabilisation of the Pomeranian terminal moraine at 16.4 ± 0.7 ka can be deduced from SED of erratic boulders (Heine et al., 2009, Rinterknecht et al., in press). A period of boulder stabilisation at 15.2 ± 0.5 ka in the area of the Gerswalde terminal moraine indicates further retreat of the active ice margin during the Gerswalde subphase. The melting of dead ice buried within the glaciofluvial sediments of the Angermünde subphase has been dated to 14.7 ± 1.0 ka.

Evidence for a twofold LGM in north-eastern Germany

Summarising the results from the previous sections, there is clear evidence for a twofold LGM in north-eastern Germany. The older advance of the Brandenburg phase occurred after ~34 ka, with first results from single grain analyses indicating a minimum age of ~24 ka. The ice advance during the Pomeranian phase occurred at around ~20 ka and therefore represents the climatic LGM as reconstructed

from the marine isotope record. It shaped the most prominent ice marginal features (terminal moraines and outwash plains) in north-eastern Germany. By contrast, there are strong indications that the ice advance to the southernmost IMP in the research area, the Brandenburg IMP, only reshaped a relief initially generated by the Saalian glaciation. Sandur sediments from the Luckenwalde outwash plain were dated to 130-150 ka (corresponding to the Warthe stage of the Saalian glaciation, cf. section 6). The results from gravel analyses at Luckenwalde further suggest that transformation of the relief was mainly linked to meltwater processes. This implies a fast-paced and short-lived ice advance to the Brandenburg IMP. This is corroborated by the different bleaching characteristics of the samples from the Pomeranian IMP and the Brandenburg IMP. Although samples were taken from sediments associated with identical sedimentary environments (outwash plains, proximal position to the former ice margin, characterised by high turbidity flow – implying possibly disadvantageous bleaching conditions) all sandur samples from the Brandenburg IMP showed incomplete resetting of the OSL signal, whereas the majority of samples from the Pomeranian IMP showed good bleaching characteristics. This might indicate a very limited reworking of the fluvioglacial sediments on the elevated outwash cones of the Brandenburg IMP, with meltwater flow from stagnant or even dead ice probably quickly shifting to the complex fluvioglacial channel system (cf. sections 6 & 2.4).

Just recently Johnsen et al. (in press) have given evidence for an interstadial from 25-20 ka in western Norway based on OSL and radiocarbon dating (similar observations from the southern Alps were reported by Monegato et al., 2007). They suggest that the area was ice-free at around 21-22 ka, dividing the LGM into two stadials. Furthermore, they argue that these effects were most likely not restricted to the western part of the SIS, but would also have affected the other sectors of the dynamic ice sheet. As stated above, there is clear evidence from the results of this study that the described scenario indeed applies to north-eastern Germany as well because OSL ages and geomorphological findings from the Brandenburg IMP indicate a fast-paced ice advance early in MIS 2, the initial boulder stabilisation in the area north of the Brandenburg IMP has been dated to ~21 ka (depending on correction factors for snow and vegetation, Heine et al., 2009), indicating ice free conditions in the area, and finally, the initial sandur formation at the Pomeranian IMP set in at around 20 ka, documenting the readvance of an active ice sheet to north-eastern Germany.

12. Overall Conclusions

Within this last section, the main findings of this study will be briefly summarised.

Although for some samples incomplete bleaching remains a limiting factor even on the single grain level and the obtained ages still have to be regarded as maximum ages, the methodological aims of the study were basically achieved. OSL dating techniques were successfully applied for the dating of Weichselian and (unexpectedly) Saalian sandur sediments and a set of tools was compiled and successfully applied to detect and correct for incomplete resetting of the OSL signal. Statistical minimum age model approaches for the evaluation of D_e datasets for incompletely bleached samples have to permit the

calibration of the statistical model according to threshold values derived from analogue well bleached samples. For future studies the analysis of single grain luminescence characteristics of individual samples is strongly recommended in order to be able to define adequate aliquot sizes (defined by the number of grains, not aliquot diameter) for single aliquot measurements.

Concerning the second methodological aim of the study, the assessment of the comparability of ages derived from OSL and SED, it was shown that different dating techniques enable the dating of different processes of the glacial landscape development. While OSL of sandur sediments enables the determination of an age for the presence of an active ice margin at an IMP, the ages obtained from SED of glacigenic boulders date the final stabilisation of the landscape surface. This causes a significant time lag between ages for IMPs derived from OSL and SED, as observed from the comparison of ages from the Pomeranian IMP. A reassessment strategy for previous exposure ages is suggested, and the use of the FMM as a maximum age model is proposed.

To reflect recently developed dynamic concepts of ice sheets, the use of age-derived isochroneity in ice marginal positions, rather than the use of morphostratigraphical definitions resulting in time transgressiveness is proposed. Based on the OSL ages from this study and a reinterpretation of ^{10}Be ages for glacigenic boulders according to the strategy laid out above, the first deglaciation pattern for north-eastern Germany based on results from numerical dating methods was established and the major aim of this study was thereby achieved. It can be summarised as follows:

- Brandenburg phase: LGM-1 (maximum extent of the Weichselian SIS in the research area), fluvioglacial reworking of Saalian outwash deposits (130-150 ka, Warthe stage, quartz OSL age, this study) at Luckenwalde and the deposition of sandur sediments on the Beelitz outwash cone at <34 ka (maximum age, quartz OSL, this study).
- First phase of boulder stabilisation in the area between the Brandenburg and Pomeranian IMP at 21-20 ka (^{10}Be SED, Heine et al., 2009).
- Pomeranian phase: LGM-2 (corresponding to the LGM derived from the marine isotope record) associated with the formation of the Pomeranian IMP at 20.1 ±1.6 ka (Althüttendorf outwash cone, quartz OSL, this study) to 19.4 ±2.4 ka (Klosterbrücke outwash fan, quartz OSL, this study).
- Final stabilisation of the Pomeranian terminal moraine at 16.4 ± 0.7 ka (^{10}Be SED, Heine et al., 2009, Rinterknecht et al., in press).
- General stabilisation of the landscape surface at around 15 ka most probably due to the termination of a periglacial activity phase indicated by:
  - A phase of boulder stabilisation in the terminal moraines associated with the recessional Gerswalde subphase (^{10}Be SED, Rinterknecht et al., in press).
  - The stabilisation of periglacial cover sediments as observed for the Beelitz outwash cone (quartz OSL, this study).

- The meltout of buried dead ice as deducible from the deposition of glaciolacustrine to glaciofluvial sediments in a developing dead ice depression at the Macherslust sampling site (quartz OSL, this study).

However, some points remain to be clarified in the course of future studies. First, the Brandenburg IMP needs to be reinvestigated in order to be able to state its precise age. Second, the geochronological position of the Frankfurt IMP, which is situated between the Brandenburg and the Pomeranian IMP, remains to be clarified. Finally, recessional IMPs and especially those associated with the Mecklenburg ice advance should also be dated in order to fully reconstruct the deglaciation pattern of the Weichselian SIS in north-eastern Germany from its maximum extent at the Brandenburg IMP to its retreat beyond the recent shoreline of the Baltic Sea.

13. Appendix

13.1. Overall reference list

Aitken, M.L., 1985. Thermoluminescence dating. Studies in archaeological science. Academic Press, London, 359 p.

Albrecht, J., 1999. Initial ice movement directions from the East and South South East during a late Weichselian readvance in NE Germany. Eiszeitalter & Gegenwart 49, 55-70.

Alexanderson, H., Eskola, K.O., Helmens, K.F., 2008. Optical dating of a late Quaternary sediment sequence from Sokli, Northern Finland. Geochronometria 32, 51-59.

Alexanderson, H., Murray, A.S., 2007. Was southern Sweden ice free at 19-25 ka, or were the post LGM glacifluvial sediments incompletely bleached?. Quaternary Geochronology 2, 229-236.

Andersen, B.G., 1981. Late Weichselian ice sheets in Eurasia and Greenland. In: Denton, G.H., Hughes, T.J., (eds.). The Last Great Ice Sheets. New York, Wiley. 3-65.

Arnold, L.J., Roberts, R.G., 2009. Stochastic modelling of multi-grain equivalent dose (D_e) distributions: Implications for OSL dating of sediment mixtures. Quaternary Geochronology 4, 204-230.

Auclair, M., Lamothe, M., Huot, S. 2003. Measurement of anomalous fading for feldspar IRSL using SAR. Radiation Measurements 37, 487-492.

Bailey, R.M., 2000. The interpretation of quartz optically stimulated luminescence equivalent dose versus time plots. Radiation Measurements 32, 129-140.

Bailey, R.M., 2003. Paper I:The use of measurement-time dependent single aliquot equivalent-dose estimates from quartz in the identifcation of incomplete signal resetting. Radiation Measurements 37, 673-683.

Bailey, R.M., Arnold, L.J. 2006. Statistical modelling of single grain quartz De distributions and an assessment of procedures for estimating burial dose. Quaternary Science Reviews 25, 2475-2502.

Bailey, R. M., Smith, B. W., Rhodes, E. J. 1997. Partial bleaching and the decay form characteristics of quartz OSL. Radiation Measurements 27, 123-136.

Balco, G., Stone, J.O.H, Porter, S.C., Caffee, M.W., 2002. Cosmogenic-nuclide ages for New England costal moraines, Martha's Vineyard and Cape Cod, Massachusetts, USA. Quaternary Science Reviews 21, 2127-2135.

Balescu, S., Lamothe, M., 1994. Comparison of TL and IRSL age estimates of feldspar coarse grains from waterlain sediments. Quaternary Geochronology 13, 437-444.

Ballarini, M., 2006. Optical dating of quartz from young deposits. IOS Press, Amsterdam.

Ballarini, M., Wallinga, J., Duller, G.A.T., Brouwer, J.C., Bos, A.J.J., Van Eijk, C.W.E. 2005. Optimizing detection filters for single-grain optical dating of quartz. Radiation Measurements 40, 5-12.

Ballarini, M., Wintle, A.G., Wallinga, J. 2006. Spatial variation of dose rate from beta sources as measured using single grains. Ancient TL 24, 1-8.

Bateman, A., Boulter, C.H., Carr, A.S., Frederick, C.D., Peter, D., Wilder, M., 2007. Detecting post-depositional sediment disturbance in sandy deposits using optical luminescence. Quaternary Geochronology 2, 57-64.

Bateman, M.D., Frederick, C.D., Jaiswal, M.K., Singhvi, A.K., 2003. Investigations into the Potential Effects of Pedoturbation on Luminescence Dating. Quaternary Science Reviews 22, 1169-1176.

Behrmann, W., 1949/50. Die Umgebung Berlins nach morphologischen Formengruppen betrachtet. Die Erde 1, 93-122.

Benn, D.I., Owen, L.A., 2002. Himalayan glacial sedimetary environments: a framework for reconstructing and dating the former extent of glaciers in high mountains. Quaternary International 97-98, 3-25.

Bennett, M.R., 2003. Ice streams as the arteries of an ice sheet: their mechanics, stability and significance. Earth-Science Reviews 61, 309-339.

Bernhardi, A., 1832. Wie kamen die aus dem Norden stammenden Felsbruchstücke und Geschiebe, welche man in Norddeutschland und den benachbarten Ländern findet, an ihre gegenwärtigen Fundorte?. Jahrbuch für Mineralogie, Geognosie, Geologie und Petrefaktenkunde 3, 257-267.

Bøe, A.-G., Murray, A., Dahl, S.O., 2007. Resetting of sediments mobilised by the LGM ice-sheet in southern Norway. Quaternary Geochronology 2, 222-228.

Böse, M., 1989. Methodisch-stratigraphische Studien und paläomorphologische Untersuchungen zum Pleistozän südlich der Ostsee. Berliner Geographische Abhandlungen 54.

Böse, M., 1994. Ice margins and deglaciation in the Berlin area between Brandenburg and Frankfurt end moraines – a review. Zeitschrift für Geomorphologie N.F., Suppl. 95, 1-6.

Böse, M., 1995. Problems of dead ice and ground ice in the central part of the North European plain. Quaternary International 28, 123-125.

Böse, M., 2005. The Last Glaciation and Geomorphology. In: Koster, E. A., (ed.). The Physical geography of Western Europe. Oxford University Press, 61-74.

Böse, M., Brande, A., 2000. Regional Pattern of Holocene Sand Transport in the Berlin-Brandenburg Area. In: Dulias, R., Pelka-Gosciniak, J. (eds.), Aeolian Processes in different Landscape Zones. University of Silesia, Faculty of Earth Sciences & Association of Polish Geomorphologists, Sosnowiec, 51-58.

Böse, M., Górska, M., 1995. Lithostratigraphical Studies in the outcrop at Uj'scie, Torún-Eberswalde Pradolina, western Poland. Eiszeitalter und Gegenwart 45, 1-14.

Böse, M., Kozarski, S., 1994. Last Ice Sheet Dynamics and Deglaciation in the North European Plain. Zeitschrift für Geomorphologie 95 (supplement), 1-6.

Bøtter-Jensen, L., Andersen, C.E., Duller, G.A.T., Murray, A.S. 2003a. Developements in radiation, stimulation and observation facilities in luminescence measurements. Radiation Measurements 37, 535-541.

Bøtter-Jensen, L., Bulur, E., Duller, G.A.T., Murray, A.S., 2000. Advances in luminescence instrument systems. Radiation Measurements 32, 523-528.

Bøtter-Jensen, L., McKeever, S.W.S., Wintle, A.G., 2003b. Optically Stimulated Luminescence Dosimetry. Elsevier, Amsterdam, 355p.

Boulton, G.S., Dongelmans, P., Punkari, M., Broadgate, M., 2001. Palaeoglaciology of an ice sheet through a glacial cycle: the European ice sheet through the Weichselian. Quaternary Science Reviews 20, 591-625.

Bowen, D.Q., Phillips, F.M., McCabe, A.M., Knutz, P.C., Sykes, G.A., 2002. New data for the Last Glacial maximum in Great Britain and Ireland. Quaternary Science Reviews 21, 89-101.

Brauer, A., Allen J.R.M., Mingram, J., Dulski, P., Wulf, S., Huntley, B., 2007. Evidence for last interglacial chronology and environmental change from Southern Europe. Proceedings of the National Academy of Sciences 104, 450-455.

Brauer, A., Tempelhoff, K., Murray, A., 2005. OSL Dating of Fine-Grained Sand Deposits and ist Implications for Glacial Stratigraphy and Landscape Evolution: Research Results from Stolzenhagen, Northeastern Brandenburg. Die Erde 136, 15-35.

Brose, F. 1978. Weichselglaziale Rückzugsstaffeln im Hinterland der Eisrandlage des Pommerschen Stadiums südlich von Angermünde. Wissenschaftliche Zeitschrift der Ernst-Moritz-Arndt-Universität Greifswald, mathematisch-naturwissenschaftliche Reihe 27-1/2, 17-19.

Brose, F., 1995. Erscheinungen des weichselzeitlichen Eisrückzuges in Ostbrandenburg. Brandenburgische Geowissenschaftliche Beiträge 1995 (1), 3-11.

Brose, F., Luckert, J., Müller, H., Schulz, R., Strahl, J., Thieke, H.-U., 2006. The Eemian of Vevais – an important geotope of the Eastern Brandenburg area. Brandenburgische Geowissenschaftliche Beiträge 13 (1/2), 155-164.

Brose, F., Piotrowski, A., Schroeder, J.H., 2003. I-3.4.1 Entwicklung des Oderbruchs: Neue Daten zur Sedimentfüllung der Oderbruchdepression. In: Schroeder, J.H., Brose, F. (eds.). Führer zur Geologie von Berlin und Brandenburg Nr. 9: Oderbruch – Märkische Schweiz – Östlicher Barnim. Berlin, 57-65.

Bubenzer, O., Hilgers, A., Riemer, H., 2007. Luminescence dating and archaeology of Holocene fluvio-lacustrine sediments of Abu Tartur, Eastern Sahara. Quaternary Geochronology (2), 314-321.

Cepek, A.G., 1965. Die Stratigraphie der pleistozänen Ablagerungen in Norddeutschen Tiefland. In: Gellert, J.F. (Ed.), Die Weichsel-Eiszeit im Gebiet der DDR, 45-65.

Davids, F., Duller, G.A.T., Roberts, H.M., 2010. Testing the use of feldspars for optical dating of hurricane overwash deposits. Quaternary Geochronology 5, 125-130.

DeCorte, F., Vandenberghe, D., Hossain, S.M., De Wispelaere, A., Van den Haute, P., 2004. The effect of different sample-calibrant composition in gamma-ray spectrometry for the assessment of the radiation dose rate in the luminescence dating of sediments. Journal of Radioanalytical and Nuclear Chemistry 262, 261-267.

Degering, D., Krbetschek, M.R., 2007. Dating of Interglacial Sediments by Luminescence Methods. In: Sirocko, F., Claussen, M., Sánchez Goñi, M.F., Litt, T. (eds.). The Climate Of Past Interglacials. Elsevier, Amsterdam, 157-172.

Duller, G. A. T. 1994. Luminescence dating of poorly bleached sediments from Scotland. Quaternary Science Reviews 13, 521–524.

Duller, G.A.T. 2003. Distinguishing quartz and feldspar in single grain luminescence measurements. Radiation Measurements 37, 161-165.

Duller, G.A.T., 2006. Single grain optical dating of glacigenic deposits. Quaternary Geochronology 1, 296-304.

Duller, G.A.T., 2007. Luminescence Analyst v3.24. Analysis Software for Data from Risø Systems. Aberystwyth Luminescence Laboratory. University of Wales.

Duller, G.A.T., 2008. Single-grain optical dating of Quaternary sediments: why aliquot size matters in luminescence dating. Boreas 37, 589-612.

Dzierzek, J., Zreda, J., 2007. Timing and style of deglaciation of northeastern Poland from cosmogenic 36Cl dating of glacial and glaciofluvial deposits. Geological Quarterly 51-2, 203-216.

Ehlers, J., 1990. Reconstructing the dynamics of the North-West European Pleistocene ice sheets. Quaternary Science Reviews 9, 71-83.

Ehlers, J., Eissmann, L., Lippstreu, L., Stephan, H.-J., Wansa, S. 2004: Pleistocene glaciations of North Germany. In Ehlers, J., Gibbard, P.L. (eds.): Quaternary Glaciations Extent And Chronology – Part I: Europe. Amsterdam, 135-146.

Ehlers, J., Gibbard, P.L. (eds.) 2004. Quaternary Glaciations Extent And Chronology – Part I: Europe. Amsterdam.

Erd, K., 1973. Pollenanalytische Gliederung des Pleistozäns der Deutschen Demokratischen Republik. Zeitschrift für Geologische Wissenschaften 1 (9), 1087–1103.

Everest, J., Bradwell, T., 2003. Buried glacier ice in southern Iceland and its wider significance. Geomorphology 52, 347-358.

Feathers, J.K., 2003. Single-grain OSL dating of sediments from the Southern High Plains, USA. Quaternary Science Reviews 22, 1035-1042.

Franz, H.-J., 1961. Morphogenese der Jungmoränenlandschaft des westlichen Brandenburger Stadiums – Teil 1: Die Eisrandlagen. In: Wissenschaftliche Zeitschrift der Pädagogischen Hochschule Potsdam, Math.-Naturw. Reihe 7 (1/2), 29-48.

Fuchs, M., Lang, A., 2001. OSL dating of coarse-grain fluvial quartz using single-aliquot protocols on sediments from NE Peloponnese, Greece. Quaternary Science Reviews 20, 783-787.

Fuchs, M., Owen, L.A., 2008. Luminescence dating of glacial and associated sediments: review, recommendations and future directions. Boreas 37, 636-659.

Fuchs, M., Straub, J., Zö ller, L., 2005. Residual luminescence signals of recent river flood sediments: a comparison between quartz and feldspar of fine- and coarse-grain sediments. Ancient TL 23, 25-30.

Fuchs, M., Wagner, G.A., 2003. Recognition of insufficient bleaching by small aliquots of quartz for reconstructing soil erosion in Greece. Quaternary Science Reviews 22, 1161-1167.

Fuchs, M., Woda, C., Bürkert, A., 2007. Chronostratigraphy of a sediment record from the Hajar mountain range in north Oman: Implications for optical dating of insufficiently bleached sediments. Quaternary Geochronology 2, 202-207.

Galbraith, R.F., Roberts, R.G., Laslett, G.M., Yoshida, H., Olley, J.M., 1999. Optical dating of single and multiple grains of Quartz from Jinmium rock shelter, northern Australia: Part I, experimental design and statistical models. Archaeometry 41 (2), 339-364.

Galbraith, R.F., Roberts, R.G., Yoshida, H., 2005. Error variation in OSL palaeodose estimates from single aliquots of quartz: a factorial experiment. Radiation measurements (39), 289-307.

Gärtner, P., Behrendt, L., Bussemer, S., Marcinek, J., Markuse, G., Schlaak, N. 1995. Quartärmorphologisches Nord-Südprofil durch Brandenburg. Berichte zur deutschen Landeskunde 69-2, 229-262.

Geikie, J. 1894. The Great Ice Age and Its Relation to the Antiquity of Man. Stanford, London.

Geikie, J. 1895. Classification of European glacial deposits. Journal of Geology 3, 241-269.

Genieser, K., 1957. Neue Daten zur Flußgeschichte der Elbe. In: Eiszeitalter und Gegenwart 13, 141-156.

Geyh, M.A., Müller, H., 2005. Numerical ^{230}Th/U dating and a palynological review of the Holsteinian/Hoxnian Interglacial. Quaternary Science Reviews 24, 1861-1872.

Geyh, M.A., Müller, H., 2006. Missing evidence for two Holstein-like Interglacials. Reply to the comments by J.D. Scourse on: Numerical ^{230}Th/U dating and a palynological review of the Holsteinian/Hoxnian Interglacial. Quaternary Science Reviews 25, 3072-3073.

Godfrey-Smith, D.I., Huntley, D.J., Chen, W.H., 1988. Optical dating studies of quartz and feldspar sediment extracts.Quaternary Science Reviews 7, 379–385.

Gosse, J.C., 2005. The Contribution of Cosmogenic Nuclides to Unraveling Alpine Paleoclimate Histories. In: Huber, U.M., Bugmann, H.K.M., Reasoner, M.A. (eds.). Global Change and Mountain Regions. Advances in Global Change Research 23, 39-49.

Gosse, J.C., Phillips, F.M., 2001. Terrestrial in situ cosmogenic nuclides: Theory and application. Quaternary Science Reviews 20, 1475-1560.

Greenwood, S.L., Clark, C., 2009. Reconstructing the last Irish Ice Sheet 1: changing flow geometries and ice flow dynamics deciphered from the glacial landform record. Quaternary Science Reviews 28, 3085-3100.

Gripp, K., 1924. Über die äußerste Grenze der letzten Vereisung in Nordwest-Deutschland. Mitteilungen der Geographischen Gesellschaft in Hamburg 36, 159-245.

Guobyte, R. 2004. A brief outline of the Quaternary of Lithuania and the history of ist investigation. In Ehlers, J., Gibbard, P.L. (eds.): Quaternary Glaciations Extent And Chronology – Part I: Europe. Amsterdam, 245-250.

Gyllencreutz, R., Mangerud, J., Svendsen, J.-I., Lohne, Ø., 2007. DATED – A GIS based reconstruction and dating database of the Eurasian deglaciation. Geological Survey of Finland, Special Paper 46, 113-120.

Hallet, B., Putkonen, J., 1994. Surface Dating of Dynamic Landforms: Young Boulders on Aging Moraines. Science 265, 937-940.

Heine, K., Reuther, A.U., Thieke, H.U., Schulz, R., Schlaak, N., Kubik, P.W., 2009. Timing of Weichselian ice marginal positions in Brandenburg (northeastern Germany) using cosmogenic in situ 10Be. Zeitschrift für Geomorphologie N.F. 53 (4), 433-454.

Hermsdorf, N., Strahl, J., 2008. Eemian deposits in the Brandenburg area. Brandenburgische Geowissenschaftliche Beiträge 15 (1/2), 23-55.

Hilgers, A., 2007. The chronology of Late Glacial and Holocene dune development in the northern Central European lowland reconstructed by optically stimulated luminescence (OSL) dating. PhD thesis, Universität zu Köln, Germany.

Hilgers, A., Murray, A.S., Schlaak, N., Radtke, U., 2001. Comparison of quartz OSL protocols using Lateglacial and Holocene dune sands From Brandenburg, Germany. Quaternary Science Reviews, 20, 731-736.

Houmark-Nielsen, M., 2003. Signature and timing of the Kattegat Ice Stream: onset of the Last Glacial Maximum sequence at the southwestern margin of the Scandinavian Ice Sheet. Boreas 32, 227-241.

Houmark-Nielsen, M., 2007. Extent and age of Middle and Late Pleistocene glaciations and periglacial episodes in southern Jylland, Denmark. Bulletin of the Geological Society of Denmark 55, 9-35.

Houmark-Nielsen, M., 2008. Testing OSL failures against a regional Weichselian glaciation chronology from Southern Scandinavia. Boreas 37, 660-677.

Houmark-Nielsen, M., Björck, S., Wohlfarth, B., 2006.'Cosmogenic 10Be ages on the Pomeranian Moraine, Poland': Comments. Boreas 35, 600-604.

Houmark-Nielsen, M., Kjær, K., 2003. Southwest Scandinavia, 40-15 kyr BP: palaeogeography and environmental change. Journal of Quaternary Science 18 (8), 769-786.

Hubbard, A., Bradwell., T., Golledge, N., Hall, A., Patton, H., Sudgen, D., Cooper, R., Stoker, M., 2009. Dynamic cycles, ice streams and their impact on the extent, chronology and deglaciation of the British-Irish ice sheet. Quaternary Science Reviews 28, 758-776.

Hultzsch, A. 1994. Althüttendorf / Groß Ziethen – Blockpackung und Sander. In Schroeder, J.H. (ed.): Führer zur Geologie von Berlin und Brandenburg Nr. 2: Bad Freienwalde – Parsteiner See. Berlin, 116-127.

Huntley, D.J., Baril, M.R., 1997. The K content of the K-feldspars being measured in optical dating or thermoluminescence dating. Ancient TL, 15-1, 11-13.

Huntley, D.J., Godfrey-Smith, D.I., Thewalt, M.L.W., 1985. Optical dating of sediments. Nature 313, 105–107.

Huntley, D.J., Lamothe, M. 2001. Ubiquity of anomalous fading in K-feldspars and the measurements and correction for it in optical dating. Canadian Journal of Earth Sciences 38, 1093-1106.

Hütt, G., Jaeck, I., Tconka, Y., 1988. Optical dating. K-feldspars optical response stimulation spectra. Quaternary Science Reviews, 7. 381-386.

Integovernmental Panel on Climate Change (ed.). 2007. Climate Change 2007: Synthesis Report. 73p.

Ivy-Ochs, S., Kerschner, H., Schlüchter, C., 2007. Cosmogenic nuclides and the dating of Lateglacial and Early Holocene glacier variations: The alpine perspective. Quaternary International 164-165, 53-63.

Ivy-Ochs, S., Kober, F., 2008. Surface exposure dating with cosmogenic nuclides. Eiszeitalter und Gegenwart 57 (1/2), 179-209.

Jacobs, Z., Duller, G.A.T., Wintle, A.G. 2006. Interpretation of single grain De distributions and calculation of De. Radiation Measurements 41, 264-277.

Jarvis, A., Reuter, H.I.,Nelson, A., Guevara, E., 2006. Hole-filled seamless SRTM data V3, International Centre for Tropical Agriculture (CIAT), available from http://srtm.csi.cgiar.org.

Jennings, C.E., 2006. Terrestrial ice streams – a view from the lobe. Geomorphology 75, 100-124.

Johnsen, F.J., Olsen, L., Murray, A.S., in press. OSL ages in central Norway support a MIS 2 interstadial (25e20 ka) and a dynamic Scandinavian ice sheet, Quaternary Science Reviews, doi:10.1016/j.quascirev.2010.10.007

Juschus, O., 2001. Das Jungmoränenland südlich von Berlin - Untersuchungen zur jungquartären Landschaftsentwicklung zwischen Unterspreewald und Nuthe, (dissertation at the Humboldt Universität zu Berlin). http://edoc.hu-berlin.de/dissertationen/juschus-olaf-2001-05-04/PDF/Juschus.pdf. 251 p. Berlin.

Juyal, N., Chamyal, L.S., Bhandari, S., Bhushana, R., Singhvi, A.K., 2006. Continental record of the southwest monsoon during the last 130 ka: evidence from the southern margin of the Thar Desert, India. Quaternary Science Reviews 25, 2632–2650.

Kalm, V., in press (2010). Ice-flow pattern and extent of the last Scandinavian Ice Sheet southeast of the Baltic Sea. Quaternary Science Reviews, in press, doi:10.1016/j.quascirev.2010.01.19.

Keilhack, K., 1895. Die Geikie'sche Gliederung der nordeuropäischen Glacialablagerungen. Jahrbuch der Königlich Preussischen geologischen Landesanstalt und Bergakademie zu Berlin 16, 111-124.

Keilhack, K., 1909. Begleitworte zur Karte der Endmoränen und Urstromtäler Norddeutschlands. Jahrbuch der Königlich Preussischen geologischen Landesanstalt und Bergakademie zu Berlin 30 (1), 507-510.

Keilhack, K., 1910. Erläuterungen zur Geologischen Karte von Preußen und benachbarten Bundesstaaten – Blatt Teltow. Königlich Preußische Geologische Landesanstalt, Berlin.

Kjær, K.H., Houmark-Nielsen, M., Richardt, N., 2003. Ice-flow patterns and dispersal of erratics at the southwestern margin of the last Scandinavian Ice Sheet: signature of palaeo-ice streams. Boreas 23, 130-148.

Klasen, N., Fiebig, M., Preusser, F., Reitner, J.M., Radtke, U., 2007. Luminescence dating of proglacial sediments from the Eastern Alps. Quaternary International 164-165. 21-32.

Kliewe, H., Jahnke, W., 1972. Verlauf und System der Marginalzonender letzten Vereisung auf dem Territorium der DDR. Wissenschaftliche Zeitschrift der Erns-Moritz-Arndt-Universität Greifswald - Mathematisch-Naturwissenschaftliche Reihe 21, 31-37.

Knight, P.G., Jennings, C.E., Waller, R.I., Robinson, Z.P., 2007. Changes in ice-margin processes and sediment routing during ice-sheet advance across a marginal moraine. Geografiska Annaler 89 A (3), 203-215.

Korn, J., 1912. Über einen interglazialen Süßwasserkalk in Vevais bei Wriezen. Jahrbuch der Königlich-Preußischen Geologischen Landesanstalt und Bergakademie 33, 41-48.

Kozarski, S., 1992. Eine auf der Radiokarbonmethode basierende Abschätzung der Rückzugschronologie des letzten Inlandeises in Nordpolen, in: Billwitz, K., Jäger, K.D., Janke, W. (eds.). Jungquartäre Landschaftsräume, Berlin, 16-22.

Kozarski, S., 1995. Deglacjacja pólnocno-zachodniej Polski: womki i trasformacja geosystema (~20 ka – 10 ka). Documentacja Geograficzna 82 (1).

Krbetschek, M.R., Degering, D., Alexowsky, W., 2008. Infrarot-Radiofluoreszenz-Alter (IR-RF) unter-saalezeitlicher Sedimente Mittel- und Ostdeutschlands. Zeitschrift der deutschen Gesellschaft für Geowissenschaften 159, 133-144.

Krbetschek, M.R., Rieser, U., Zöller, L., Heinicke, J., 1994. Radioactive Disequilibria in palaeodosimetric dating of sediments. Radiation Measurements 23, 485-489.

Krbetschek, M.R., Trautmann, T., Dietrich, A., Stolz, W., 2000. Radioluminescence dating of sediments: methodological aspects. Radiation Measurements 32 (5-6), 493-498.

Kühl, N., Litt, T., Schölzel, C., Hense, A., 2007. Eemian and Early Weichselian temperature and precipitation variability in northern Germany. Quaternary Science Reviews 26 (25/28), 3311-3317.

Kulig, G., 2005. Erstellung einer Auswertesoftware zur Altersbestimmung mittels Lumineszenzverfahren unter spezieller Berücksichtigung des Einflusses radioaktiver Ungleichgewichte in der 238-U-Zerfallsreihe. Bakkalaureusarbeit Network Computing, TU Freiberg.

Lagerlund, E., Malmberg Persson, K., Kryszkowski, D., Johansson, P., Dobracka, E., Dobracki, R., Panzig, W.-A., 1995. Unexpected ice flow directions during the late Weichselian deglaciation of the south baltic area indicated by a new lithostratigraphy in NW Poland and NE Germany. Quaternary International 28, 127-144.

Lang, A., Lindauer, S., Kuhn, R., Wagner, C.A., 1996. Procedures used for optically and infrared stimulated luminescence dating of sediments in Heidelberg. Ancient TL 14. 7-11.

Leeuween, R.J.W., Beets, D.J., Bosch, J.H.A., Burger, A.W., Cleveringe, P., Harten, D. van, Herngreen, GFW., Kruk, R.W., Langereis, C.G., Meijer, T., Pouwer, R., Wolf, H. de, 2000. Stratigraphy and integrated facies analysis of the Saalian and Eemian sediments in the Amsterdam-Terminal borehole, the Netherlands. Geologie en Mijnbouw / Netherlands Journal of Geosciences 79 (2/3), 161-196.

Lepper, K., McKeever, W.S., 2002. An objective methodology for dose distribution analysis. Radiation Protection Dosimetry 101 (1-4), 349-352.

Li, S.-H., 1994. Optical dating: insufficiently bleached sediments. Radiation Measurements 23, 563-567.

Li, S.-H., 2001. Identification of well-bleached grains in the optical dating of quartz. Quaternary Science Reviews 20, 1365-1370.

Lian, O. B., Roberts, R. G., 2006. Dating the Quaternary: progress in luminescence dating of sediments. Quaternary Science Reviews (25), 2449-2468.

Libby, W.F., 1952. Radiocarbon Dating. University of Chicago Press, Chicago.

Liedtke, H., 1956/57: Beiträge zur Entwicklung des Thorn-Eberswalder Urstromtales zwischen Oder und Havel. Wissenschaftliche Zeitschrift der Humboldt-Universität zu Berlin, Mathematisch-naturwissenschaftliche Reihe 6, 3-49.

Liedtke, H., 1975. Die Nordischen Vereisungen in Mitteleuropa. Forschungen zur deutschen Landeskunde 204, Bonn - Bad Godesberg.

Liedtke, H., 1981. Die Nordischen Vereisungen in Mitteleuropa. Forschungen zur deutschen Landeskunde 204 (2nd edition), Trier.

Liedtke, H., 1996. Die eiszeitliche Gestaltung des Oderbruchs. Heidelberger Geographische Arbeiten 104, 327-351.

Liedtke, H., 2001. Das nordöstliche Brandenburg während der Weichseleiszeit. In Bussemer, S. (ed.): Das Erbe der Eiszeit, Langenweißbach, 119-133.

Linge, H., Brook, E.J., Nesje, A., Raisbeck, G.M., Yiou, F., Clark, H., 2006. In situ 10Be exposure ages from southeastern Norway: implications for the geometry of the Weichselian Scandinavian ice sheet. Quaternary Science Reviews 25, 1097-1109.

Lippstreu, L., 1995. Brandenburg. In: Benda, L. (ed.), Das Quartär Deutschlands. 116-147.

Litt, T., Behre, K.-E., Meyer, K.-D., Stephan, H.-J., Wansa, S., 2007. Stratigraphical Terms for the Quaternary of the North German Glaciation Area. In: Litt, T. (ed.): Stratigraphie von Deutschland – Quartär. E&G Quaternary Science Journal 56 (1/2), 7-65.

Litt, T., Gibbard, P., 2008. A proposal for the definition of a Global Stratotype Section and Point (GSSP) for the base of the Upper (Late) Pleistocene Subseries (Quaternary System/Period) Episodes, 31, No.2, 260- 263.

Lomax, J., Hilgers, A., Twidale, C.R., Bourne, J.A., Radtke, U., 2007. Treatment of broad palaeodose distributions in OSL dating of dune sands from the western Murray Basin, South Australia. Quaternary Geochronology 2, 51-56.

Lukas, S., Spencer, J.Q.G., Robinson, R.A.J., Benn, D.I., 2007. Problems associated with luminescence dating of Late Quaternary glacial sediments in the NW Scottish Highlands. Quaternary Geochronology 2, 243-248.

Lunkka, J.P., Saarnisto, M., Gey, V., Demidov, I., Kiselova, V., 2001. Extent and age of the Last Glacial Maximum in the southeastern sector of the Scandinavian ice Sheet. Global and Planetary Change 31, 407-425.

Lüthgens, C., Böse, M., 2007. Reassessment of the geomorphological development of the Rangsdorf lake area. E&G Quaternary Science Journal 57, 256-282.

Lüthgens, C., Böse, M., in press (2010). From morphostratigraphy to geochronology e on the dating of ice marginal positions. Quaternary Science Reviews, doi:10.1016/j.quascirev.2010.10.009.

Lüthgens, C., Böse, M., Krbetschek, M.R., 2010a. On the age of the young morainic morphology in the area ascribed to the maximum extent of the Weichselian glaciation in north-eastern Germany. Quaternary International 222, 72-79.

Lüthgens, C., Böse, M., Lauer, T., Krbetschek, M., Strahl, J., Wenske, D., in press (2010b). Timing of the last interglacial in Northern Europe derived from Optically Stimulated Luminescence (OSL) dating of a terrestrial Saalian–Eemian–Weichselian sedimentary sequence in NE-Germany. Quaternary International, doi:10.1016/j.quaint.2010.06.026.

Lüthgens, C., Böse, M., Preusser, F., submitted for publication (2010c). The age of the Pomeranian ice marginal position in north-eastern Germany determined by Optically Stimulated Luminescence (OSL) dating of glaciofluvial (sandur) sediments. Boreas.

Lüthgens, C., Krbetschek, M.R., Böse, M., Fuchs, M.C., 2010d. Optically Stimulated Luminescence Dating of fluvioglacial (sandur) sediments from north-eastern Germany. Quaternary Geochronology 5, 237-243.

Lüttig, G., 1958. Methodische Fragen der Geschiebeforschung. Geologisches Jahrbuch 75, 361-418.

Lüttig, G., 2005. Geschiebezählungen im westlichen Mecklenburg. Archiv für Geschiebekunde 4 (9), 569-600.

Maizels, J., 1997. Jökulhlaup deposits in proglacial areas. Quaternary Science Reviews 16, 793-819.

Marcinek, J., 1961. Über die Entwicklung des Baruther Urstromtales zwischen Neiße und Fiener Bruch. Wissenschaftliche Zeitschrift der Humboldt-Universität zu Berlin, Math.-Naturw. Reihe 10, 13-46.

Marcinek, J., Brose, F., 1995. Brandenburger Eisrandlage und Baruther Urstromtal. In: Schroeder, J.H. (Ed.). Führer zur Geologie von Berlin und Brandenburg Nr. 3: Lübbenau – Calau. Berlin, 189-197.

Marcinek, J., Schulz, I. 1995. Im klassischen gebiet der norddeutschen Eiszeitforschung – Im Raum der Pommerschen Eisrandlage um Chorin und der Finow. Berliner Geographische Studien 40, 197-213.

Marks, L., 2002. Last Glacial Maximum in Poland. Quaternary Science Reviews 21, 103-110.

Marks, L., in press (2010). Timing of the Late Vistulian (Weichselian) glacial phases in Poland. Quaternary Science Reviews, in press, doi:10.1016/j.quascirev.2010.08.008.

Marshall, S.J., 2005. Recent advances in understanding ice sheet dynamics. Earth and Planetary Science Letters 240. 191-204.

Mayya, Y.S., Morthekai, P., Murari, M.K., Singhvi, A.K., 2006. Towards quantifying beta microdosimetric effects in single-grain quartz dose distributions. Radiation Measurements 41, 1032-1039.

McKerrell, H.V. and Mejdahl V., 1981. Progress and problems with automated TL dating, Proceedings of the 16th International Symposium of Archaeometry, National Museum of Antiquities of Scotland, Edinburgh: pp. 36.

Mejdahl, V., Christiansen, H.H., 1994. Procedures used for luminescence dating of sediments. Quaternary Science Reviews 13, 403-406.

Monegato, G., Ravazzi, C., Donegana, M., Pini, R., Calderoni, G., Wick, L., 2007. Evidence of a two-fold glacial advance during the last glacial maximum in the Tagliamento end moraine system (eastern Alps). Quaternary Research 68, 284-302.

Murray, A., Buylaert, J.-P., Henriksen, M., Svendsen, J.-I., Mangerud, J., 2008. Testing the reliability of quartz OSL ages beyond the Eemian. Radiation Measurements 43, 776-780.

Murray, A., Funder, S., 2003. Optically stimulated luminescence dating of a Danish Eemian coastal marine deposit: a test of accuracy. Quaternary Science Reviews 22, 1177-1183.

Murray, A., Svendsen, J. I., Mangerud, J., Astakhov, V. I., 2007. Testing the accuracy of quartz OSL dating using a known-age Eemian site on the river Sula, northern Russia. Quaternary Geochronology 2 (1-4), 102-109.

Murray, A.S., Wintle, A.G., 2000. Luminescence dating of Quartz using an improved single aliquot regenerative dose protocol. Radiation Measurements 32, 57-73.

Murray, A.S., Wintle, A.G., 2003. The single aliquot regenerative dose protocol: potential for improvements in reliability. Radiation Measurements 37, 377-381.

Napieralski, J., Hubbard, A., Yingkui, L., Harbor, J., Stroeven, A.P., Kleman, J., Alm, G., Jansson, K.N., 2007. Towards a GIS assessment of numerical ice-sheet model performance using geomorphological data. Journal of Glaciology 53 (180), 71-83.

Olley, J.M., Caitchton, G.G., Murray, A.S., 1998. The distribution of apparent dose as determined by optically stimulated luminescence in small aliquots of fluvial quartz: implications for dating young sediments. Quaternary Science Reviews 17, 1033-1040.

Pawley, S.M., Bailey, R.M., Rose, J., Moorlock, B.S.P., Hamblin, R.J.O., Booth, S.J., Lee, J.R., 2008. Age limits on Middle Pleistocene sediments from OSL dating, north Norfolk, UK. Quaternary Science Reviews 27, 1363-1377.

Penck, A. 1879. Die Geschiebeformation Norddeutschlands. Zeitschrift der Deutschen geologischen Gesellschaft 31, 117-203.

Penck, A. 1882. Die Vergletscherung der deutschen Alpen: ihre Ursachen, periodische Wiederkehr und ihr Einfluss auf die Bodengestaltung. Barth, Leipzig.

Penck, A., Brückner, E., 1909. Die Alpen im Eiszeitalter. Tauchnitz, Leipzig.

Pisarska-Jamroży, M., 2006. Transitional deposits between the end moraine and outwash plain in the Pomeranian glaciomarginal zone of NW Poland: a missing component of ice-contact sedimentary models. Boreas 35, 126-141.

Preusser, F., 1999. Lumineszenzdatierung fluviatiler Sedimente; Fallbeispiele aus der Schweiz und Norddeutschland. Kölner Forum Geologie Paläontologie 3, 1-62.

Preusser, F., Blei, A., Graf, H., Schlüchter, C. 2007. Luminescence dating of Würmian (Weichselian) proglacial sediments from Switzerland: methodological aspects and stratigraphical conclusions. Boreas 36, 130-142.

Preusser, F., Degering, D. 2007. Luminescence dating of the Niederweningen mammoth site, Switzerland. Quaternary International 164-165, 106-112.

Preusser, F., Degering, D., Fuchs, M., Hilgers, A., Kadereit, A., Klasen, N., Krbetschek, M., Richter, D., Spencer, J.Q.G., 2008. Luminescence dating: basics, methods and applications. Eiszeitalter und Gegenwart – Quaternary Science Journal 57 (1/2), 95-149.

Preusser, F., Kasper, H.U., 2001. Comparison of dose rate determination using high-resolution gamma spectrometry and inductively coupled plasma-mass spectrometry. Ancient TL 19, 19-23.

Putkonen, J., Swanson, T., 2003. Accuracy of cosmogenic ages for moraines. Quaternary Research 59, 255-261.

Rasmussen, S. O., Andersen, K.K., Svensson, A.M., Steffensen, J.P., Vinther, B.M., Clausen, H.B., Siggaard-Andersen, M.L., Johnsen, S.J., Larsen, L.B., Dahl-Jensen, D., Bigler, M., Röthlisberger, R., Fischer, H., Goto-Azuma, K., Hansson, M.E., Ruth, U. 2006: A new Greenland ice core chronology for the last glacial termination. Journal of Geophysical Research 111, D06102, doi:10.1029/2005JD006079.

Raukas, A., Stankowski, W., 2005. Influence of sedimentological composition on OSL dating of glaciofluvial deposits: Examples from Estonia. Geological Quarterly 49 (4), 463-470.

Reuther, A.U., Ivy-Ochs, S., Heine, K., 2006. Application of surface exposure dating in glacial geomorphology and the interpretation of moraine ages. Zeitschrift für Geomorphologie N.F. 142, 335-359.

Rinterknecht, V.R., Bitinas, A., Clark, P.U., Raisbeck, G.M., Yiou, F., Brook, E.J., 2008. Timing of the last deglaciation in Lithuania. Boreas 37, 426-433.

Rinterknecht, V.R., Braucher, R., Böse, M., Bourlès, D., Mercier, J.-L., in press (2010). Late Quaternary ice sheet extents in northeastern Germany inferred from surface exposure dating. Quaternary Science Reviews, in press, doi:10.1016/j.quascirev.2010.07.026.

Rinterknecht, V.R., Clark, P.U., Raisbeck, G.M., Yiou, F., Bitinas, A., Brook, E.J., Marks, L., Zelčs, V., Lunkka, J.-P., Pavlovskaya, I.E., Piotrowski, J.A., Raukas, A., 2006a. The Last Deglaciation of the Southeastern Sector of the Scandinavian Ice Sheet. Science 311, 1449-1452.

Rinterknecht, V.R., Marks, L., Piotrowski, J., Raisbeck, G.M., Yiou, F., Brook, E.J., Clark, P.U., 2005. Cosmogenic 10Be ages on the Pomeranian Moraine, Poland. Boreas 34, 186-191.

Rinterknecht, V.R., Marks, L., Piotrowski, J., Raisbeck, G.M., Yiou, F., Brook, E.J., Clark, P.U., 2006b. 'Cosmogenic 10Be ages on the Pomeranian Moraine, Poland': Reply to comments. Boreas 35, 605-606.

Rinterknecht, V.R., Pavlovskaya, I.E., Clark, P.U., Raisbeck, G.M., Yiou, F., Brook, E.J., 2007. Timing of the last deglaciation in Belarus. Boreas 36, 307-313.

Roberts, R.G., Galbraith, R.F., Yoshida, H., Laslett, G.M., Olley, J.M., 2000. Distinguishing dose populations in sediment mixtures: a test of single-grain optical dating procedures using mixtures of laboratory-dosed quartz. Radiation Measurements 32, 459-465.

Roberts, R.G., Yoshida, H., Galbraith, R., Laslett, G.M., Smith, M.A.,1998. Single-aliquot and single-grain optical dating confirm thermoluminescence age estimates at Malakunanja II rock shelter in northern Australia. Ancient TL 16, 19–24.

Rodnight, H., 2006. Developing a luminescence chronology for late Quaternary fluvial change in South African floodplain wetlands. Unpublished PhD thesis. University of Wales, Aberystwyth.

Rodnight, H. 2008. How many equivalent dose values are needed to obtain a reproducible distribution?. Ancient TL 26, 3-9.

Saks, T., Zelčs, V., Kalvāns, A., 2009. A glacial dynamic study of Apriki tongue: Implications for deglaciation history. International Field Symposium of the INQUA Peribaltic Working Group, Tartu, September 13-17, 2009 - Abstracts. Available from: http://www.ut.ee/orb.aw/class=file/action=preview/id=629667/INQUA+Peribaltic+2009+Abstr+%26+Guide.pdf. last visited 01/03/2010.

Schaetzl, R.J., Forman, S.L., 2008. OSL ages on glaciofluvial sediment in northern Lower Michigan constrain expansion of the Laurentide ice sheet. Quaternary Research 70, 81-90.

Schirrmeister, L. 2004. Macherslust. Glazilakustrische Ablagerungen. In Schroeder, J.H. (ed.): Führer zur Geologie von Berlin und Brandenburg – Nr. 5: Nordwestlicher Barnim – Eberswalder Urstromtal, Berlin, 236-245.

Schokker, J., Cleveringa, P., Murray, A., 2004. Palaeoenvironmental reconstruction and OSL dating of terrestrial Eemian deposits in the southeastern Netherlands. Journal of Quaternary Science 19 (2), 193-202.

Scourse, J., 2006. Comment on: Numerical 230Th/U dating and a palynological review of the Holsteinian/Hoxnian Interglacial by Geyh and Mü ller. Quaternary Science Reviews 25, 3070-3071.

Sefstrom, N.G., 1843. An investigation of the furrows which traverse the Scandinavian mountains in certain directions, together with the probable cause of their origin. In: Taylor, R. (ed.). Scientific memoirs selected from the transactions of foreign academies of science and learned societies, and from foreign journals. London, 81-144.

Seibold, E., Seibold, I., 2003. Erratische Blöcke - erratische Folgerungen: ein unbekannter Brief von Leopold von Buch von 1818. International Journal of Earth Sciences 92 (3), 426-439.

Singarayer, J. S., Bailey, R. M., Ward, S., Stokes, S. 2005: Assessing the completeness of optical resetting of quartz OSL in the natural environment. Radiation Measurements 40, 13-25.

Smed, O., 1989. Sten I det danske landskab. Geografforlaget, Brenderup.

Smed, P., 1994. Steine aus dem Norden: Geschiebe als Zeugen der Eiszeit in Norddeutschland (German translation by J. Ehlers). Bornträger, Stuttgart.

Smith, L.C., Sheng, Y., Magilligan, F.J., Smith, N.D., Gomez, B., Mertes, L.A.K., Krabill, W.B., Garvin, J.B., 2006. Geomorphic impact and rapid subsequent recovery from the 1996 Skeiðarársandur jökulhlaup, Iceland, measured with multi-year airborne lidar. Geomorphology 75, 65-75.

Steffen, D., Preusser, F., Schlunegger, F., 2009. OSL quartz age underestimation due to unstable signal components. Quaternary Geochronology 4, 353-362.

Stokes, C.R., 2002. Identification and mapping of palaeo-ice stream geomorphology from satellite imagery: implications for ice stream functioning and ice sheet dynamics. International Journal of Remote Sensing 8 (23), 1557-1563.

Stokes, C.R., Clark, C.D., 2001a. Palaeo-ice streams. Quaternary Science Reviews 20, 1437-1457.

Stokes, C.R., Clark, C., 2001b. Identifying Palaeo-Ice Stream Tracks Using Remote Sensing. Slovak Geological Magazine 7 (3), 242-262.

Stokes, C.R., Clark, C.D., Storrar, R., 2009. Major changes in ice stream dynamics during deglaciation of the north-western margin of the Laurentide Ice Sheet. Quaternary Science Reviews 28, 721-738.

Stone, A.E.C., Thomas, D.S.G. 2008. Linear dune accumulation chronologies from the southwest Kalahari, Namibia: challenge of reconstructing Late Quaternary palaeoenvironments from aeolian landforms. Quaternary Science Reviews 27 (17-18), 1667-1681.

Stuiver, M. Reimer, P.J., Bard, E., Beck,J.W., Burr, G.S., Hughen, K.A., Kromer, B., McCormac, F.G., Plicht, J., Spurk, M., 1998. INTCAL98 Radiocarbon age calibration 24,000

Svendsen, J.I., Alexanderson, H., Astakhov, V.I., Demidov, I., Dowdeswell, J.A., Funder, S., Gataullin, V., Henriksen, M., Hjort, C., Houmark-Nielsen, M., Hubberten, H.W., Ingólfsson, Ó., Jakobsson, M., Kjær, K., Larsen, E., Lokrantz, H., Lunkka, J.P., Lysså, A., Mangerud, J., Matiouchkov, A., Murray, A., Möller, P., Niessen, F., Nikolskaya, O., Polyak, L., Saarnisto, M., Siegert, C., Siegert, M.J., Spielhagen, R.F., Stein, R., 2004. Late Quaternary ice sheet history of northern Eurasia. Quaternary Science Reviews 23, 1229-1271.

Tabachnick, B.G., Fidell, L.S. 1996: Using multivariate statistics (3rd ed.). Harper Collins, New York.

Terberger, T., Klerk, P. de, Helbig, H., Kaiser, K., Kühn, P., 2004. Late Weichselian landscape development and human settlement in Mecklenburg-Vorpommern (NE Germany). Eiszeitalter und Gegenwart 54, 138-175.

Thomsen, K. J., Jain, M., Murray, A. S., Denby, P. M., Roy, N., Bøtter-Jensen, L., 2008. Minimizing feldspar OSL contamination in quartz UV-OSL using pulsed blue stimulation. Radiation Measurements 43, 752-757.

Thrasher, I.M., Mauz, B., Chiverrell, R.C., Lang, A., 2009. Luminescence dating of glaciofluvial deposits: A review. Earth-Science Reviews 97, 133-146.

Torell, O., 1875. Ueber das norddeutsche Diluvium, in: Beyrich, V., Rammelsberg, W., Weiss, O.: Verhandlungen der Gesellschaft – Protokoll der November-Sitzung. Zeitschrift der Deutschen geologischen Gesellschaft 27, 958-962.

Trautmann, T., Krbetschek, M.R., Dietrich, A., Stolz, W., 1999. Feldspar radioluminescence: AA new dating method and ist physical background. Journal of Luminescence 85, 45-58.

Tschudi, S., Ivy-Ochs, S., Schlüchter, C., Kubik, P., Rainio, H., 2000. 10Be dating of Younger Dryas Salpausselkä I formation in Finland. Boreas 29, 287-293.

Tsukamoto, S., Denby, P.M, Murray, A.S., Bøtter-Jensen, L., 2006. Time-resolved luminescence from feldspars: New insight into fading. Radiation Measurement 7-8, 790-795.

Vaikmäe, R., Böse, M., Michel, A., Moormann, B. J., 1995. Changes in Permafrost Conditions. Quaternary International 28, 113-118.

Van Veen, F., 2008. Early ideas about erratic boulders and glacial phenomena in The Netherlands. In: Grapes, R., Oldroyd, D., Grigelis, A., (eds.). History of Geomorphology and Quaternary Geology. Geological Society Special Publication 301, 159-169.

Vandenberghe, D., Hossain, S.M., De Corte, F., Van de haute, P., 2003. Investigations on the origin of the equivalent dose distribution in a Dutch coversand. Radiation Measurements 37, 433-439.

Wagner, G. A., 1998. Age determination of Young Rocks and Artifacts – Physical and Chemical Clocks in Quaternary Geology and Archaeology. Springer, Berlin, Heidelberg, New York, 466 p.

Wallinga, J., 2002. On the detection of OSL age overestimation using single-aliquot techniques. Geochronometria 21, 17-26.

Wintle, A.G., 1973. Anomalous Fading of Thermoluminescence in Mineral Samples. Nature 245, 143-144.

Wintle, A.G., 2008a. Fifty years of luminescence dating. Archaeometry 50 (2), 276-312.

Wintle, A.G., 2008b. Luminescence dating. Where it has been and where it is going. Boreas 37, 471-482.

Wintle, A.G., Huntley, D.J., 1979. Thermoluminescence dating of a deep sea core. Nature 279, 710-712.

Wintle, A.G., Murray, A.S., 2006. A review of quartz optically stimulated luminescence characteristics and their relevance in single-aliquot regeneration dating protocols. Radiation Measurements 41, 369-391.

Woda, C., Fuchs, M., 2008. On the applicability of the leading edge method to obtain equivalent doses in OSL dating and dosimetry. Radiation Measurements 43, 26-37.

Woldstedt, P., 1925. Die großen Endmoränenzüge Norddeutschlands. Zeitschrift der Deutschen Geologischen Gesellschaft 77, 172-184.

Wysota, W., Molewski, P., Sokolowski, R.J., 2009. Record of the Vistula ice lobe advances in the late Weichselian glacial sequence in north-central Poland. Quaternary International 207, 26-41.

List of Maps

Bundesanstalt für Geowissenschaften und Rohstoffe (ed.). Geologische Übersichtskarte 1:200.000
© BGR 2011

CC 3142 (1998) – Neubrandenburg
CC 3150 (1998) – Schwedt (Oder)
CC 3942 (1998) – Berlin
CC 3950 (2003) – Frankfurt (Oder)

Königlich Preussische Geologische Landesanstalt (ed.).
Geologische Specialkarte von Preußen 1:25 000
By kind permission of the Landesamt für Bergbau, Geologie und Rohstoffe (LBGR) Brandenburg

3048 (1912) – Joachimsthal
3148 (1899) – Eberswalde
3149 (1899) – Hohenfinow
3250 (1908) – Freienwalde
3350 (1895) – Möglin
3743 (1875) – Beelitz

Königlich Preußische Geologische Landesanstalt (ed.).
Geologische Karte von Preußen und benachbarten Bundesstaaten 1:25 000
By kind permission of the Landesamt für Bergbau, Geologie und Rohstoffe (LBGR) Brandenburg

3049 (1891) – Groß Ziethen

Preußische Geologische Landesanstalt (ed.).
Geologische Karte von Preußen und benachbarten Bundesstaaten 1:25 000
By kind permission of the Landesamt für Bergbau, Geologie und Rohstoffe (LBGR) Brandenburg

3844 (1922) – Hennickendorf
3845 (1922) – Schöneweide
3944 (1922) – Zinna
3945 (1922) – Luckenwalde

Landesvermessungamt Brandenburg (ed.). Topographische Karte 1:25 000
TK25 © GeoBasis-DE/LGB 2011, GB-D 07/11 www.geobasis-bb.de

3048 (1998) – Joachimsthal
3049 (1998) – Chorin
3148 (1996) – Eberswalde
3149 (1996) – Falkenberg-Mark
3250 (1996) – Bad Freienwalde
3350 (1996) – Beerfelde
3743 (1993) – Beelitz
3844 (1994) – Hennickendorf
3845 (1994) – Woltersdorf
3944 (1994) – Kloster Zinna
3945 (1994) – Luckenwalde

Liedtke, H., 1981. Die Nordischen Vereisungen Mitteleuropas 1: 1 000 000. Trier.

Lippstreu, L., Hermsdorf, N., Sonntag, A., 1997. Geologische Übersichtskarte des Landes Brandenburg 1:300 000. Potsdam.

Woldstedt, P., 1935. Geologisch-morphologische Übersichtskarte des norddeutschen Vereisungsgebietes 1:1 500 000. Preußische Geologische Landesanstalt, Berlin.

13.2. Supplementary maps

13.2.1. North-eastern Germany – topography and research areas

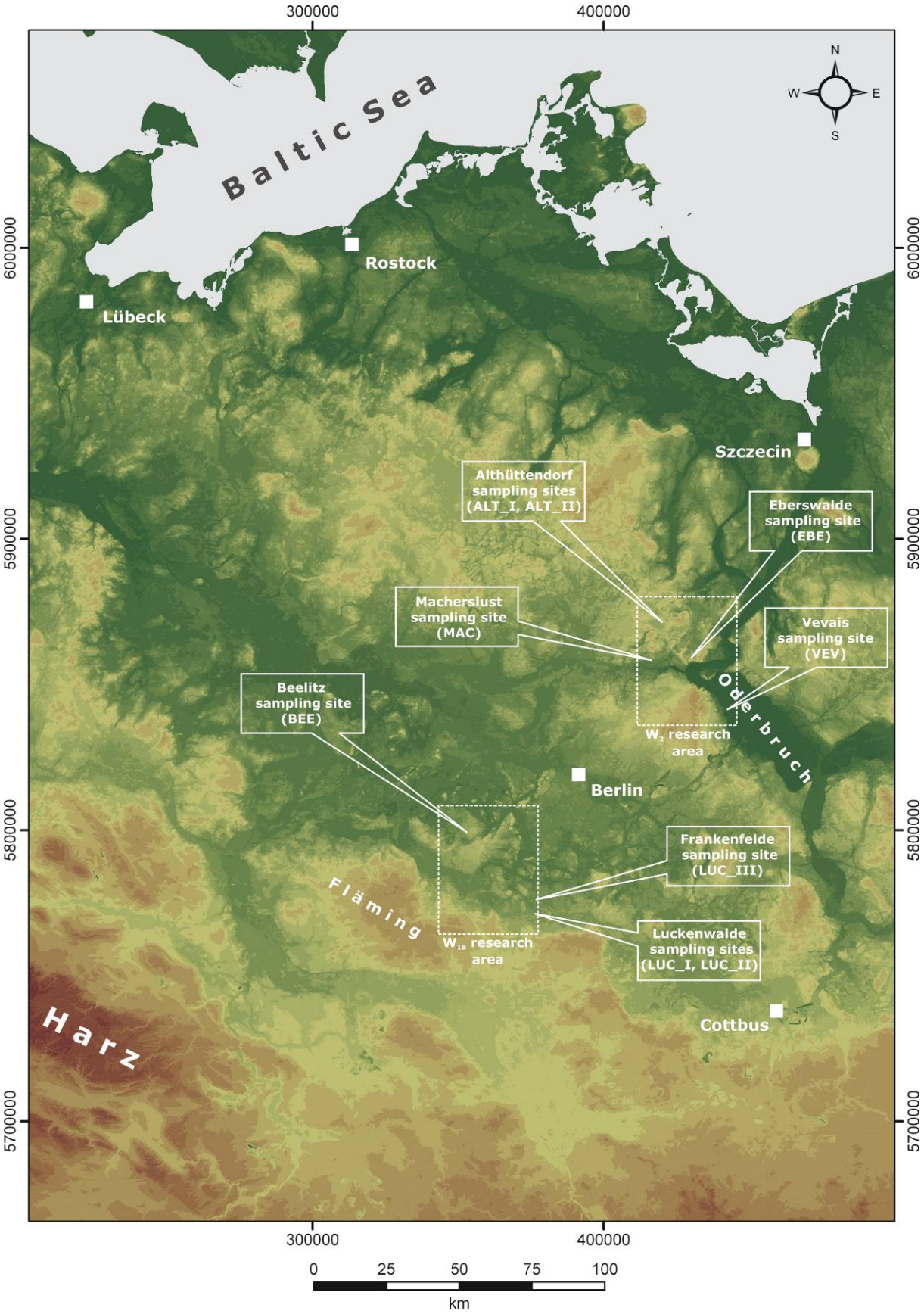

Topography of north-eastern Germany and neighbouring areas, based on a digital elevation model (DEM) from hole-filled seamless SRTM data (processed by Jarvis et al., 2006), 90 m resolution, UTM, WGS 1984.

13.2.2. W_{1B} research area – topography and sampling sites

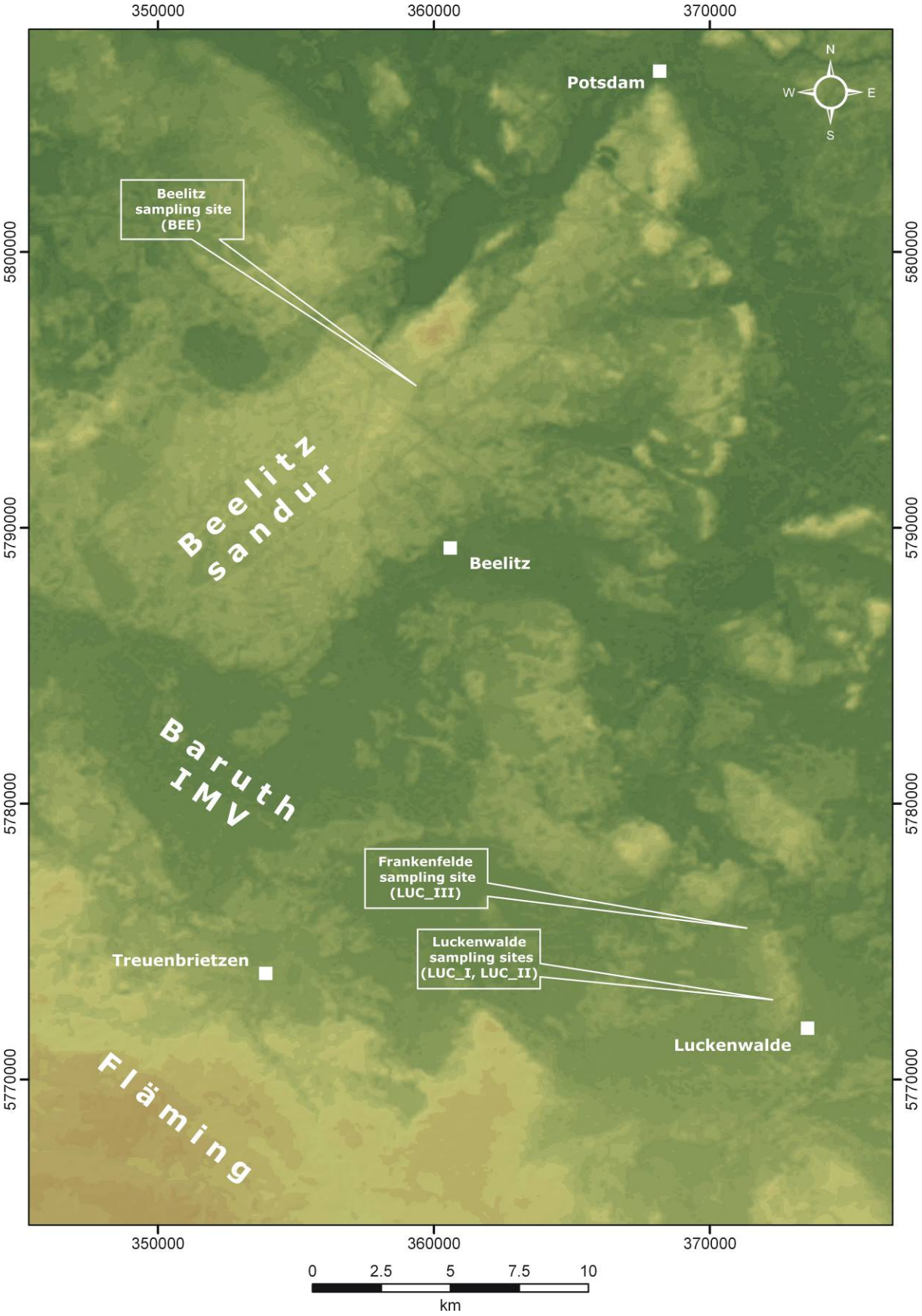

Topography of the W_{1B} research area, map based on a digital elevation model (DEM) derived from hole-filled seamless SRTM data (processed by Jarvis et al., 2006), 90 m resolution, UTM, WGS 1984.

13.2.3. W_{1B} research area – GÜK200

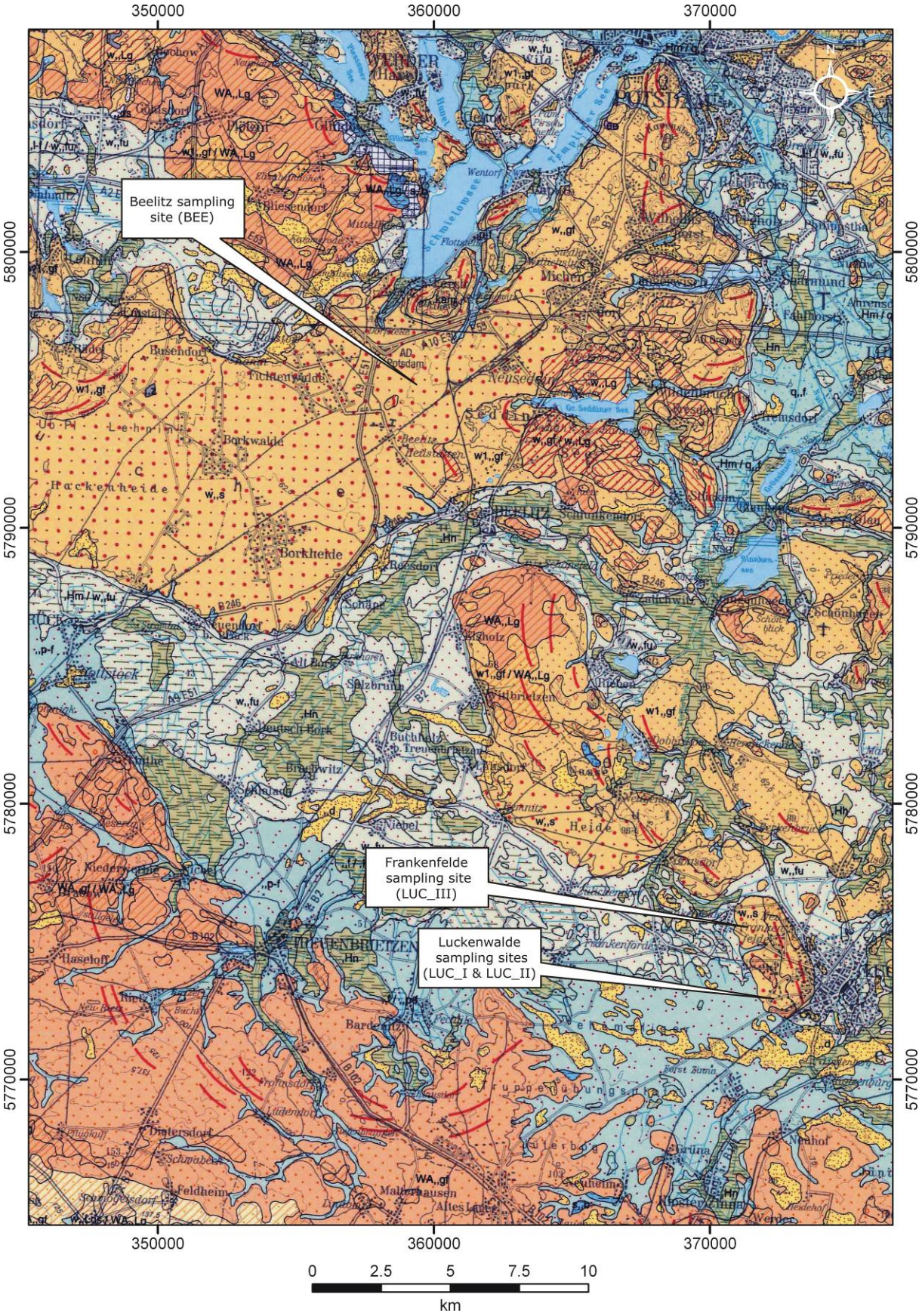

Excerpt from the geological map 1:200,000 (based on GÜK CC 3942 © BGR Hannover - Bundesanstalt für Geowissenschaften und Rohstoffe, 1998). UTM, WGS 1984. Selected map legend see appendix 13.2.6.

13.2.4. W_2 research area – topography and sampling sites

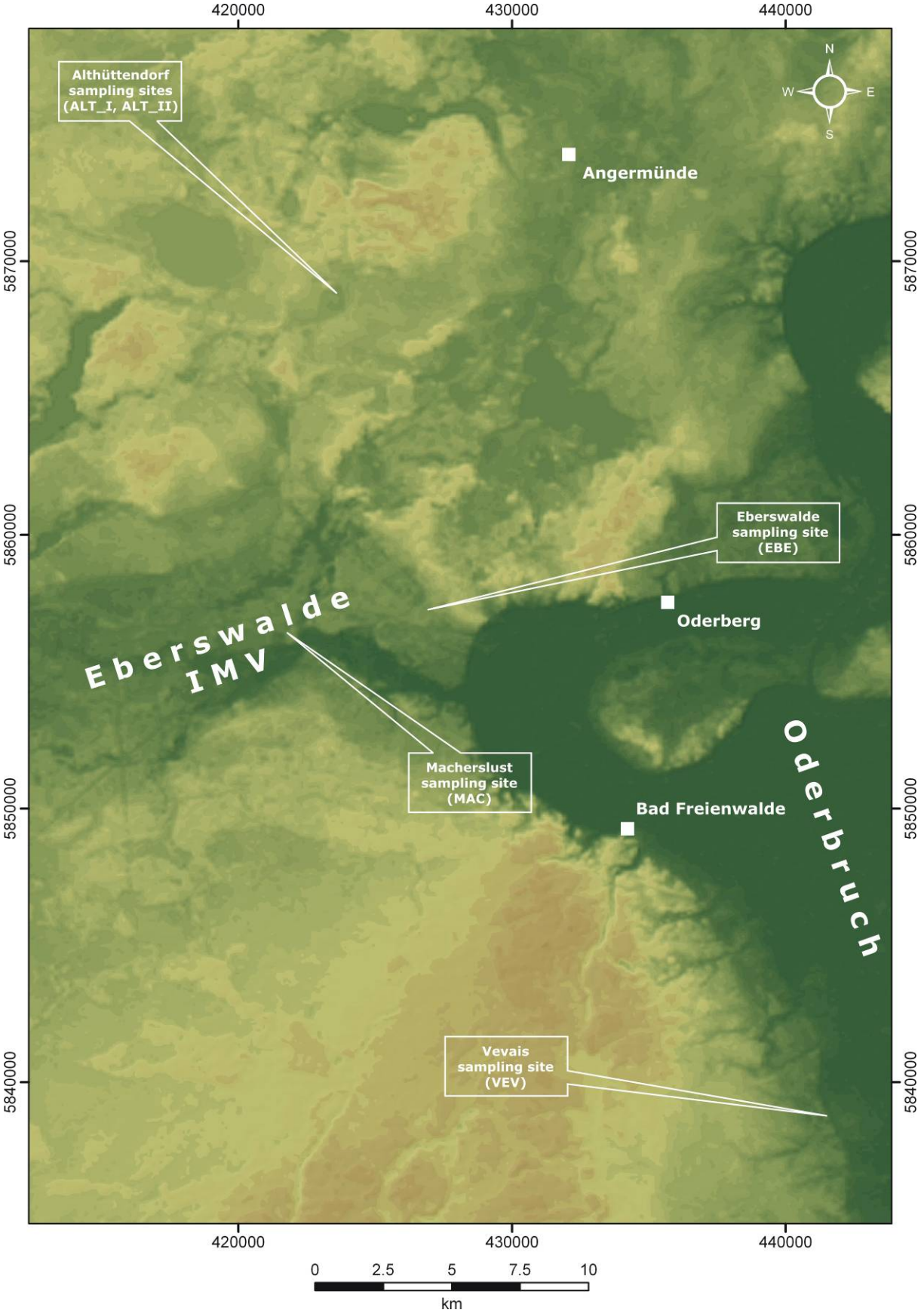

Topography of the W_2 research area, map based on a digital elevation model (DEM) derived from hole-filled seamless SRTM data (processed by Jarvis et al., 2006), 90 m resolution, UTM, WGS 1984.

13.2.5. W_2 research area – GÜK200

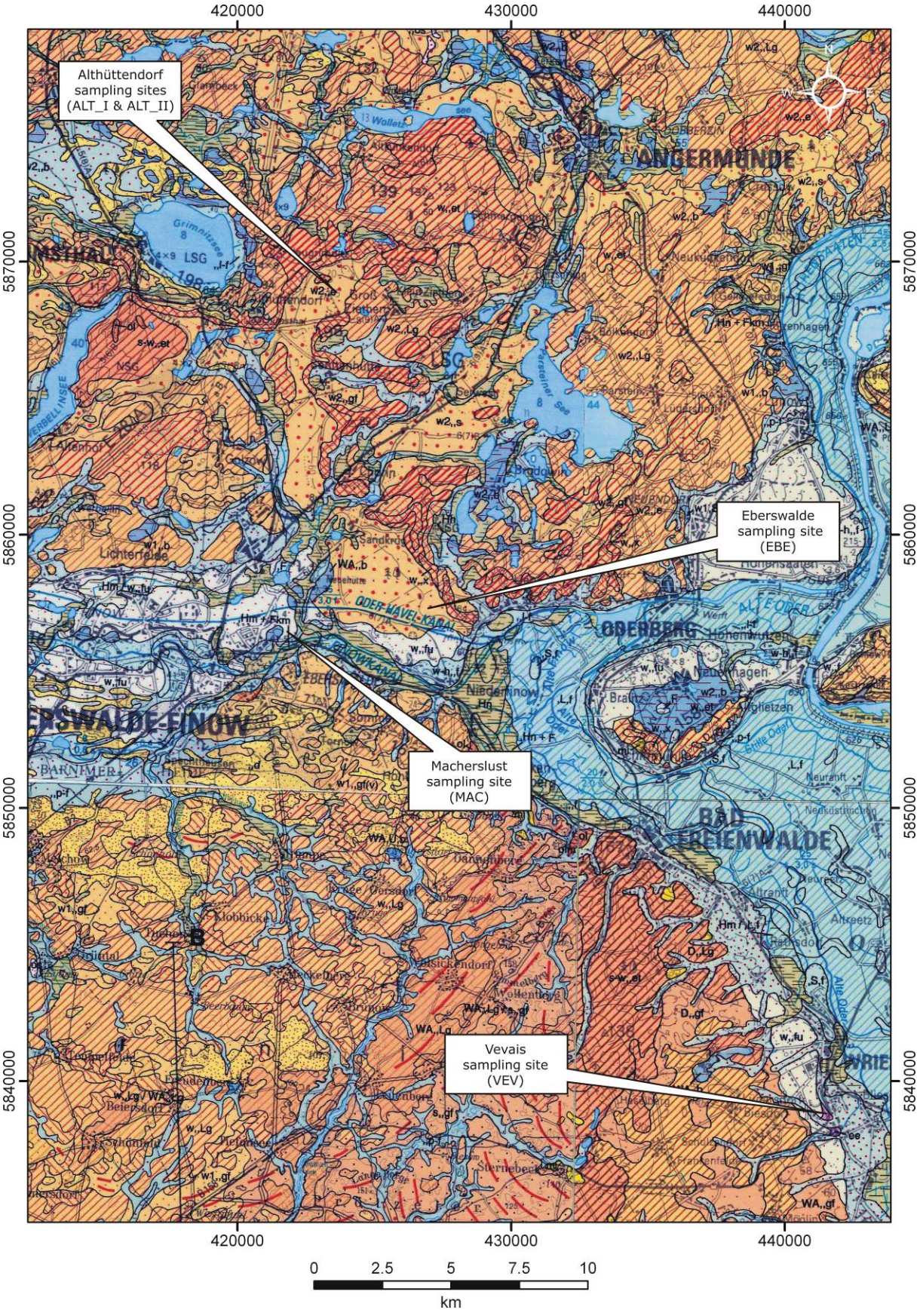

Excerpt from the geological map 1:200,000 (GÜK CC 3142, 3150, 3942, 3950 © BGR Hannover - Bundesanstalt für Geowissenschaften und Rohstoffe, 1998, 2003). UTM, WGS 1984. Map legend see appendix 13.2.6.

13.2.6. GÜK200 map legend (selection)

KÄNOZOIKUM Quartär Holozän

,L,f	*fluviatile Ablagerungen (Auelehm, z.T. unter Überflutungssanden)*	Schluff bis Ton, ± sandig; unter Sand
,M,f	*fluviatile Ablagerungen (Auemergel)*	Schluff, tonig, feinsandig, oft humos, karbonatisch
,S,f	*fluviatile Ablagerungen (Auesand; Auekies)*	Meist Sand; Kies, sandig; humos
,,l-f	*limnisch-fluviatile Ablagerungen*	Fein- und Mittelsand, ± humos; dünne Lagen von Mudden und / oder verschwemmtem Torf
,,z	*Abschlämmmassen*	Zusammensetzung je nach Ausgangsgestein
,Hm	*Anmoor (Moorerde)*	Schluff, Sand; stark humos; Humus, sandig
,Hm + Mw	*Anmoor (Moorerde) mit Kalkausfällungen*	Gemischtkörnige Sedimente mit 10-30 % organischer Substanz, Nester und Lagen von Moor- und Wiesenmergel
,Hn	*Niedermoor*	Bruchwald-, Schilf- und Seggentorf, meist stark zersetzt
,Fkm	*limnische Ablagerungen Faulschlamm, karbonatisch ("Moormergel"; Kalkmudde; Seekreide)*	Schluff, tonig, kalkig, humusreich

Pleistozän, z.T. Holozän

,,d	*äolische Ablagerungen (Dünen und Flugsandfelder)*	Fein- bis Mittelsand
,S,a	*Flugsand*	Fein- bis Mittelsand

Pleistozän

Weichsel-Kaltzeit

,,p-f	*periglaziale bis fluviatile Ablagerungen (periglazial-fluviatile bis -limnische Tal- und Beckenfüllungen, auch Hangsande, Schwemmkegel und Fließerden)*	Sand; schluffig in Schwemmkegeln z.T. kiesig, in Moränengebieten auch Schluff, sandig, mit Steinen
w,,fu	*Ablagerungen der Urstromtäler einschließlich ihrer Nebentäler (Niederterrasse der Urstromtäler; "Talsande")*	Sand, fein- und mittelkörnig, schwach grobkörnig, schwach kiesig
w,,f	*fluviatile Ablagerungen (Hoch- und spätglaziale Niederterrassen; überdeckt von periglazialen Hangsanden oder Schwemmkegeln)*	Sand; (schwach) kiesig
N3	Untere Niederterrasse (unteres Niveau) *fluviatile Ablagerungen*	Sand, Kies
N2	Untere Niederterrasse (mittleres Niveau) *fluviatile Ablagerungen*	Sand, Kies
N1	Untere Niederterrasse (oberes Niveau) *fluviatile Ablagerungen*	Sand, Kies
w,,b	*Beckenablagerungen (glazilimnisch), ungegliedert*	Ton bis Sand
w2,,s	Pommersches Stadium *glazifluviatile Ablagerungen (Sander im morphologischen Sinne)*	Sand, (schwach) kiesig
w1,,s	Brandenburger Stadium *glazifluviatile Ablagerungen (Sander im morphologischen Sinne)*	Sand; (schwach) kiesig

Map legend (part 1 of the selection) for the previously presented geological maps 1:200,000 (GÜK200 © BGR Hannover). The legend is presented as is (in German language).

w1,,gf(v)	Brandenburger Stadium *glazifluviatile Ablagerungen* *(Vorschüttphase)*	Sand; (schwach) kiesig
w1,,gf	Brandenburger Stadium *glazifluviatile Ablagerungen* *(Eiszerfallsphase)*	Sand; (schwach) kiesig
w1,,gf(o)	Brandenburger Stadium *glazifluviatile Ablagerungen* *(höherer Teil)*	Sand, ± kiesig
w1,,Lg	Brandenburger Stadium *Grundmoräne (Geschiebelehm, Geschiebemergel)*	Schluff, stark sandig, schwach kiesig; Steine
w1,,kam	Brandenburger Stadium *Kames*	Sand - Kies
w1,,os	Brandenburger Stadium *Oser* *(Schmelzwasserablagerungen in Tunneltälern)*	Sand, (schwach) kiesig; geröllführend; Geschiebemergelkern
w1,,e	Brandenburger Stadium *Endmoräne* *(auch eisrandnahe glazifluviatile Aufschüttungen)*	Sand, Kies, Steine, Geschiebemergel, z.T. glazigen deformiert
w1,,et	Brandenburger Stadium *Stauchendmoräne*	Sand, Kies, Schluff, Geschiebemergel; glazigene Schollen; glazigen deformiert
w1,,b	Brandenburger Stadium *Beckenablagerungen* *auch der Eiszerfallsphase*	Meist Schluff und Ton; Bänderschluff und -tonmergel
w1,S,b	Brandenburger Stadium *Beckenablagerungen* *(Beckensand), auch der Eiszerfallsphase*	Meist Feinsand
Saale- und Weichsel-Kaltzeit		
s-w,,et	Stauchmoräne, meist saalezeitlich, weichselzeitlich überprägt	Sand, Kies, Schluff, Geschiebemergel; glazigene Schollen; glazigen deformiert
Eem-Warmzeit, z.T. Weichsel-Frühglazial		
ee	*limnische Ablagerungen* *z.T. limnisch-fluviatile Ablagerungen*	Kalk- und Detritusmudde, Ton, Schluff, Sand mit organogenen Beimengungen oder Torf
Saale-Kaltzeit		
WA,,gf	Warthe-Stadium *glazifluviatile Ablagerungen* *(auch der Vorschüttphase)*	Sand, ungleichkörnig; Kies
WA,,Lg	Warthe-Stadium *Grundmoräne (Geschiebemergel, Geschiebelehm)*	Schluff, tonig, sandig, kiesig; Steine
WA,,b	Warthe-Stadium *Beckenablagerungen* *auch der Eiszerfallsphase*	Meist Schluff und Ton; Bänderschluff und -tonmergel
WA,S,b	Warthe-Stadium *Beckenablagerungen* *auch der Eiszerfallsphase*	Meist Feinsand; Schluff bis Ton
D,,gf	Drenthe-Stadium *glazifluviatile Ablagerungen* *auch der Vorschüttphase*	Sand, ungleichkörnig, (schwach) kiesig glazigen deformiert
D,,Lg	Drenthe-Stadium *Grundmoräne (Geschiebemergel, Geschiebelehm)*	Schluff, tonig, sandig, kiesig; Steine glazigen deformiert
D,,b	Drenthe-Stadium *Beckenablagerungen* *auch der Eiszerfallsphase*	Feinsand, Schluff, Ton; Bänderschluff und -tonmergel glazigen deformiert

Map legend (part 2 of the selection) for the previously presented geological maps 1:200,000 (GÜK200 © BGR Hannover). The legend is presented as is (in German language).

13.2.7. Althüttendorf (ALT_I & ALT_II) – TK25

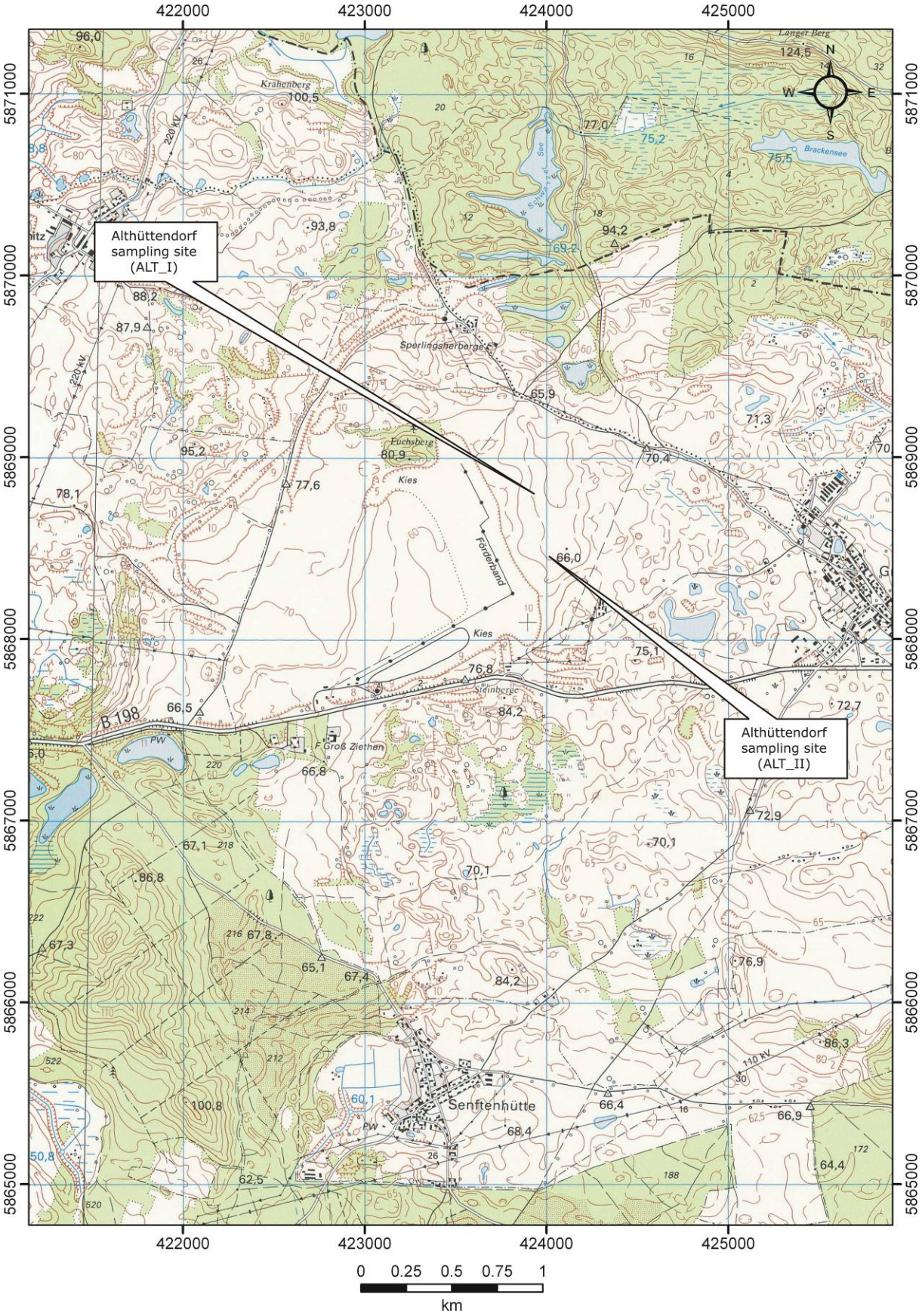

Excerpt from the topographical map 1:25,000 (TK25 3048, 3049 © GeoBasis-DE/LGB 2011, GB-D 07/11 www.geobasis-bb.de - Landesvermessungsamt Brandenburg, 1998). UTM, WGS 1984. Selected map legend see appendix 13.2.19.

13.2.8. Althüttendorf (ALT_I & ALT_II) – GK25

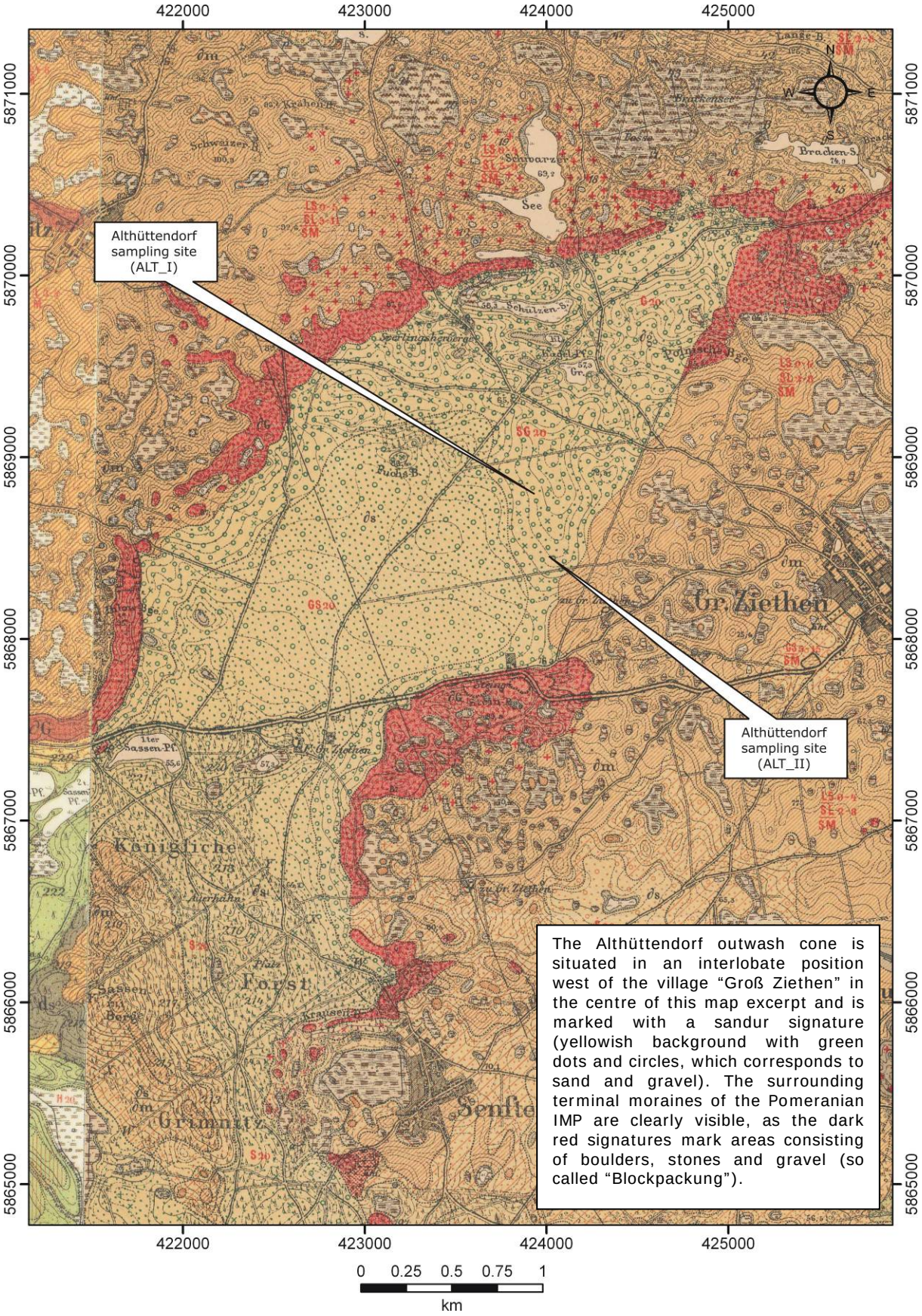

Excerpt from the geological map 1:25,000 (GK25 3048, 3049 © LBGR 2011 - Königlich Preußische Geologische Landesanstalt, 1912, 1891). UTM, WGS 1984. Please also see remarks in appendix 13.2.20.

13.2.9. Beelitz (BEE) – TK25

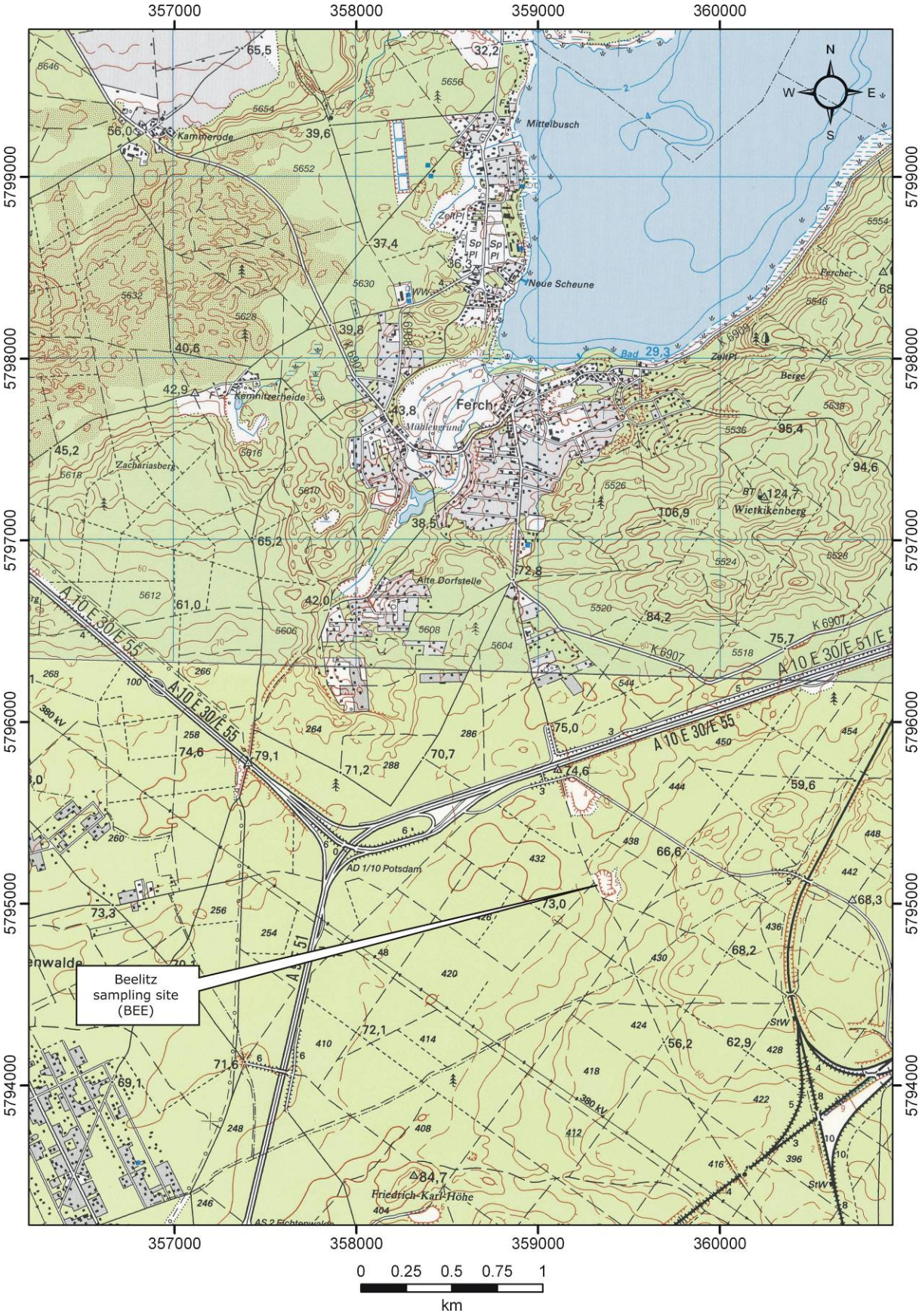

Excerpt from the topographical map 1:25,000 (TK25 3743 © GeoBasis-DE/LGB 2011, GB-D 07/11 www.geobasis-bb.de - Landesvermessungsamt Brandenburg, 1993). UTM, WGS 1984. Selected map legend see appendix 13.2.19.

13.2.10. Beelitz (BEE) – GK25

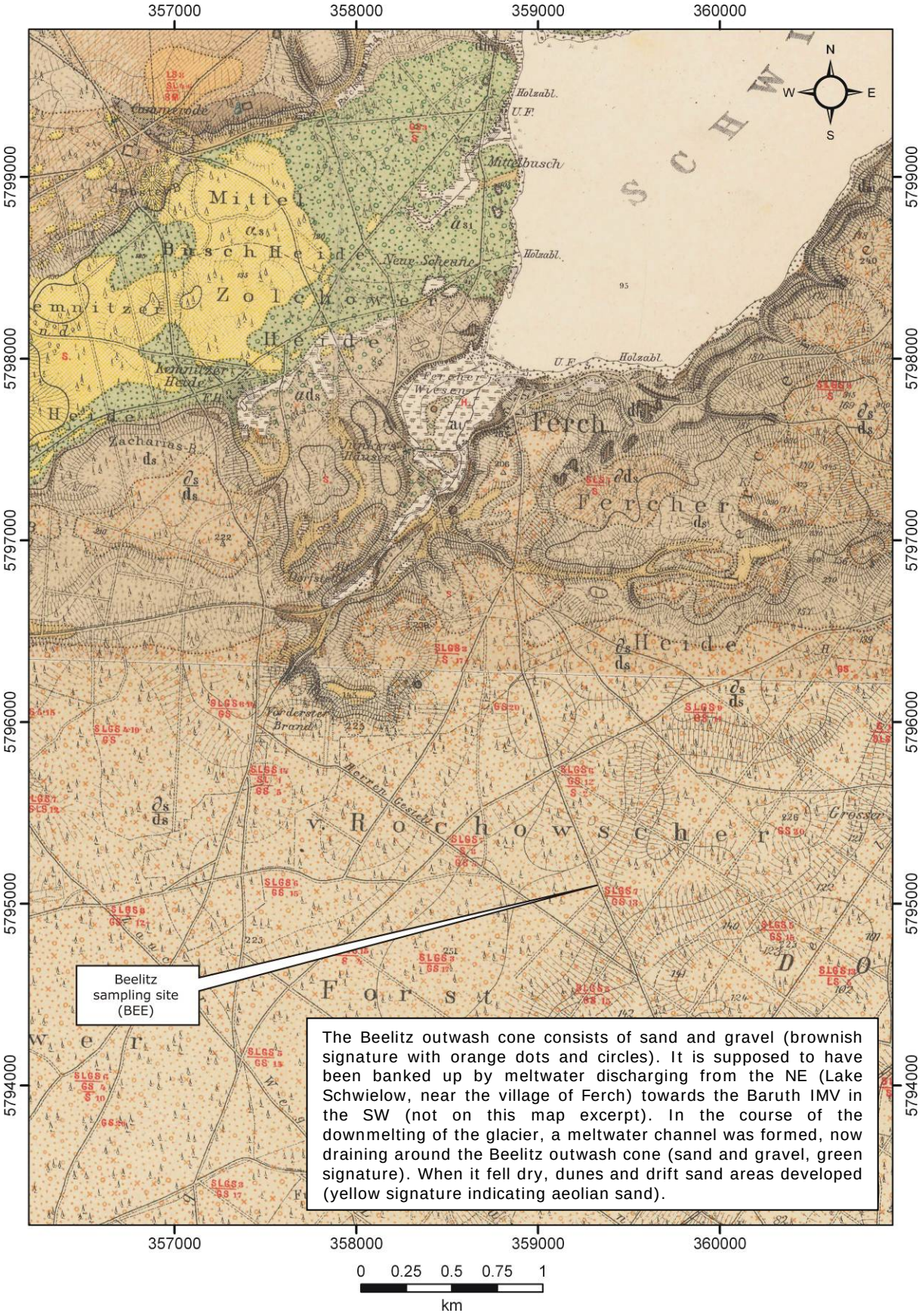

Excerpt from the geological map 1:25,000 (GK25 3743 © LBGR 2011 - Königlich Preußische Geologische Landesanstalt, 1875). UTM, WGS 1984. Please also see general remarks in appendix 13.2.20.

13.2.11. Eberswalde (EBE) – TK25

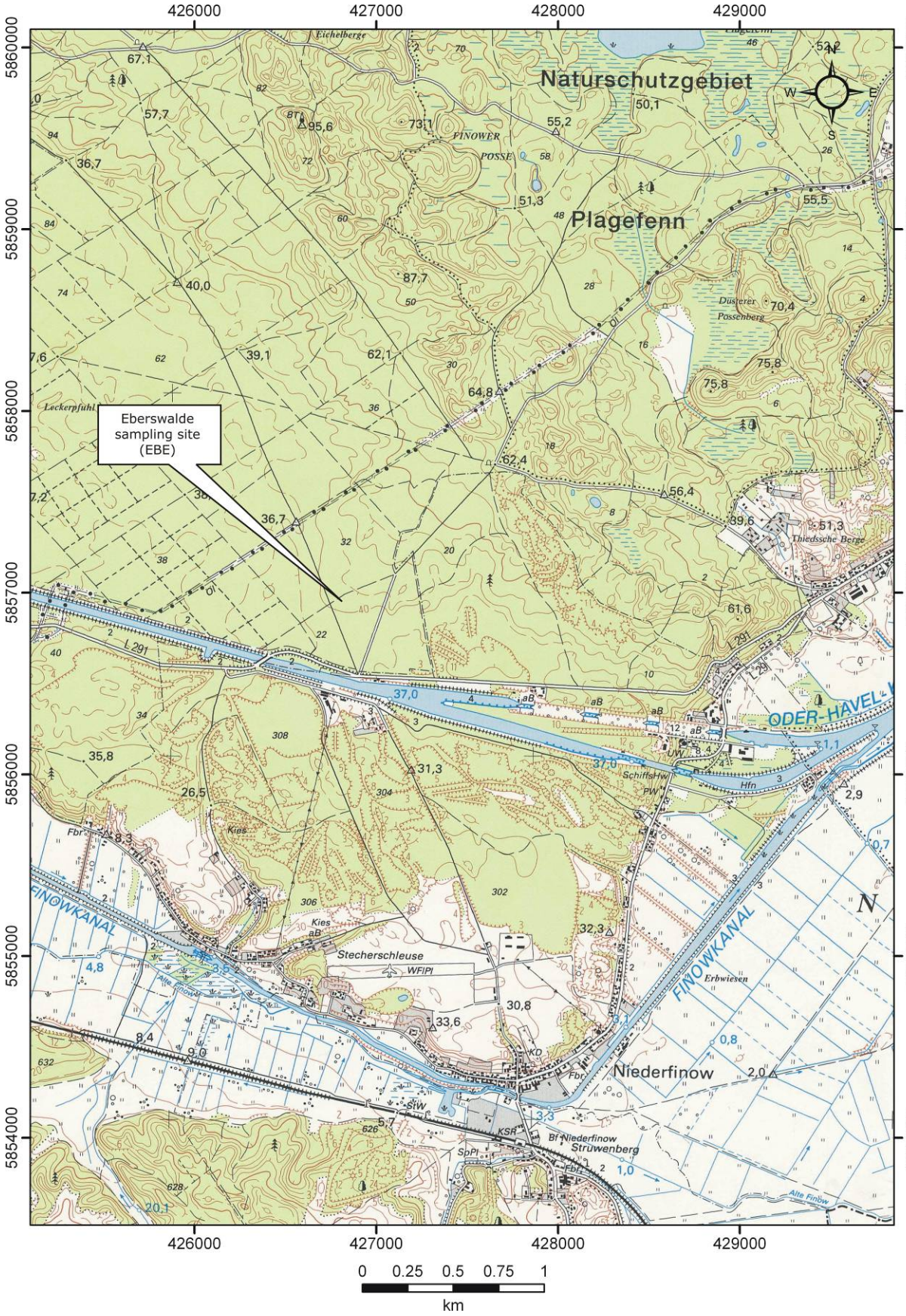

Excerpt from the topographical map 1:25,000 (TK25 3149 © GeoBasis-DE/LGB 2011, GB-D 07/11 www.geobasis-bb.de - Landesvermessungsamt Brandenburg, 1996). UTM, WGS 1984. Selected map legend see appendix 13.2.19.

13.2.12. Eberswalde (EBE) – GK25

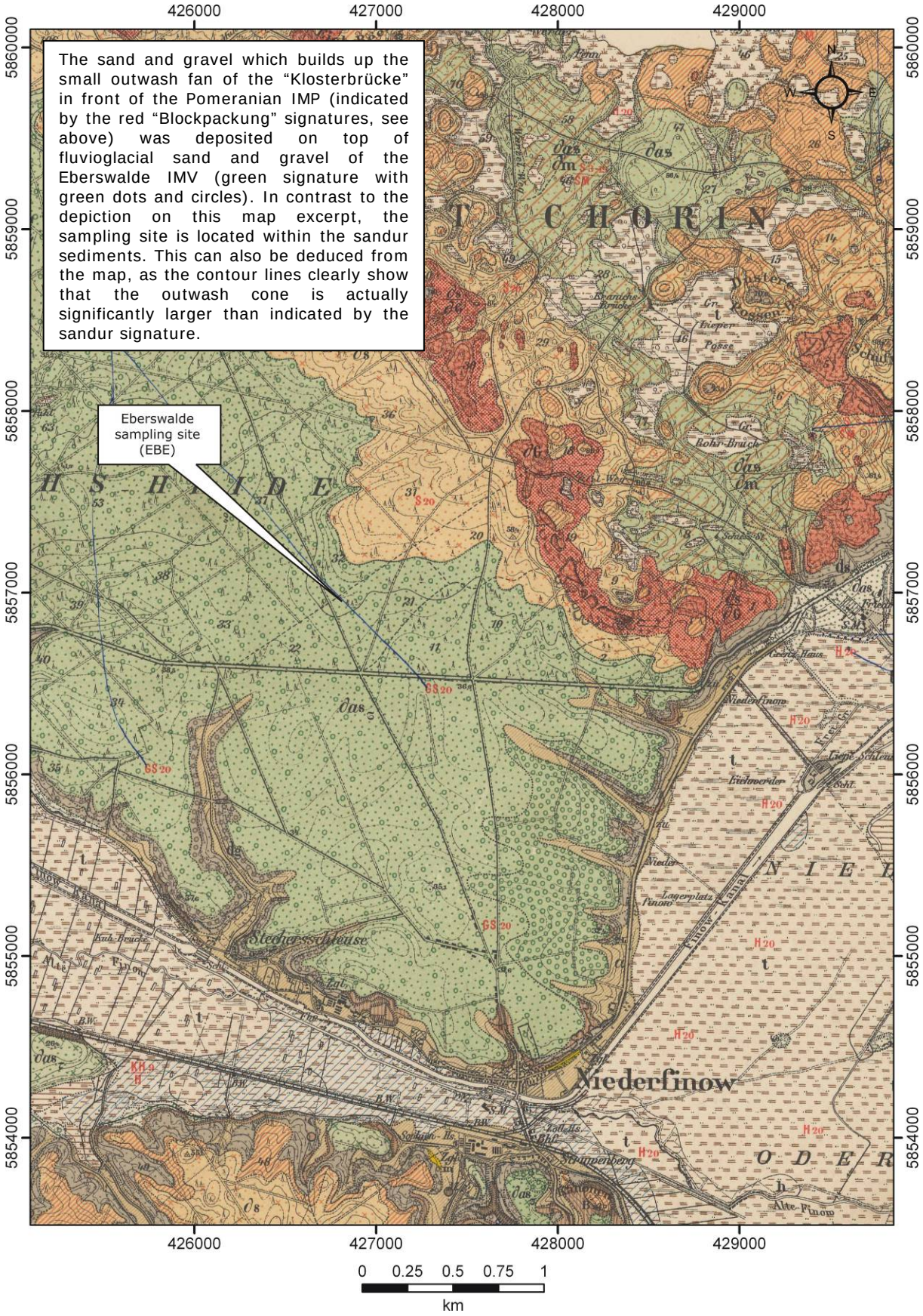

Excerpt from the geological map 1:25,000 (GK25 3149 © LBGR 2011 - Königlich Preußische Geologische Landesanstalt, 1899). UTM, WGS 1984. Please also see general remarks in appendix 13.2.20.

13.2.13. Frankenfelde (LUC_III) & Luckenwalde (LUC_I & LUC_II) – TK25

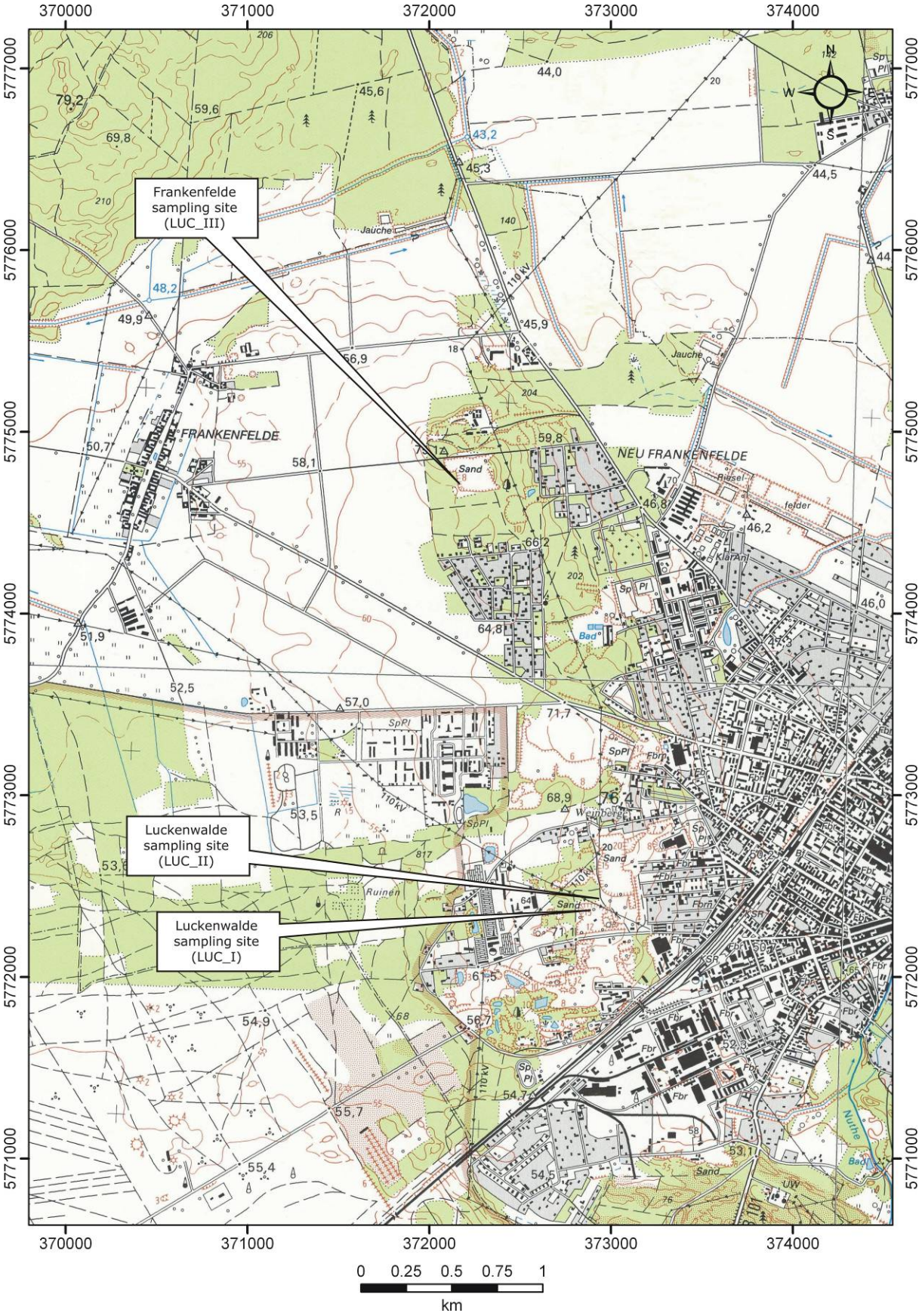

Excerpt from the topographical map 1:25,000 (TK25 3844, 3845, 3944, 3945 © GeoBasis-DE/LGB 2011, GB-D 07/11 www.geobasis-bb.de - Landesvermessungsamt Brandenburg, 1994). UTM, WGS 1984. Selected map legend see appendix 13.2.19.

13.2.14. Frankenfelde (LUC_III) & Luckenwalde (LUC_I & LUC_II) – GK25

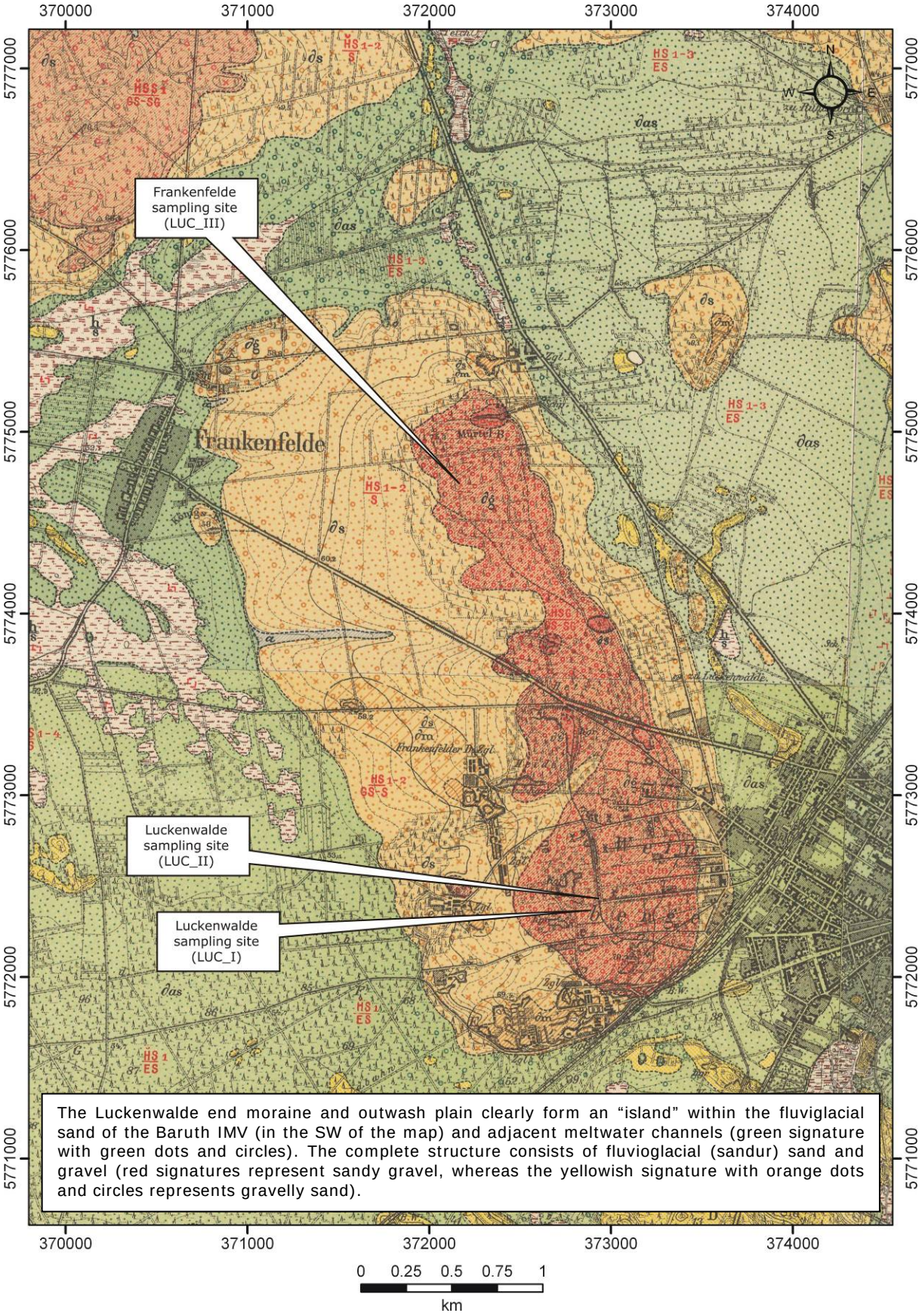

The Luckenwalde end moraine and outwash plain clearly form an "island" within the fluviglacial sand of the Baruth IMV (in the SW of the map) and adjacent meltwater channels (green signature with green dots and circles). The complete structure consists of fluvioglacial (sandur) sand and gravel (red signatures represent sandy gravel, whereas the yellowish signature with orange dots and circles represents gravelly sand).

Excerpt from the geological map 1:25,000 (GK25 3844, 3845, 3944, 3945 © LBGR 2011 - Preußische Geologische Landesanstalt, 1922). UTM, WGS 1984. Please see remarks in appendix 13.2.20.

13.2.15. Macherslust (MAC) – TK25

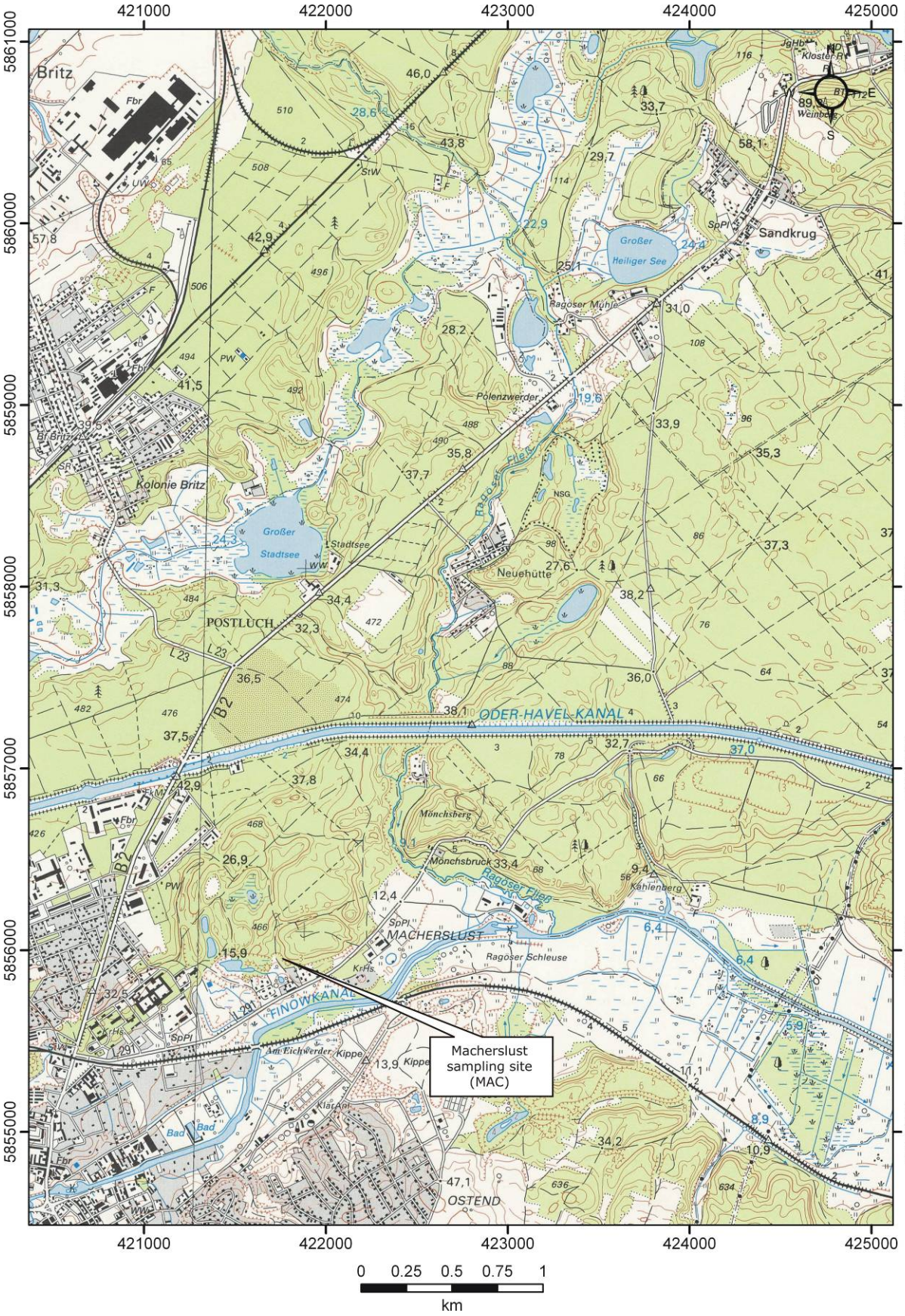

Excerpt from the topographical map 1:25,000 (TK25 3148, 3149 © GeoBasis-DE/LGB 2011, GB-D 07/11 www.geobasis-bb.de - Landesvermessungsamt Brandenburg, 1996). UTM, WGS 1984. Selected map legend see appendix 13.2.19.

13.2.16. Macherslust (MAC) – GK25

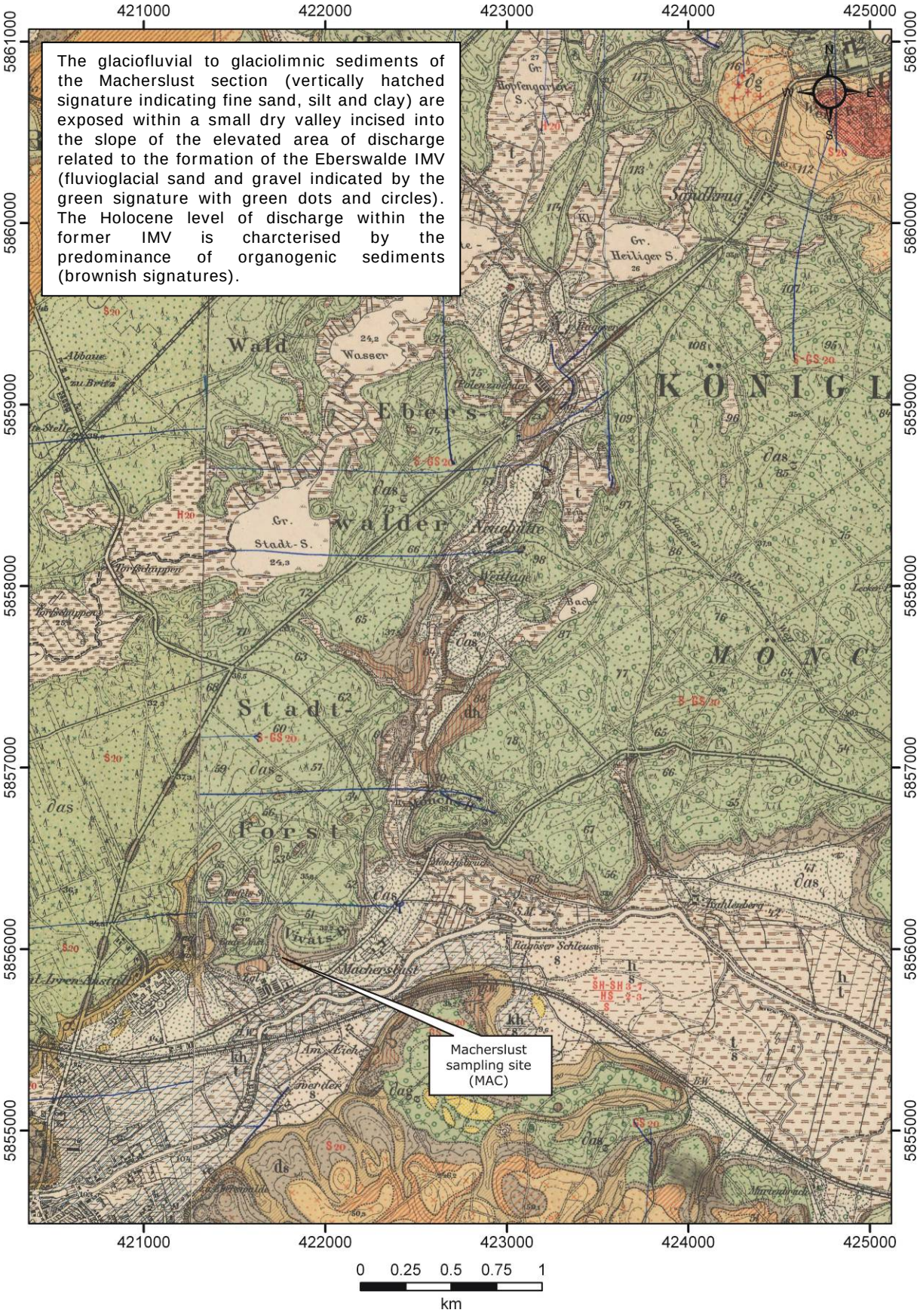

Excerpt from the geological map 1:25,000 (GK25 3148, 3149 © LBGR 2011 - Königlich Preußische Geologische Landesanstalt, 1899). UTM, WGS 1984. Please also see general remarks in appendix 13.2.20.

13.2.17. Vevais (VEV) – TK25

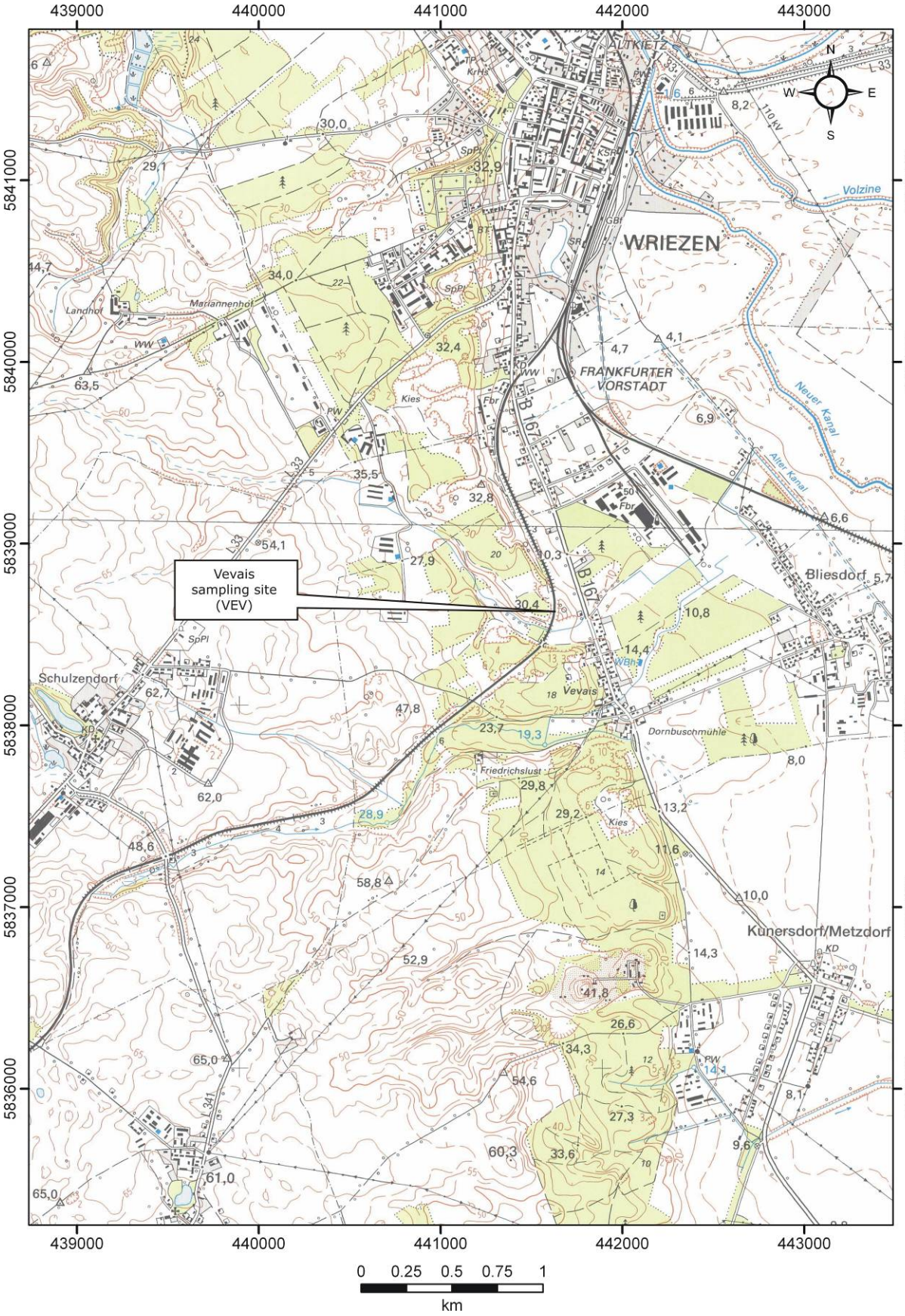

Excerpt from the topographical map 1:25,000 (TK25 3250, 3350 © GeoBasis-DE/LGB 2011, GB-D 07/11 www.geobasis-bb.de - Landesvermessungsamt Brandenburg, 1996). UTM, WGS 1984. Selected map legend appendix 13.2.19.

13.2.18. Vevais (VEV) – GK25

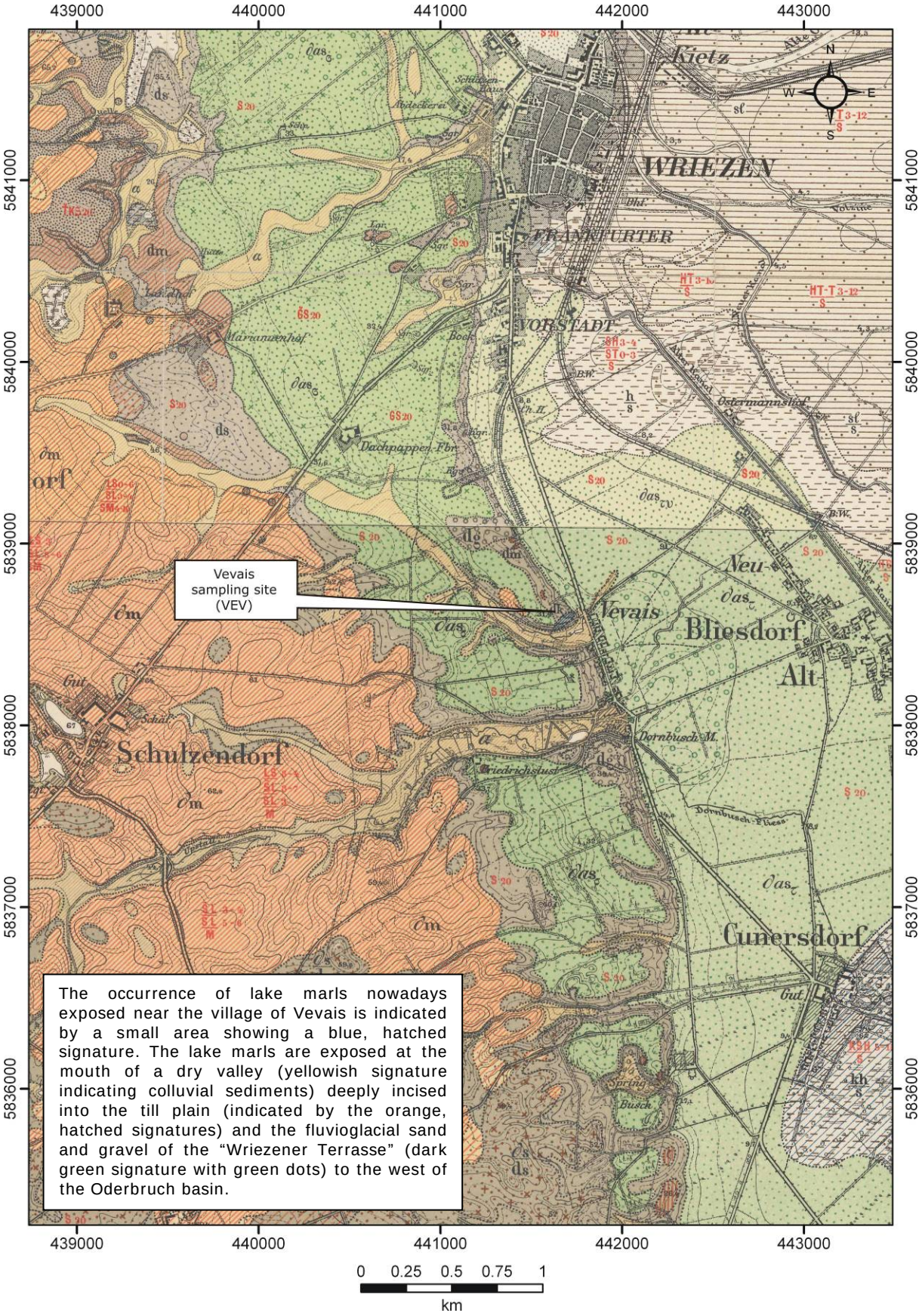

Excerpt from the geological map 1:25,000 (GK25 3250, 3350 © LBGR 2011 - Königlich Preußische Geologische Landesanstalt, 1908, 1895). UTM, WGS 1984. Please also see remarks in appendix 13.2.20.

13.2.19. TK25 map legend (selection)

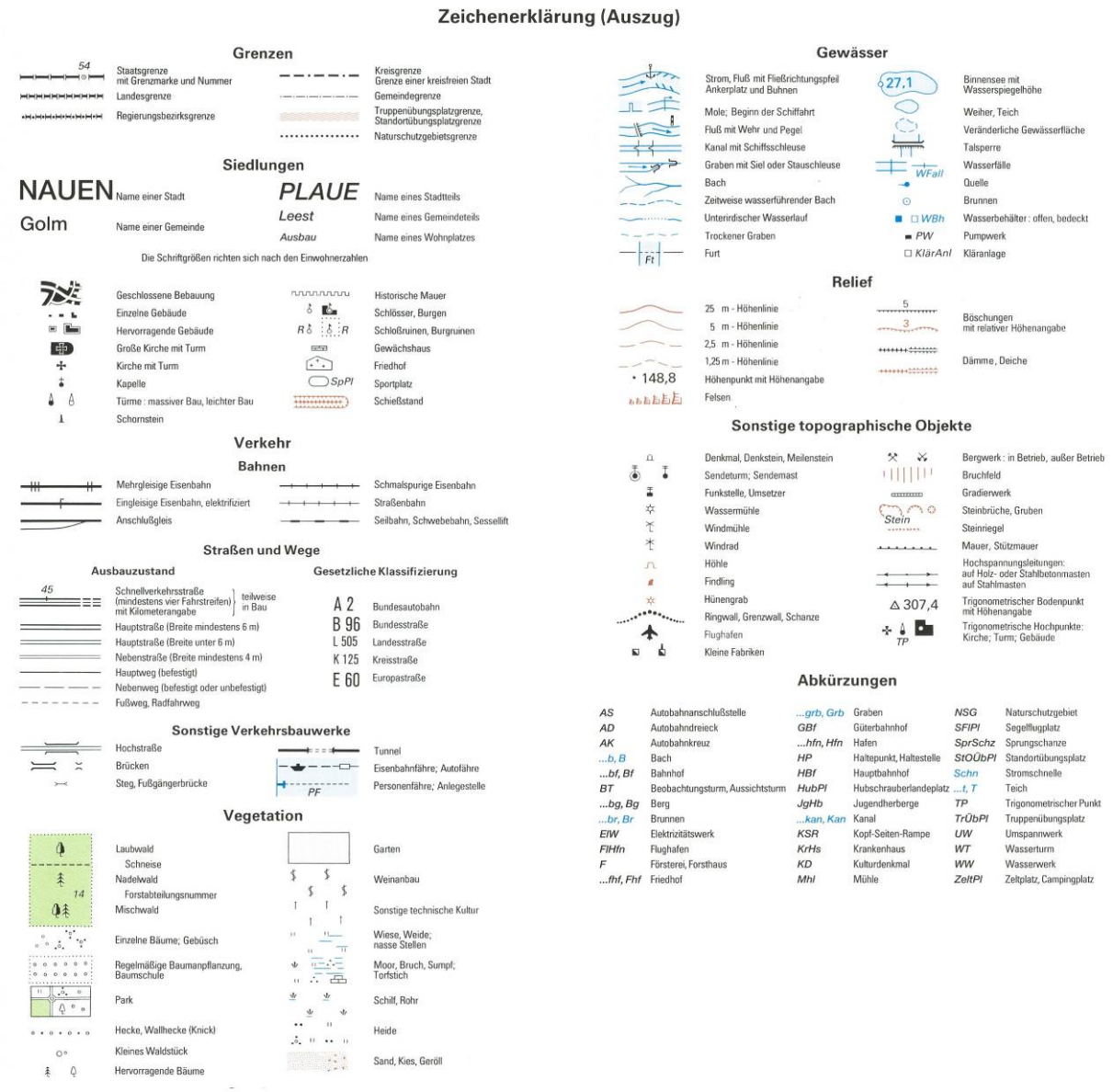

Map legend (selection) for the previously presented topographical maps 1:25,000 (TK25 © GeoBasis-DE/LGB 2011, GB-D 07/11 www.geobasis-bb.de). The legend is presented as is (in German language), because it is mostly self-explanatory.

13.2.20. GK25 map legend – general remarks

The geological maps 1:25,000 (GK25) presented in the preceding sections represent the most detailed geological field survey available for the research area. However, as the oldest maps were published in the late 19th century already and the newest maps also date back to the beginning of the 20th century, the interpretation of the mapped data is in many cases outdated. In addition, the signatures used for identical strata on maps from different editions differ significantly. For those reasons a detailed map legend is not presented here, but the most important information to be inferred from the map excerpts is provided along with the individual maps (used by kind permission of the Landesamt für Bergbau, Geologie und Rohstoffe (LBGR) Brandenburg).

.

List of publications

Lüthgens, C., Böse, M., 2007. Reassessment of the geomorphological development of the Rangsdorf lake area. E&G Quaternary Science Journal 57, 256-282.

Lüthgens, C., Böse, M., in press (2010). From morphostratigraphy to geochronology e on the dating of ice marginal positions. Quaternary Science Reviews, doi:10.1016/j.quascirev.2010.10.009.

Lüthgens, C., Böse, M., accepted manuscript (2011). Chronology of Weichselian main ice marginal positions in north-eastern Germany. E&G Quaternary Science Journal.

Lüthgens, C., Böse, M., Krbetschek, M.R., 2010a. On the age of the young morainic morphology in the area ascribed to the maximum extent of the Weichselian glaciation in north-eastern Germany. Quaternary International 222, 72-79.

Lüthgens, C., Böse, M., Lauer, T., Krbetschek, M., Strahl, J., Wenske, D., in press (2010b). Timing of the last interglacial in Northern Europe derived from Optically Stimulated Luminescence (OSL) dating of a terrestrial Saalian–Eemian–Weichselian sedimentary sequence in NE-Germany. Quaternary International, doi:10.1016/j.quaint.2010.06.026.

Lüthgens, C., Böse, M., Preusser, F., in press (2010c). Age of the Pomeranian ice marginal position in north-eastern Germany determined by Optically Stimulated Luminescence (OSL) dating of glaciofluvial sediments. Boreas, doi:10.1111/j.1502-3885.2011.00211.x.

Lüthgens, C., Krbetschek, M.R., Böse, M., Fuchs, M.C., 2010d. Optically Stimulated Luminescence Dating of fluvioglacial (sandur) sediments from north-eastern Germany. Quaternary Geochronology 5, 237-243.

Wenske, D., Böse, M., Frechen, M., Lüthgens, C., in press (2010). Late Holocene mobilisation of loess-like sediments in Hohuan Shan, high mountains of Taiwan. Quaternary International, doi:10.1016/j.quaint.2009.10.034.

List of conference presentations

2011
Lüthgens, C., Böse, M., (2011): A new deglaciation chronology for north-eastern Germany inferred from OSL dating of sandur sediments and a reinterpretation of surface exposure ages of erratic boulders. XVIII INQUA Congress, Bern, Switzerland, 21-27.07.2011 (poster – accepted).

2010
Böse, M., Lüthgens, C. (2010): On the ice marginal positions in north-eastern Germany between the Brandenburg Phase and the Gerswalde Subphase. 35. Hauptversammlung der Deutschen Quartärvereinigung DEUQUA e.V.; 12th Annual meeting of the INQUA PeriBaltic Working Group (oral)

Lüthgens, C., Krbetschek, M., Böse, M. (2010): Optically Stimulated Luminescence (OSL) dating of Weichselian sandur sediments from NE Germany – a comparison of results using medium aliquots, small aliquots and single grains of quartz. EGU General Assembly 2010, Vienna, Austria, 06.05.2009. (poster).

Lüthgens, C., Wenske, D., Tsukamoto, S., Böse, M., Frechen, M. (2010): Optically Stimulated Luminescence dating of deposits from the Tachia river catchment (Taiwan) - a test for suitability. EGU General Assembly 2010, Vienna, Austria, 05.05.2009. (poster).

Wenske, D., Böse, M., Frechen, M., Lüthgens, C. (2010): Sedimentation of loess-like sediments on fluvial terraces in the high mountains of Taiwan and its implications for assessing Quaternary morphodynamics. EGU General Assembly 2010, Vienna, Austria, 05.05.2009. (poster).

Lüthgens, C. (2010): Zur Zeitstellung weichselzeitlicher Eisrandlagen in Nordostdeutschland - Datierung von glazifluviatilen Sanden mit Hilfe von Optisch Stimulierter Lumineszenz (OSL). Vortrag im Colloquium des Institutes für Geographische Wissenschaften der Freien Universität Berlin. (oral)

2009
Böse, M., Lüthgens, C. (2009): From Morphostratigraphy to Geochronology - The Glacial Landscape in North-East Germany. Exploratory workshop on the frequency and timing of glaciations in northern Europe (including Britain) during the Middle and Late Pleistocene. Berlin, Germany. 16.-20.02.2009 (keynote)

Lüthgens, C., Böse, M., Krbetschek, M. (2009a): Towards a new understanding of the Last Glacial Maximum (LGM) in NE Germany – Results from Optically Stimulated Luminescence (OSL) Dating and their implications. Exploratory workshop on the frequency and timing of glaciations in northern Europe (including Britain) during the Middle and Late Pleistocene. Berlin, Germany. 16.-20.02.2009 (poster).

Lüthgens, C., Böse, M., Krbetschek, M. (2009b): Towards a new understanding of the Last Glacial Maximum (LGM) in NE Germany – Results from Optically Stimulated Luminescence (OSL) Dating and their implications. EGU General Assembly 2009, Vienna, Austria, 19.-24.04.2009. (poster).

Lüthgens, C., Böse, M., Krbetschek, M. (2009c): OSL ages from fluvioglacial (sandur) sediments of the Pomeranian ice marginal position in north-eastern Germany -results and methodological implications. German Meeting on Luminescence and ESR Dating 2009, Hannover, Germany, 09.-11.10.2009 (poster).

Lüthgens, C., Böse, M., Krbetschek, M. (2009d): The last glacial history of north-eastern Germany – From morphostratigraphy to geochronology. International Field Symposium of the INQUA Peribaltic Working Group, Tartu, Estonia, 13.-17.09.2009 (oral).

2008

Böse, M., Lüthgens, C. (2008a): Is the Young Morainic Morphology really “Young“? Ice Marginal Positions in North-East Germany. EGU General Assembly 2008, Vienna, Austria, 13.-18.04.2008. (oral).

Böse, M., Lüthgens, C. (2008b): Zum Alter von Reliefformen in weichselzeitlichen Eisrandlagen Nordost-Deutschlands. 3. Mitteleuropäische Geomorphologietagung, Salzburg, Österreich, 23.-28.09.2008. (oral).

Böse, M., Lüthgens, C., Krbetschek, M.R. (2008): Morphology and stratigraphy of the Weichselian ice marginal positions south of Berlin. International Field Symposium “The Quaternary of the Gdansk Bay and Lower Vistula regions in North Poland: stratigraphy, depositional environments and palaeoegeography”, Warsaw, Poland, 14-19.09.2008. (oral).

Lüthgens, C., Krbetschek, M.R., Böse, M., Fuchs, M. (2008): Optically Stimulated Luminescence Dating of fluvioglacial (sandur) sediments from North-Eastern Germany. 12th International Conference on Luminescence and Electron Spin Resonance Dating, Beijing, China, 18.-22.09.2008. (poster).

Lüthgens, C., Böse, M., Krbetschek, M.R. (2008a): Optically Stimulated Luminescence Dating of the Weichselian Ice Advances in North-Eastern Germany. EGU General Assembly 2008, Vienna, Austria, 13.-18.04.2008. (poster).

Lüthgens, C., Böse, M., Krbetschek, M.R. (2008b): Zur Zeitstellung weichselzeitlicher Eisrandlagen in Nordostdeutschland. DEUQUA Tagung 2008, Wien, Österreich, 31.08.-06.09.2008. (oral).

2007

Krbetschek, M.R., **Lüthgens, C.**, Böse, M. (2007): Optically Stimulated Luminescence Dating of the Weichselian Ice Advances in North-Eastern Germany. XVII INQUA Congress 2007, Cairns, Australia, 28.07.-03.08.2007. (poster).

Lüthgens, C., Böse, M., Krbetschek, M.R. (2007a): Datierung der weichselzeitlichen Haupteisrandlagen mit Hilfe von physikalischen Methoden (OSL und IR-RF) - Werkstattbericht. 74. Tagung der Arbeitsgemeinschaft Norddeutscher Geologen, Hamburg, Deutschland, 29.05.-01.06.2007. (oral).

Lüthgens, C., Böse, M., Krbetschek, M.R. (2007b): Questionable LGM Landforms in North-Eastern Germany. XVII INQUA Congress 2007, Cairns, Australia, 28.07.-03.08.2007. (poster).

Lüthgens, C., Krbetschek, M.R., Böse, M. (2007): OSL-dating of fluvioglacial sands in northeastern Germany - work in progress. Deutsches Lumineszenz und ESR Treffen, Wien, Österreich, 30.11.-02.12.2007. (oral).

Presenting author indicated by **bold** letters.

Curriculum Vitae

For reasons of data protection, the curriculum vitae is not included in the online version.

Berlin, 03.12.2010

Eidesstattliche Erklärung

Hiermit erkläre ich, dass ich die vorgelegte Arbeit selbständig und ohne fremde Hilfe verfasst und andere als die angegebenen Hilfsmittel nicht benutzt habe. Die Beiträge der Co-Autoren der wissenschaftlichen Veröffentlichungen sind im Rahmen der Danksagung (Acknowledgements) dargelegt. Ich erkläre, dass ich die Arbeit erstmalig und nur am Fachbereich Geowissenschaften der Freien Universität Berlin eingereicht habe und keinen entsprechenden Doktorgrad besitze.

Der Inhalt der dem Verfahren zugrunde liegenden Promotionsordnung ist mir bekannt.

Christopher Lüthgens